AD-A185 409 MOLECULAR MOTION AND ENERGY MIGRATION IN POLYMERS(U) 1/2
ROYAL INSTITUTION OF GREAT BRITAIN LONDON (ENGLAND)
D PHILLIPS JUN 85 DAJA37-82-C-0265

UNCLASSIFIED F/G 7/6 NL

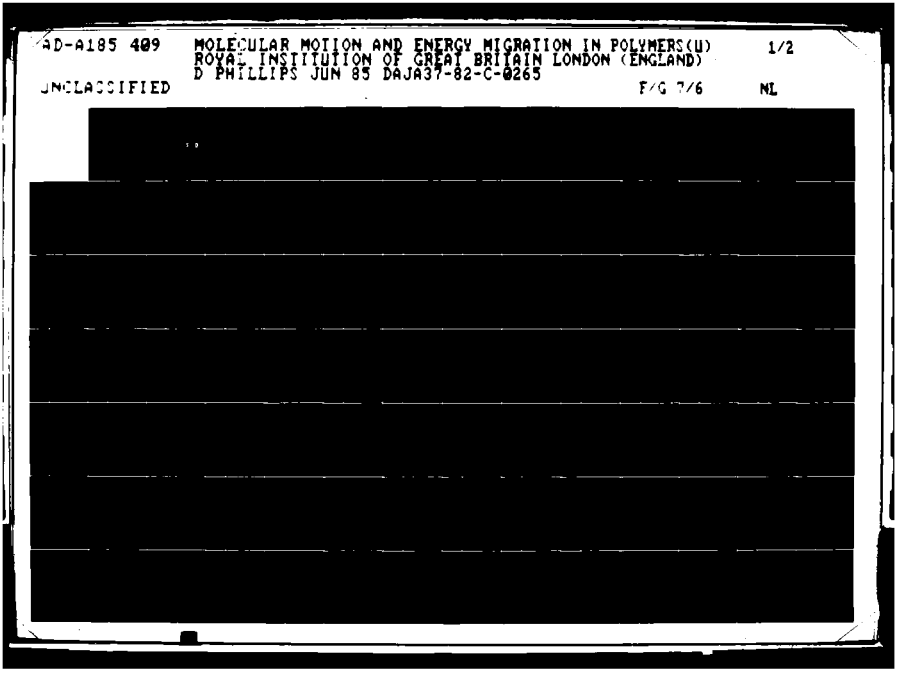

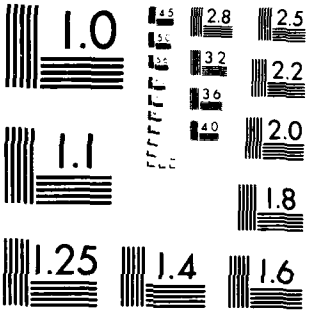

AD-A185 409

DTIC ACCESSION NUMBER

PHOTOGRAPH THIS SHEET

LEVEL

INVENTORY

MOLECULAR MOTION AND ENERGY MIGRATION IN POLYMERS

DOCUMENT IDENTIFICATION

JUNE 85

This document has been approved for public release and sale; its distribution is unlimited.

DISTRIBUTION STATEMENT

ACCESSION FOR	
NTIS GRA&I	X
DTIC TAB	
UNANNOUNCED	
JUSTIFICATION	
BY	
DISTRIBUTION /	
AVAILABILITY CODES	
DIST	AVAIL AND/OR SPECIAL
A-1	

DISTRIBUTION STAMP

DTIC COPY INSPECTED

DTIC ELECTE S OCT 2 7 1987 D E

DATE ACCESSIONED

DATE RETURNED

87 10 20 184

DATE RECEIVED IN DTIC

REGISTERED OR CERTIFIED NO.

PHOTOGRAPH THIS SHEET AND RETURN TO DTIC-FDAC

DTIC FORM 70A MAR 86

DOCUMENT PROCESSING SHEET

PREVIOUS EDITION MAY BE USED UNTIL STOCK IS EXHAUSTED.

MOLECULAR MOTION AND ENERGY MIGRATION IN POLYMERS

Professor David Phillips

June 1985

US Army European Research Office of the US Army,
London, England.

Contract Number DAJA 37-82-C-0265
PROFESSOR DAVID PHILLIPS

Unclassified

SECURITY CLASSIFICATION OF THIS PAGE *(When Data Entered)*

REPORT DOCUMENTATION PAGE		READ INSTRUCTIONS BEFORE COMPLETING FORM
1. REPORT NUMBER	2. GOVT ACCESSION NO.	3. RECIPIENT'S CATALOG NUMBER
4. TITLE *(and Subtitle)* Molecular Motion and Energy Migration in Polymers		5. TYPE OF REPORT & PERIOD COVERED Final Technical Report 6. PERFORMING ORG. REPORT NUMBER
7. AUTHOR(s) Professor David Phillips		8. CONTRACT OR GRANT NUMBER(s) DAJA37-82-C-0265
9. PERFORMING ORGANIZATION NAME AND ADDRESS The Royal Institution 21 Albemarle Street, London, W1, UK		10. PROGRAM ELEMENT, PROJECT, TASK AREA & WORK UNIT NUMBERS 61102A 1L161102BH57 08
11. CONTROLLING OFFICE NAME AND ADDRESS USARDSG-UK PO Box 65, FPO NY 09510		12. REPORT DATE June 1985 13. NUMBER OF PAGES 58 + 60 pages of Appendix
14. MONITORING AGENCY NAME & ADDRESS*(if different from Controlling Office)*		15. SECURITY CLASS. *(of this report)* Unclassified 15a. DECLASSIFICATION/DOWNGRADING SCHEDULE

16. DISTRIBUTION STATEMENT *(of this Report)*

Approved for public release; distribution is unlimited.

17. DISTRIBUTION STATEMENT *(of the abstract entered in Block 20, if different from Report)*

18. SUPPLEMENTARY NOTES

19. KEY WORDS *(Continue on reverse side if necessary and identify by block number)*

Synthetic polymer, fluorescence, anisotropy, time-resolved, laser, picosecond, photon-counting, polarisation, poly(styrene), copolymer, methyl methacrylate, methyl acrylate, acrylonitrile, butadiene, vinyl naphthalene acenaphthylene, poly(diacetylenes), 4,4' - diphenylene diphenyl vinylene, energy transfer, migration, segmental motion, rotational relaxation.

20. ABSTRACT *(Continue on reverse side if necessary and identify by block number)*

Extensive studies have been carried out on the time-resolved fluorescence, and fluorescence anisotropy, of a variety of synthetic polymers in dilute solution, disordered glasses, and solid state. Picosecond lasers were used for excitation and time-correlated single-photon counting for detection. Polymers studied included poly(styrene) and copolymers with methyl methacrylate, acrylonitrile and butadiene; polymethyl acrylate and methacrylate tagged with vinyl naphthalene and acenaphthylene; various poly(diacetylenes), and 4,4' - diphenylene diphenyl vinylene.

DD FORM 1 JAN 73 1473 EDITION OF 1 NOV 65 IS OBSOLETE

Unclassified

SECURITY CLASSIFICATION OF THIS PAGE *(When Data Entered)*

TABLE OF CONTENTS

1. Introduction

It was the technical aim of this work to investigate by nanosecond and sub-nanosecond time-resolved fluorescence and fluorescence anisotropy techniques the interactions between chromophores in poly(vinyl aromatic) polymers, the sub-group motion of such polymers, and energy migration in these systems. It was envisaged that studies on polymers in dilute solution would be completed, and extended to concentrated solutions, solid polymers, and where feasible, polymer melts.

In dilute fluid solution, we have carried out an extensive study of styrene containing polymers and copolymers, reported below, in which excimer formation is related to excitation migration and segmental motion. Some steady-state anisotropy measurements were also made.

In solid state, very extensive studies on the fluorescence of poly(diacetylene) polymers were made, again with particular emphasis on exciton diffusion in ordered crystals, and disordered polymers in solvent glasses at low temperatures.

A major experimental objective of the work was to design apparatus capable of very accurate measurements of time-resolved fluorescence anisotropy of 'labelled' synthetic polymers. This proved to be difficult, but was eventually achieved, and the equipment was used to study the vinyl aromatic tagged acrylic polymers in dilute and concentrated solution which was proposed originally.

The results achieved are discussed in detail below.

2. Experimental methods used

The experiments were carried out using two pieces of apparatus in which pulsed laser excitation was used to excite fluorescence in a sample, which was monitored using the well-tried technique of time-correlated single-photon counting[1].

System 1[2]

In this system, shown in Figure 1, the excitation source was a 4W Argon-ion laser (Spectra Physics 166) operated as a cavity-dumped only device. The resultant pulses were approximately 10ns full width at half maximum intensity (FWHM) and at repetition rates variable from single to 5MHz. Although these pulses are broad, the system has been shown to extract subnanosecond fluorescence lifetimes with confidence. Tuning of the output wavelength of the laser using an intracavity prism, enabled pulsed output of most of the Argon-ion 'lasing' lines (514.5, 501.7, 496.5, 488.0, 476.5, 472.7, 465.8, '457.9 + 454.5', 437.1nm). For excitation of the samples under study, it was necessary to frequency double the 514.5nm output to 257.25nm in order to obtain the desired wavelength. This was accomplished by focussing the output of the laser to a beam waist at the centre of a temperature-tuned non-linear crystal (ADP) (Coherent model 440 UV generator).

This ion laser was operated as a cavity-dumped only device, as the electronics were not sufficiently stable to simultaneously mode-lock and cavity dump, although use of an rf synthesiser (Racal Dana 8082) enabled it to be successfully mode-locked, synchronisation with the cavity dumper proved unsuccessful. New electronics are currently being built to overcome this problem. It should also be noted that this system was made prior to integer + 1/2 technology, thus even when fully working, pulse suppression will be a problem, especially as the cavity length is shorter and hence the mode-locked pulses are even closer together (10ns). In this system the mode-locker frequency, 48.5MHz, is 1/8th of the cavity dumper frequency, with the pulse repetition frequency related in the same way as previous, giving rates of 4.85MHz, 970KHz, etc... Replacement of the Spectra Physics 466 driver with a Coherent/Harris 101 introduced a different range of repetition rates (3.8MHz, 760KHz, etc) related to the Coherent CR18 laser, operating with a mode locker frequency of 38.5MHz, (1/10th of the cavity dumper frequency).

The major problem with this system operating in this configuration, is the structure within the cavity dumped envelope. This system has been operated previously using the cavity dumper in a CW dye laser. However, by small adjustments of the Bragg cell, elimination of the structure was possible, assumed to be due to dephasing of the two interfacing beams. The temporal resolution of this spectrometer was also lower and thus with the increased resolution of the present spectrometer the structure became more of a problem. Figure 2a shows a cavity-dumped pulse detected using the photon counting detection system,

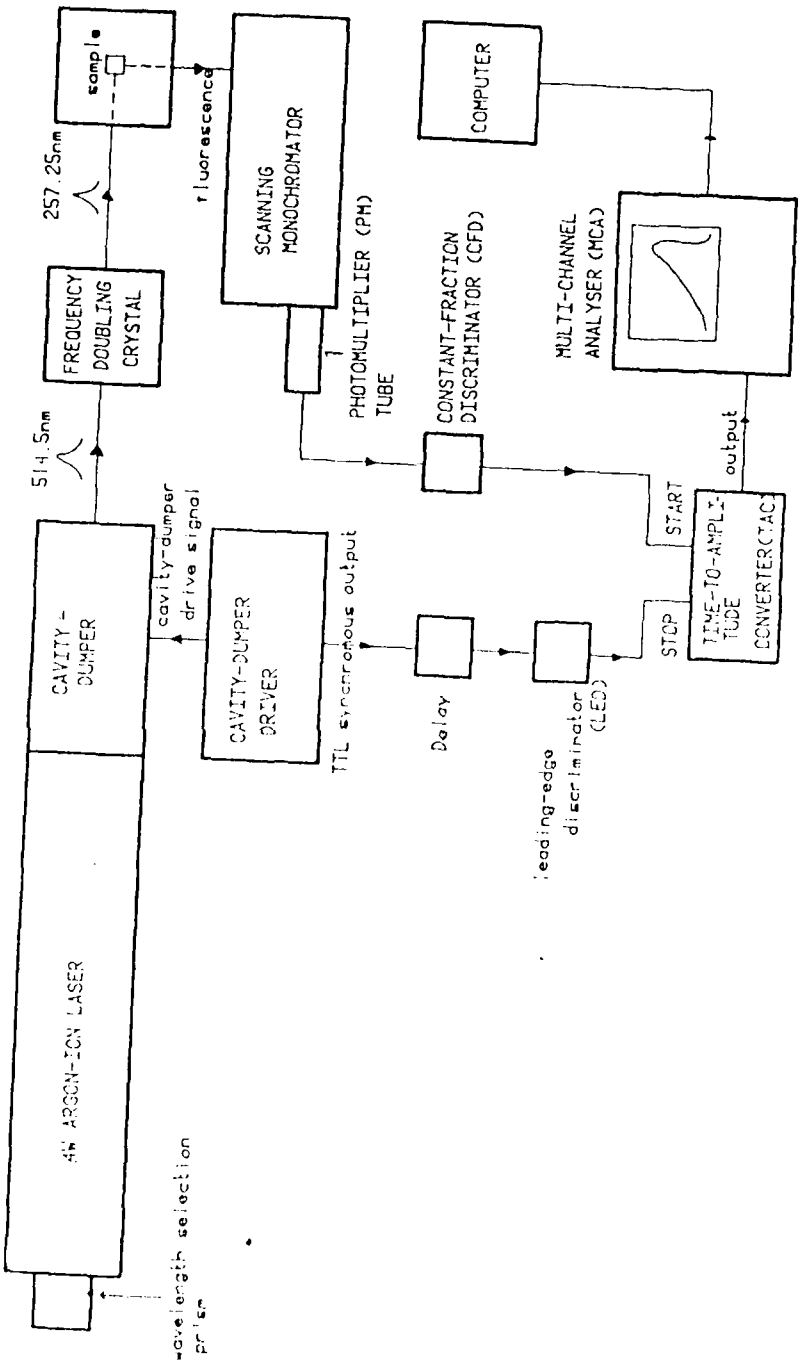

Figure 1 Schematic of spectrometer incorperating cavity-dumped argon-ion laser

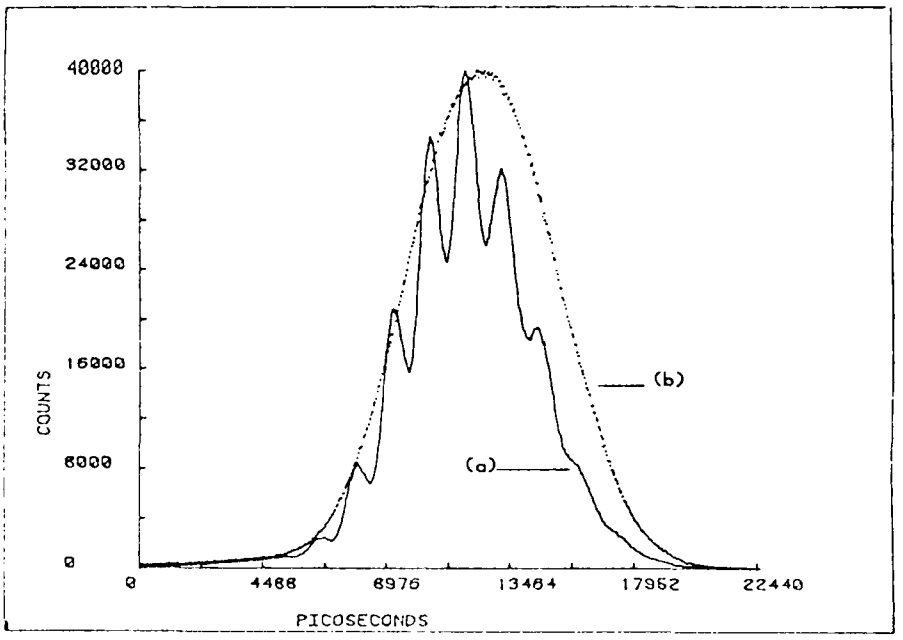

Figure 2 Cavity dumped pulses detected using single-photon detection
(a) Double pass configuration
(b) Single pass configuration

demonstrating the structure within the pulse. Using the aforementioned 'dephasing' technique was both difficult and unreliable. Figure 2b shows another pulse detected under the same conditions as previously but here the structure has been removed successfully by eliminating the first diffracted beam and thus avoiding interference of the two output beams. This method proved far superior and was now adopted for general use.

System 2[2]

The second system shown in Figure 3 compromised an activity mode-locked (Spectra Physics 342) 12W Argon-ion laser (Spectra Physics 171), synchronously pumping a Rhodamine 6G dye laser (Spectra Physics 375) with an intracavity dumper (Spectra Physics 344). Pulses produced were 10ps FWHM and at repetition rates variable from single shot to 4MHZ 'lasing' of Rhodamine 6G was possible over the wavelength range of 570-620nm and selection of the desired wavelength was achieved using a dielectronically coated tuning wedge. This wavelength range was unsuitable for the molecules of interest and thus frequency doubling was also applied here, using an angle-tuned ADP crystal (JK Lasers Ltd).

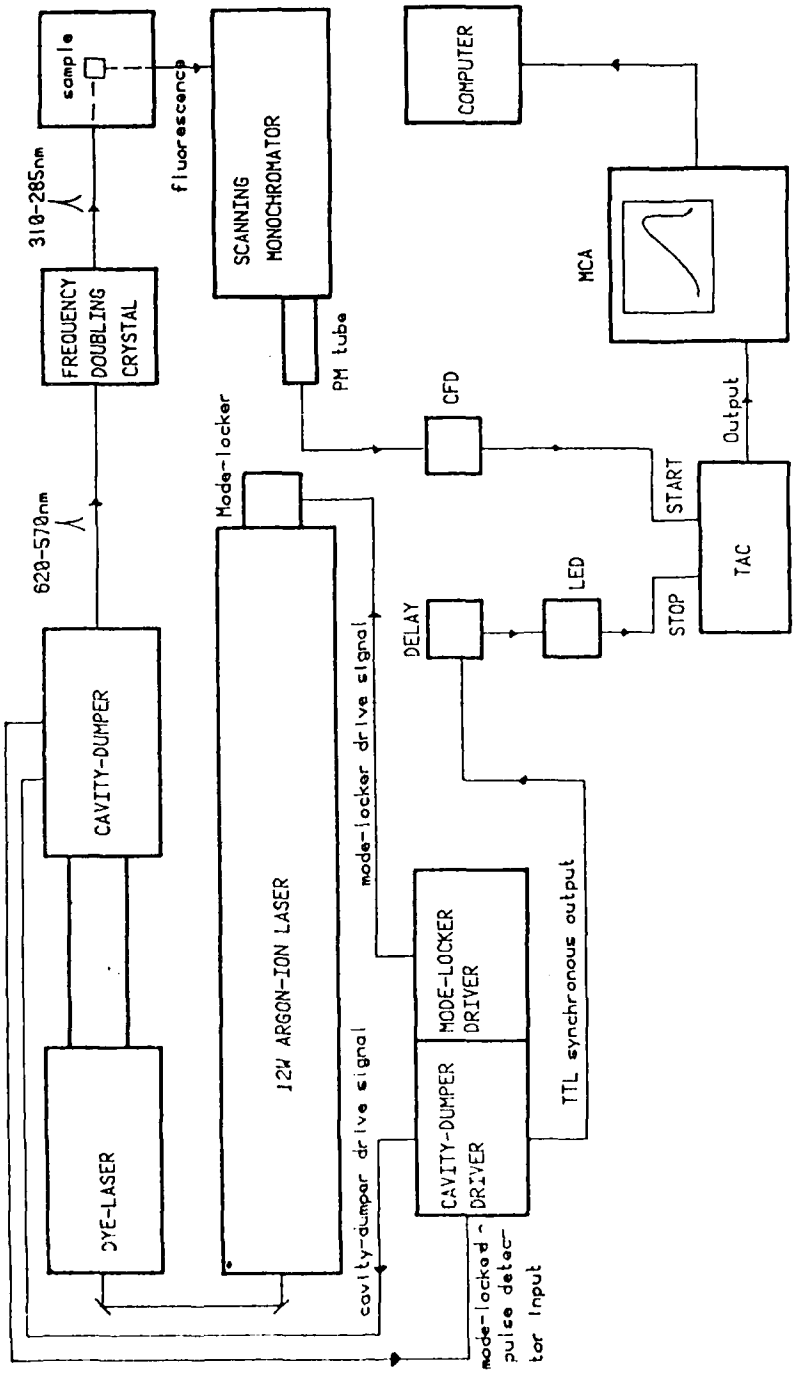

Figure 3 Schematic pf spectrometer incorporating cavity-dumped, synchronoulsy pumped dye laser

The detection electronics of both systems were identical in operation but differed in models used. The make and models quoted below in parenthesis are for the System 1 and System 2 laser systems, respectively.

Solution-phase samples were contained in $1cm^3$ suprasil quartz cuvettes with facilities for degassing by the freeze-pump-thaw technique. Fluorescence was monitored perpendicular to the direction of excitation, by focusing the light using a 3cm focal length lens on to the slits of a high resolution monochromator (Rank-Precision Monospek 1000, Rank-Precision D330). Fluorescence was detected using a fast photomultiplier (PM) tube (Philips 56DUVP, Philips XP2020Q) wired for single-photon counting and biased at 2.3KV by a Farnell E2 stablised power supply. The output signal from the PM tube was fed to a constant fraction discriminator (Ortec 463, Ortec 934), the output of which was then delayed (to centralise decay on screen of MCA) using nanosecond delay lines (S.E.N. FE290, Ortec 425A) and applied to the START input of the time-to-amplitude converter (TAC) (Ortec 437A/467, Ortec 457). In the conventional set up this is the STOP input, however, owing to the high repetition rate of the laser, an inverted mode of TAC operation is employed. The STOP input to the TAC was obtained from a TTL signal from the rear of the cavity-dumper driver (Spectra Physics 466/Harris 101; Spectra Physics 454) which is synchronised with the cavity-dumper drive signal. No difference was observed in using this method in place of the conventional technique of using a photodiode, and was thus used for convenience.

The output voltage from the TAC was fed to the MCA (Northern NS600/Norland Inotech 5300, Canberra series 30) operating in the pulse-height analysis mode. One half of the memory (256/512, 512 channels) used to store the fluorescence decay, and the other half to store the instrument response function. Data was collected to a minimum of 30000 counts in the channel of maximum intensity in order to obtain a good signal-to-noise ratio, which is required to justify the use of complex fitting functions. The TAC range was chosen to allow the fluorescence intensity to decay through at least three decades of intensity and thus prevent omission of any long lived fluorescence species.

Data was transferred to a Perkin-Elmer 7/32C minicomputer and then analysed using an iterative, non-linear least squares reconvolution program, written in Fortran 4.

Analysis of data is discussed in the relevant sections below, and in Appendix I. The use of the apparatus to make time-resolved anisotropy measurements is discussed in Appendix II.

3. Luminescence of poly(styrene) and copolymers

Poly(styrene) is a characteristic vinyl aromatic polymer in that it exhibits strong excimer fluorescence, an excimer being an excited state dimer, the formation and decay of which follows the Birks kinetic Scheme 1 for free chromophores in solution[3]. For the case of vinyl(naphthalenes) we showed in earlier work[4-7] on the basis of analysis of monomer fluorescence that Scheme 2 was most compatible with the observations. The results were based upon the empirical fitting of fluorescence decay curves to a sum of three weighted exponentials, and have been criticized on the grounds that more complex mathematical models can in some circumstances be mimicked by three exponential terms (i.e., a six parameter fit)[10]. We have responded to these criticisms in a recent article reproduced here as Appendix I. We believe in particular that the methods of analysis used here are particularly valid in the case of poly(styrenes), and we thus present here our conclusions based upon this analysis, the basis of which is outlined below.

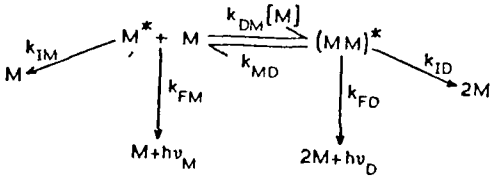

Scheme 1 Kinetic scheme for excimer formation and decay after Birks

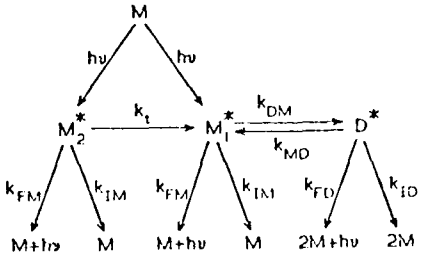

Scheme 2 Possible scheme for excimer kinetics in copolymers of vinyl(naphthalene)

Scheme 2

In this photophysical scheme it is proposed that M_i and D* interact by an exciton diffusion mechanism. M_2* is considered to be an isolated naphthalene chromophore which can transfer energy into M_1* with a transfer rate characterised by the rate coefficient k_t. Reverse transfer from M_1* to M_2* is considered unimportant for the following reason. Exciton diffusion is expected to be very efficient within sequences of naphthalene

chromophores within the chain, comprising the M_1^* sites. In view of the reduced lifetime of M_1^* relative to M_2^* and of the delocalised nature of the energy within extended chromophore sequences which increases the effective separation of M_1^* and M_2^*, M_1^* to M_2^* energy transfer by Foster or Dexter mechanisms is diminished relative to the M_2^* to M_1^* process.

Analysis of results

In Scheme 2 the emissions from M_1^* and M_2^* will be spectrally indistinguishable and if it is assumed that

$$k_M = k_{FM} + k_{IM} \quad (1)$$

is identical for each species, then the decay profiles $i_M(t)$ and $i_D(t)$ recorded for monomer and excimer, respectively, may be derived as

$$i_M(t) = A_1 \exp(-\lambda_1 t) + A_2 \exp(-\lambda_2 t) + A_3 \exp(-\lambda_3 t) \quad (2)$$

and

$$i_D(t) = A_4 \exp(-\lambda_1 t) + A_5 \exp(-\lambda_2 t) + A_6 \exp(-\lambda_3 t) \quad (3)$$

where

$$\lambda_{1,2} = 1/2[(X + Y) \pm \{(Y - X)^2 + 4k_{MD}\, k_{DM}[M]\}1/2] \quad (4)$$

and

$$X = k_M + k_{DM}[M], \quad Y = k_D + k_{MD}$$

where

$$k_D = k_{FD} + k_{ID}$$

and

$$\lambda_1 + \lambda_2 = k_M + k_{DM}[M] + k_D + k_{MD} \quad (5)$$

and

$$\lambda_3 = k_t + k_M \text{ for Scheme 2} \quad (6)$$

Equation (2) is compatible with the observation of triple components in the decay of monomer fluorescence in all polymers studied. The model may thus be used to yield rate-constants in the following way.

Determination of rate coefficients

For low molar mass species in which intermolecular excimer formation results from a diffusion controlled interaction, individual rate parameters may be determined by the following methods, summarised in Table 1.

(1) From a study of the concentration dependence of λ_1 and λ_2 rate parameters may be extracted from the empirical data by a variety of extrapolation techniques.

(a) k_M may be estimated from the unquenches monomer lifetime.
(b) Since $\lambda_1 \rightarrow k_M$ as $[M] \rightarrow 0$, k_M may be estimated from the intercept of λ_1 as a function of [M].
(c) Since $(\lambda_1 + \lambda_2)/[M] = k_{DM}$, k_{DM} is conveniently estimated as the slope of plot of $(\lambda_1 + \lambda_2)$ against [M].
(d) As $[M] \rightarrow \infty$, $\lambda_2/[M] \rightarrow k_{DM}$; k_{DM} may be obtained, as an alternative to method (c), from a plot of λ_2 as a function of $[M]^{-1}$.
(e) Since $(\lambda_1 + \lambda_2) \rightarrow k_M + k_{MD} + k_D$ as $[M] \rightarrow 0$ the intercept of $(\lambda_1 + \lambda_2)$ against [M] may be used in combination with (a) or (b) or estimate $(k_{MD} + k_D)$.
(f) Since $(\lambda_1\lambda_2) \rightarrow k_M(k_{MD} + k_D)$ as $[M] \rightarrow 0$, $(k_{MD} + k_D)$ may be estimated as an alternative to method (e) from a plot of $(\lambda_1\lambda_2)$ as a function of [M] through substitution of k_M from (a) or (b).
(g) The slope of $(\lambda_1\lambda_2)$ vs. [M] furnishes $k_{DM}k_D$. Thus, k_D may be estimated using the value of k_{DM} from either (c) or (d).
(h) As $[M] \rightarrow \infty$, $\lambda_1 \rightarrow k_D$.
(i) k_{MD} may be estimated by combinations of (e) and (f) with (g) and (h).

The results obtained by these procedures on poly(styrene) and copolymers with methyl methacrylate can be summarised as follows.

Styrene homopolymers[12]

Fluorescence decay curves were recorded in the regions of monomer emission (at 270 and 290nm), and excimer emission (at 340nm). The monomer decay $i_M(t)$ was poorly described by a single exponential function but was well characterised by a dual exponential fit of the form

$$i_M(t) = A_a \exp(-t/\tau_a) + A_b \exp(-t/\tau_b) \qquad (7)$$

where

$A_a = 1.15$ $\qquad$ $A_b = 0.004$

$\tau_a = 0.88\ (+\ 0.10)$ns $\qquad$ $\tau_b = 14.9\ (+\ 0.8)$ns

The excimer decay $i_D(t)$ was poorly described by single and double exponential fits. The inadequacy of the double exponential fit may be due in part to instrumental distortion experienced in analyses of emission data subject to large energy displacements from that of excitation. However, analysis of the fluorescence response excluding the rising portion of the decay profile yielded a lifetime of 15.3 (+ 0.2)ns. This long decay time may be assigned to that of the excimer consistent with a previous report.

Table 1 Procedures for derivation of rate constants

Method	Procedure	Function derived	Derived parameter
(a)	Measurement of unquenched monomer lifetimes	k_M	k_M
(b)	Extrapolation of λ_1 to $[M] = 0$	k_M	k_M
(c)	$\frac{\partial(\lambda_1 + \lambda_2)}{\partial[M]}$	k_{DM}	k_{DM}
(d)	$\frac{\partial\lambda_2}{\partial[M]}$ k_{DM} as $[M] \rightarrow \infty$	k_{DM}	k_{DM}
(e)	$(\lambda_1 + \lambda_2) \rightarrow k_M + k_{MD} + k_D$ as $[M] \rightarrow 0$	$k_M + k_{MD} + k_D$	$k_{MD} + k_D$ by combination with (a) or (b)
(f)	$(\lambda_1\lambda_2) \rightarrow k_M(k_{MD} + k_D)$ as $[M] \rightarrow 0$	$k_M(k_{MD} + k_D)$	$k_{MD} + k_D$ by combination with (a) or (b)
(g)	$\frac{\partial(\lambda_1\lambda_2)}{\partial[M]} = k_{DM}k_D$	$k_{DM}k_D$	k_D by combination with (c) or (d)
(h)	$\lambda_1 \rightarrow k_D$ as $[M] \rightarrow \infty$	k_D	k_D
(i)	(e) or (f) plus (g) or (h)	k_{MD}	k_{MD}

Consideration of the relative magnitudes of the pre-exponential factors A_a and A_b and decay times τ_a and τ_b (equation 7) reveals that the subnanosecond component dominates the fluorescence decay (constituting 94.4% of the emission profile). Comparison of τ_b with the value obtained for that of the excimer described above indicates that τ_b may be associated with the excimer dissociation to produce excited state monomer. Hence in contrast with previous reports the reverse dissociation pathway, although of rather minor significance, is not completely absent. Conclusive evidence of this fact is provided by the time resolved emission spectra presented in Figure 4.

The early gated spectra are dominated by monomer fluorescence. However, as the time interval, Δt, between excitation and analysis is increased the relative proportion of excimer to monomer, i_D/i_M, is observed to increase. This is consistent with the observation of a longer lived excimer and with the proposition that excimer may be generated from excited state monomer. More importantly it should be noted that in the late gated spectra, sampled at times at which emission from

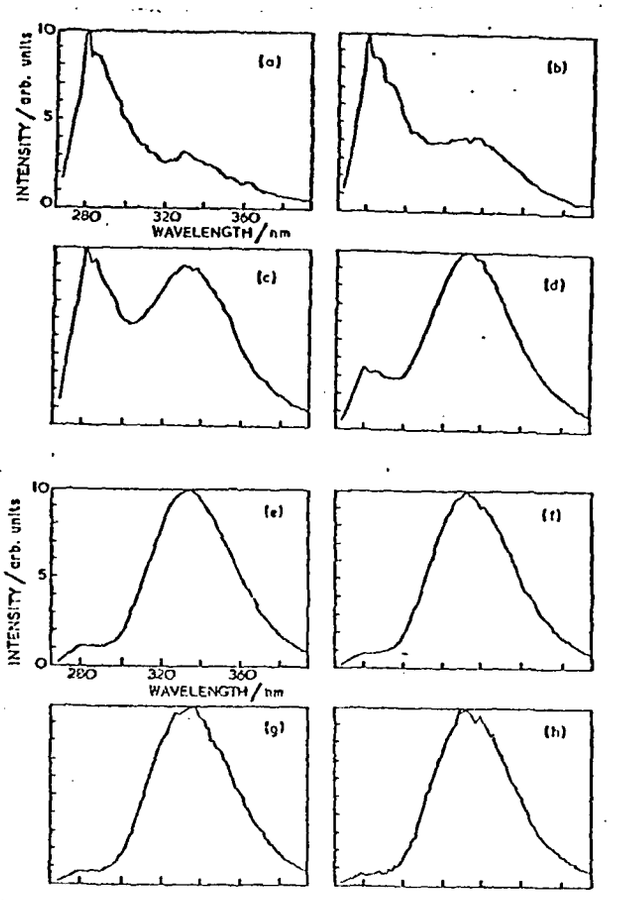

Figure 4 Time resolved fluorescence spectra of poly(styrene) in degassed dichloromethane recorded at delays of (a) 0ns; (b) 3.8ns; (c) 7.7ns; (d) 11.5ns; (e) 15.4ns; (f) 19.3ns; (g) 28.8ns; (h) 38.4ns following excitation. A gate width of 3.2ns was used throughout.

directly excited monomer would not be extant a small contribution from monomer emission is observable. Additionally the ratio i_D/i_M tends to a constant value at long times indicative that the monomer emission observed in these spectra results from reverse dissociation of excimer.

The principal differences between the photophysical behaviour of poly(styrene) and poly(vinyl naphthalene)[5] or poly(1-naphthylmethacrylate)[8] are that (i) in the poly(styrene) homopolymer monomer the emission decay is well described by a dual exponential function. Consequently there is no evidence in these dates for the presence of an 'isolated' monomer as postulated to explain the triple exponential fits in naphthalene containing polymers. (ii) The reverse dissociation of excimer

appears to be of less importance in poly(styrene) than in the polymers bearing naphthyl chromophores.

Styrene-methyl methacrylate-copolymers[12]

Table 2 lists the parameters governing polymer microcomposition necessary for the description of the photophysical behaviour of the copolymers. The derivation and significance of the functions f_s (mole fraction of aromatic) f_{ss} (fraction of bonds between styrene derived species) and l_s (mean sequence length of aromatic in the copolymers) have been discussed in paper 12 listed in this report.

As with the homopolymer fluorescence decay curves were recorded in the spectral regions corresponding to monomer and excimer fluorescence. The emission intensity decay of the excimer could not be described well by single or dual exponential functions. Triple exponential fitting is not justified due to uncertainties introduced by instrumental distortions consequent upon large spectral displacements from the excitation wavelength. Consequently, excimer 'lifetimes', τ_E, were obtained by a similar 'tail fitting' treatment as described for the homopolymer and are collated in Table 3.

Table 2 Composition data for Styrene-methylmethacrylate copolymers

Sample	f_s	f_{ss}	s
1	0.04	0.000	1.01
2	0.17	0.009	1.05
3	0.28	0.400	1.13
4	0.36	0.057	1.25
5	0.46	0.132	1.36
6	0.49	0.163	1.54
7	0.60	0.286	1.87
8	0.66	0.375	2.31
9	0.75	0.518	3.26
10	0.87	0.737	6.73
11	0.94	0.891	18.00

Table 3 Decay data for Styrene-methylmethacrylate copolymers

Sample	A_1	τ_1/ns	A_2	τ_2/ns	A_3	τ_3/ns	τ_E/ns
1			0.018	7.91	0.165	21.63	
2			0.017	8.80	0.146	22.51	
3			0.033	5.28	0.154	19.51	
4			0.062	4.88	0.143	17.74	
5			0.109	4.77	0.124	14.00	17.16
6			0.130	4.37	0.115	13.54	16.26
7	0.026	15.9	0.162	2.4(8)	0.127	7.80	15.89
8	0.010	15.3	0.287	1.8(4)	0.147	5.70	15.47
9	0.011	15.2	0.297	1.3(6)	0.119	4.20	15.33
10	0.009	16.7	1.090	0.8(5)	0.031	2.4(1)	14.19
11	0.006	14.6	0.648	0.9(4)	0.183	2.0(9)	15.28

The time dependence of fluorescence intensity in the region of monomer emission $i_M(t)$ could not be adequately characterised in terms of a single exponential function for any composition of styrene examined. In the lower styrene composition range (samples 1-6; styrene content 4-49%) $i_M(t)$ was well described by a dual exponential function of the form of equation (7). However, at aromatic contents of 60 mole % and greater it was necessary to invoke triple exponential functions of the form

$$i_M(t) = a_1 \exp(-t/\tau_1) + A_2 \exp(-t/\tau_2) + A_3 \exp(t/\tau_3) \quad (8)$$

The data are shown in Table 3. Interpretation of these results with reference to Scheme 2 yields the rate coefficients given in Table 4. The results are described in full elsewhere[12], but the main conclusions reached are:-

(1) It is apparent that the mechanism proposed for the description of intramolecular excimer formation in naphthalene-containing polymers is a feasible kinetic scheme for the phenomena in macromolecules containing styrene.
(2) The photophysical behaviour of poly(styrene) is different from that of the homopolymers of the vinylnaphthalenes and 1-napthyl methacryacrylate. It would appear that in poly(styrene) there is no detectable influence from 'isolated' monomeric groups, M_2*. Consequently it may be inferred that M_2* sites in styrene

copolymers are associated with physically isolated chromophores. In naphthalene polymers M_2^* sites are evident in

Table 4 Rate coefficients for Styrene-methyl methacrylate copolymers derived by procedures listed in Table 1

Rate coefficient	Value/10^{-7} s^{-1}	Method
k_M	8.74	(a)
	6.0 (+ 1.0)	(b)
αk_{DM}	51.1 (+ 6.4)	(c)
	47.2 (+ 6.4)	(d)
$k_{MD} + k_D$	13.5 (+ 2.7)	(e)
	15.6 (+ 2.7)	(f)
k_D	6.9 (+ 1.0)	(g)
	6.9 (+ 0.5)	(h)
k_{MD}	7.7 (+ 2.0)	(i)

the absence of 'spectroscopic spacers' and can be associated with species whose kinetic isolation is not solely consequent upon separation from similar chromophores.
(3) Population of excited state monomers by reverse dissociation of excimer does occur in poly(styrene).

Styrene acrylonitrile copolymers

A series of styrene-acrylonitrile copolymers, of composition shown in Table 5 has been the subject of a similar investigation. Results will be reported in full elsewhere[13], and thus only a digest of the work is given here. Thus we can compare the tendency for excimer formation in the styrene-acrylonitrile copolymer series with that of the styrene-methyl methacrylate series. This is hampered by the fact that the two copolymer systems do not show the same function dependence of I_D/I_M upon chain microcomposition. Hence a direct comparison is not possible and simple comparison of the I_D/I_M of two polymers of the same mole fractioon of chromophores is meaningless.

The series may however be compared in two ways.

(i) The styrene-acrylonitrile copolymer sample 1 (cf. Table 5) has an f_s of 0.49 and happens to have a similar I_D/I_M to that of a stryrene-methyl methacrylate copolymer of the same mole fraction (Table 2). Comparison of the values of f_{ss} for the two polymers, however, reveals that for the styrene-acrylonitrile

copolymer f_s = 0.08 (Table 5) whereas for the styrene-methyl methacrylate copolymer f_{ss} = 0.16[12] illustrating the greater facility for excimer formation in the acrylonitrile copolymer series.

Table 5 Styrene-acrylonitrile copolymer microcomposition data[13]

Copolymer	F_s	f_s	f_{ss}	P_{ss}	l_s
1	0.295	0.49	0.08	0.17	1.20
2	0.404	0.55	0.13	0.24	1.32
3	0.434	0.56	0.13	0.23	1.30
4	0.602	0.62	0.24	0.39	1.64
5	0.621	0.63	0.25	0.40	1.65
6	0.739	0.64	0.32	0.51	2.04
7	0.743	0.65	0.32	0.49	1.97
8	0.844	0.69	0.42	0.61	2.58
9	0.882	0.68	0.38	0.56	2.27
10	0.925	0.80	0.62	0.77	4.40

(ii) Alternatively the extent of excimer formation may be compared for two polymers of similar microcomposition. The styrene-acrylonitrile sample 9, f_s = 0.68 (Table 5) has a very similar chain microcomposition to that of the methyl methacrylate analogue of f_s = 0.66 (Table 2). For both polymers f_{ss} = 0.38 yet the value of I_D/I_M exhibited by the styrene-acrylonitrile polymer exceeds that of its methyl methacrylate counterpart by a factor of about 2.5.

Observation such as these demonstrate that the efficiency of excimer emission relative to monomer is enhanced in the acrylonitrile series compared to methyl methacrylate copolymers. Whilst it is very tempting to interpret these trends in terms of reduced steric bulk of of the comonomer enhancing the energy migration or the concentration of trap sites such effects are not the only possible causes of the observed trends. For example, enhanced deactivation of the excited monomeric or dimeric states as a result of differing environments that the chromophores experience in the two copolymeric systems could alter the ratio of I_D/I_M. In principle, fluorescence data obtained under transient excitation conditions can considerably enhance the steady state information and provide further information in the role of the comonomer in controlling the extent to which excimer emission is observed in styrene copolymers. The results obtained

yield values of k_{DM} (scheme 2) of $1.5 \times 10^9\ s^{-1}$, whereas that in the styrene methyl methacrylate system was $5 \times 10^8\ s^{-1}$. k_D by contrast was measured to be $7.0 \times 10^7\ s^{-1}$, very similar to the value in the styrene-methyl methacrylate case. This is as would be expected, since the intrinsic decay of the styrene excimer should not depend upon comonomer. k_{MD} was found here to be $3.9 \times 10^8\ s^{-1}$, considerably larger than that in the styrene-MMA case. Thus both formation and dissociation of styrene excimer are enhanced by copolymerisation with the less bulky acrylonitrile comonomer.

(iii) Styrene-butadiene block copolymers[14]. The polymers identified in Table 6 were studied.

Table 6 Kinetic parameters for Poly(styrene) homopolymers and copolymers

Sample[a]	N_s	A_1	τ_1/ns	A_2	τ_2/ns	$k_{DM}[m]/10^7\ s^{-1}$	$k_D 10^7\ s^{-1}$	$k_{MD}/10^7\ s^{-1}$
H1	15	0.93	1.09	0.044	10.13	83.9	10.1	3.4
H2	16	0.30	1.14	0.004	11.07	83.6	9.1	0.6
H3	17	1.03	0.89	0.015	14.73	106.5	6.8	1.5
H4	23	1.21	0.84	0.006	11.77	115.2	8.5	0.5
H5	27	1.04	0.81	0.011	14.14	118.8	7.1	1.2
H6	168	1.44	0.68	0.011	13.22	142.7	7.6	1.0
H7	1060	1.40	0.72	0.004	13.54	135.0	7.4	0.4
B1	16	0.79	1.34	0.003	11.68	70.7	8.6	0.2
B2	21	1.03	1.02	0.003	12.12	94.1	8.3	0.3
B3	40	0.86	0.80	0.002	13.91	130.4	7.2	0.2
B4	82	1.49	0.81	0.014	11.28	118.5	8.9	1.0
D1	6	0.53	1.51	0.037	11.49	50.7	9.2	3.1
D2	9.5	0.81	1.19	0.009	11.65	79.1	8.6	0.7
D3	21	1.07	1.00	0.031	11.84	93.3	8.6	2.4
D4	25	0.84	0.96	0.050	11.47	95.4	9.0	5.1
D5	45	1.25	0.81	0.021	14.57	118.1	6.9	1.9
D6	96	1.26	0.77	0.008	12.53	125.5	8.0	0.8

[a] H refers to homopolymers, B to single block copolymers of the type SB and D to block copolymers of the type SBSB.
[b] Number of Styrene units in the sequence length. Values listed for D1-D6 are the arithmetic means of the two individual sequence lengths.

Molar mass dependence of rate parameters

Reference to the data presented in Table 6 reveals that the rate coefficients for excimer deactivation by dissociation to monomer, k_{MD}, and by all other photophysical means, k_D, are (within the considerable errors incurred in the analysis) independent of chromophore sequence length.

Figure 5 shows the dependence of the term $k_{DM}[M]$ upon the number of styrene-derived chromophores in a continuous sequence length in the homopolymer, single block copolymer, and dual block copolymer systems. A smooth curve, concave to the molar mass axis, is produced, provided the data for the copolymers containing two styrene sequence lengths are calculated assuming negligible interaction between the separate chromophoric blocks. The general trend in the data compares well with that reported by Ishii et al.[15] for the rate constant for excimer formation in poly(styrene) homopolymers and those reported for steady-state excimer to monomer ratios[15,16,17] a function of styrene sequence length.

The superposition of dual block excimer formation rate data upon those of the homopolymers and single-block species under these conditions emphasizes the negligible influence of long-range interactions (whether of a diffusive or energy-transfer nature) upon the photophysical behaviour. Indeed the lack of involvement of long-range interactions is reinforced by the

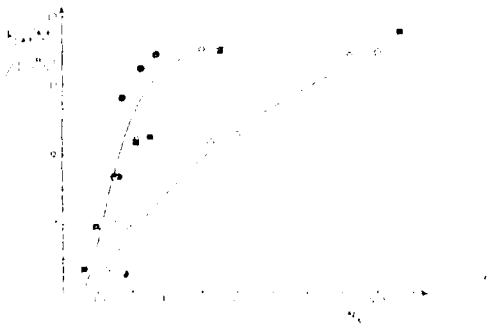

Figure 5 Plot of $k_{DM}[M]$ vs. N_S: (●) homopolymers; (○) block copolymers of type SB; (■) double block copolymers of type SBSB; (◇) double block copolymers, plotted with N_S representing the total number of Styrene units in the polymer.

polymer.
distinct incompatibility of the dual block copolymer data when the overall styrene composition is considered (cf. Figure 5). The derived decay parameters and their molecular weight dependence allow firm conclusions to be reached regarding the nature of the kinetic sites and their mutual interactions.

The kinetic treatment outlined above has assumed that the dual decay parameter combination of $\lambda_{1,2}$ results from the existence of one excited monomeric species that is capable of interacting to form an excimeric state. In this scheme the longer decay time is consequent upon the feedback to excited monomer through excimer dissociation.

The alternative interpretation which would be implied by the suggestions of MacCallum[18,19] that kinetic discrimination is resultant upon differences in compositional environment within the chain may be discounted as discussed below. According to thse arguments the dual-exponential decay in the region of monomer emission would be ascribable to the decay of styryl units located in environments of the type -SSS- and -BSS- i.e., at sequence interiors and termimi, respectively. Furthermore, it is assumed that excimer dissociation to excited monomer does not occur. This model is not consistent with the observed photophysical behaviour for the following reasons.

(1) Intuitively, it could be reasoned that if the differences in kinetic activity of -SSS- and -BSS- are solely the result of reduced probability of excimer formation as a consequence of the 2:1 ratio of potential excimer sites (and modification of rotational mobility by differences in geometric constraints in the two triad situations), the ratio of the two decay times would be much greater than observed. In other words, it would be expected to a first approximation that given a value of ca. 1ns for λ_1 descriptive of -SSS- decay, λ_2 for -BSS- triads would be expected to have a value in the region of 2-3ns (provided k_M k_{DM}). Reference to the decay data of Table 6 for these block copolymers or those reported for homopolymers and random Styrene copolymers reveals that λ_2 in all instances is much greater than λ_1 and of the order of magnitude observed for that of excimer from decay analysis in the spectral region of excimer emission.
(2) Recent work in which the emission of styrene sequences was quenched by intramolecular energy acceptors, discussed below, has shown that not only do two decay rates exist in such a situation but that the long-lived emission is unquenched. Those observations would not be anticipated from the MacCallum model since the ends of sequence styrene chromophores are located adjacent to the energy traps. Consequently, regardless of the mechanism of energy quenching the terminal groups should be subject to severe quenching as a result of considerations of distance and long unquenched lifetime.
(3) The qualitative reasoning presented in (1) and (2)

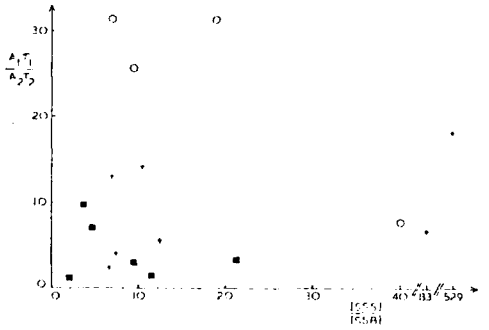

Figure 6 Plot of relative contributions of component 1 to component 2 vs. ratio of mid groups to end groups in the polymer

assessment of the model. If τ_1 and τ_2 are associated with excited states of the type -SSS- and -SSB-, respectively, then the relative contributions to the decay profiles, $A_1\tau_1/A_2\tau_2$, should be directly proportional to the ratio of the number of styrene chromophores situated in -SSS- triads to that in -BSS- triads. The data are presented in Figure 6. It is apparent that the relation between $A_1\tau_1/A_2\tau_2$ and N_{SSS}/N_{SSB} is characterised by an extremely low degree of correlation. Consequently, we have no evidence for the kinetic discrimination between excited monomeric sites in styrene polymers which might be induced by differences in location within the chain.

To summarise, we believe that the dual exponential decays obtained in the region of monomer emission in styrene polymers are not the result of the existence of two excited-state monomeric species distinguished by microcompositional difference but rather a consequence of the existence of two monomeric excited states separated in lifetime through their mode of creation: One state occurs as a result of energy absorption and is quenched by excimer formation. The other excited state is formed upon dissociation of the excimer. Both τ values are averaged quantities representative of the total assemblage of excited-state chromophores within the system.

Following the above discussion it is possible to reconsider the nature of the molar mass dependence of excimer formation in poly(styrene).

Reference to Figure 5 reveals that there are two distinct kinetic regimes. Below ca. 25 styrene units, $k_{DM}[M]$ increases in an almost linear fashion with increasing styrene content. Above ca. 35 styrene units, the function $k_{DM}[M]$ becomes independent of molar mass. Since we have shown that the results are inconsistent with the existence of two kinetically distinct excited monomeric species in these block copolymers, it is

difficult to explain the form of the molecular weight dependence without invoking the concept of energy migration.

The function $k_{DM}[M]$ is a composite term comprising a rate coefficent k_{DM} that will reflect contributions from exciton migration and micro-Brownian rotational motions of the chormophoric groups. The concentration term [M] represents the distribution of potential excimer sites within the diffusion length of exciton. In the low molecular weight range the exciton path length is defined by the chromophore block length and consequently the kinetic behaviour is determined by the concentration of potential excimer sites within the block. The probability of energy trapping by an excimeric site is dictated by the probability of excimer site creation, which, in turn, depends upon the number of chromophore pairs within the block length. Consequently, $k_{DM}[M]$ increases with styrene sequence length.

In the high molecular weight region $k_{DM}[M]$ tends to a constant value, which is indicative that once the styrene sequence length exceeds ca. 35, the probability of energy population of an excimer site is no longer dictated by the number of chromophoric pairs. This implies that the energy is delocalised over an average about 35 styrene units and is limited to this extent by an energy trapping at excimer sites. Similar considerations will apply to the dependence of I_D/I_M upon molecular weight studied in steady-state excitation.

Electronic energy migration in poly(styrene)

The phenomenon of singlet energy migration in aromatic polymers, with trapping at intramolecular low-energy impurity sites, has been the subject of several investigations in recent years. No clear conclusion has been reached concerning the nature of the energy transfer processes. Some authors have suggested that transfer occurs mainly from the monomeric moiety in he polymer, some have favoured a mechanism including successive migration from monomer excimer guest, whilst others have proposed schemes involving transfer from both monomer and excimer.

We have reported in detail results on a poly(styrene) polymer[20] labelled with a copolymerised phenyl oxazole moiety. Results are summarised in Figure 7, and are explicable in terms of the kinetic scheme shown in Scheme 3, where S* is the styrene monomer, D* the styrene excimer, and P* the phenyl oxazole trap. This kinetic scheme may be solved exactly to yield the following forms for the decay of the monomer ($i_S(t)$), excimer ($i_D(t)$) and label ($i_P(t)$):

$$i_S(t) = A_1 \exp(-\lambda_1 t) + A_2 \exp(-\lambda_2 t) \quad (9)$$

$$i_D(t) = A_3[\exp(-\lambda_2 t) - \exp(-\lambda_1 t)] \quad (10)$$

$$i_P(t) = A_4 \exp(-\lambda_1 t) + A_5 \exp(-\lambda_2 t) + A_6 \exp(-\lambda_3 t) \quad (11)$$

where

$$\lambda_{1,2} = 1/2[(X + Y + k_{PS} + k_{PD}) \pm \{(X + k_{PS} - Y - k_{PD})^2 + 4k_{DS}k_{SD}\}^{1/2}] \quad (12)$$

$$X = k_S + k_{DS} \quad (13)$$

$$Y = k_D + k_{SD} \quad (14)$$

$$\lambda_3 = k_P \quad (15)$$

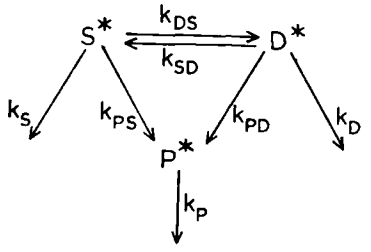

Scheme 3

The pre-exponential factors A_1, A_2, ..., A_7 are complex functions of the individual rate constants in the kinetic scheme together with the initial excited-state concentrations.

The experimentally observed decay profiles recorded at 290 and 425nm (Figure 7) may be associated with the proposed decay functions for S* and P* (equations (9) and (11), respectively). The decay at 325nm will be described by a combination of equations (10) and (11) due to the spectral overlap of excimer and label fluorescence at this wavelength. Thus a triple exponential decay scheme is predicted in good agreement with the observed decay.

From equation (12) it may be shown that:

$$\lambda_1 + \lambda_2 = (X + Y) + k_{PS} + k_{PD} \quad (16)$$

$$\lambda_1\lambda_2 = (X + k_{PS})(Y + k_{PD}) - k_{DS}k_{SD} \quad (17)$$

For poly(styrene), with no POS label, the fluorescence decay may be characterised by two decay parameters λ_1 and λ_2 where:

$$\lambda_1 + \lambda_2 = X + Y \quad (18)$$

$$\lambda_1\lambda_2 = XY - k_{DS}k_{SD} \quad (19)$$

Combinations of equations (16)-(19) with the values of λ_1, λ_2 (from the present work), and k_{DS}, k_{SD}, X, Y (from previous studies above[12], yielded the following values for k_{PS} and k_{PD}:

$$k_{PS} = 3.6 \times 10^8 \ s^{-1}$$

$$k_{PD} = -0.05 \times 10^{8}\ s^{-1} = 0$$

The following conclusions may be drawn from the above results.

(1) Energy transfer does occur from the poly(styrene) polymer to the guest POS moities.
(2) Energy transfer to the guest species from the monomer is more important than from the excimer ($k_{PS} >> k_{PD}$). Time-resolved fluorescence spectra demonstrate, however, that the excimer is involved, in some respect, in the activation of the label, since the excimer lifetime is observed as a component of the POS decay curve. Results from the kinetic analysis ($k_{PS} >> k_{PD}$) would suggest that this is due to reverse dissociation of the excimer to re-form excited monomer which then activates the label, rather than direct excitation of the POS from the excimer.
(3) It is perhaps surprising that energy transfer to the POS label is less favoured from the excimer than from the monomer given the fluorescence decay times and spectral overlap of these species. One possible explanation is that

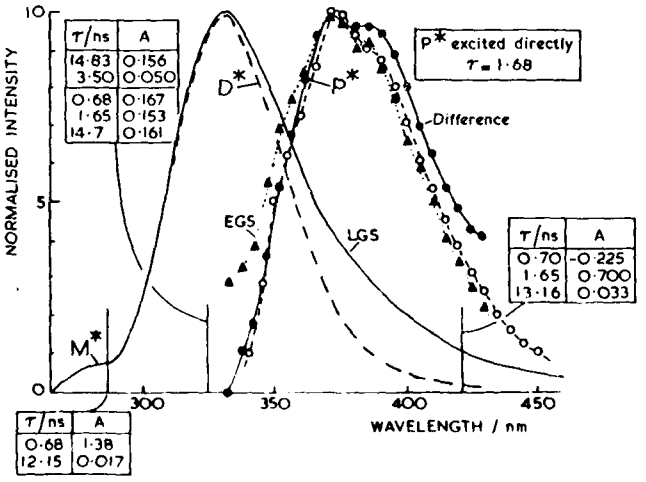

Figure 7 Fluorescence spectra and decay characteristics of POS containing poly(styrene). M*, styrene monomer region, dual decay kinetics. D*, styrene excimer region, triple decay characteristics (double fit shown does not correlate with other wavelengths, thus meaningless). P* is POS fluorescence, triple decay characteristics when styrene excited (see box), but single, τ = 1.68ns when excited directly. EGS is early-gated time-resolved spectrum which matches closely spectrum of D* excited directly, and difference between late-gated spectrum LGS and known spectrum of D*.

the concentration of excimer sites in the polymer is low compared to the monomric chromophores. In this case the high yield of excimer to monomer fluorescence observed for poly(styrene) must imply singlet energy migration in the polymer so that any exciton may have a reasonable probability of encountering a potential excimer-forming site.

(v) Fluorescence anisotropy measurements in poly(styrene)

As outlined above, the time-resolved results obtained on POS labelled poly(styrene) suggest that energy migration perhaps occurs in poly(styrene) in dilute solution. This hypothesis is inconsistent with earlier reports that the fluorescence of poly(styrene) is polarised, even in dilute solution[22,23]. This conflict of opinion has led us to a brief investigation of the steady-state and time-resolved fluorescence of poly(styrene) in dilute solution[24]. Steady-state fluroescence polarisations for poly(styrene)-POS polymers and for poly(styrene) were measured on a Hitachi Perkin-Elmer MPF-4 instrument using HNP'B (Polaroid Corp.) polarisers.

In the two types of experiment (laser excitation and steady-state fluorescence), polarisations were corrected for anisotropy produced by the diffraction gratings of the monomchromator. In the laser experiment, a dilute solution of toluene in dichloromethane was used to determine the instrument bias for polarisation at 335nm. In the steady-state experiments, the correction for anisotropy, which is wavelength dependent, was measured for each experiment. The degree of polarisation is defined by

$$P = \frac{I_{VV} - G.I_{VH}}{I_{VV} + G.I_{VH}} \qquad (20)$$

where $G = I_{HV}/I_{HH}$ is the correction factor for the anisotropy induced by the instrument, and V and H refer respectively to vertical and horizontally polarised excitation or analysing polarisers. As a check in the methods used, the polarisation of an aqueous solution of fluorescein (10^{-5} M, 22°C, pH = 7) was found to be 0.017 + 0.005, in good agreement with published data. Measurements on PS and POS are recorded in Table 7. The following points can be made:

(a) In poly(styrene), excimer emission is completely depolarised.
(b) In the POS polymers, selective excitation of the styrene moiety at 265nm results in complete depolarisation of the excimer emission at 335nm and of the phenyl oxazole trap at 380nm. The small increase in measured polarisation over that in PS itself at 335nm is due to a very small amount of direct excitation of the oxazole moiety in POS polymers (see Figure 7).
(c) Direct excitation of the oxazole moiety at 320nm yields

a measureable polarisation. This is entirely compatible with time-resolved measurements of anisotropy of POS polymers excited with a dye laser at 300nm (Figure 8) which show a decay from an initial value of 0.4 to zero. This is compatible with segmental motion of the polymer causing time-dependent depolarisation when the trap is excited directly. Following excitation of the styrene moiety however, the time-dependences of oxazole trap fluorescence polarised parallel and perpendicular to excitation radiation, on a time-scale longer than 200ps, were

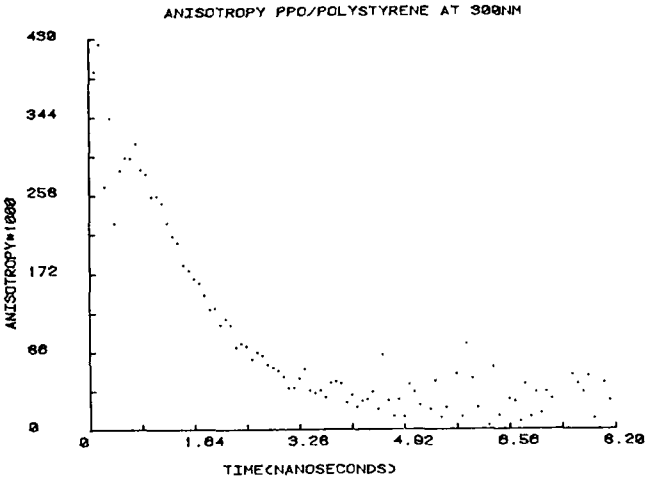

Figure 8 Time-resolved anisotropy, $r(t)[I_{\parallel}(t) - I_{\perp}(t)]/[I_{\parallel}(t) + 2I_{\perp}(t)]$ for poly(styrene) with POS label; label excited directly at 300nm.

identical, in agreement with observation of total depolarisation in the steady-state experiments[25].

These results are then in good agreement with those of Gupta et al[26], but directly contradict those of MacCullum[22,23]. We do however feel that in view of the inconsistencies in published data to date by this author, which were not commented upon; and the agreement here between time-resolved and steady-state measurements in the present experiments, the results here are correct, and establish with some certainty that under the conditions of our experiments, electronic energy transfer does indeed occur in poly(styrene).

Table 7 Degree of fluorescence polarisation in poly(styrene) solutions[24]

Method	Sample	λexc./nm	λem/nm	P
Laser	PS	257.25	335	0.005 + 0.050
Steady-state	PS	265	335	0.005 + 0.020
Steady-state	POS (0.058%)	265	335	-0.006 + 0.020
	POS (0.11%)	265	335	0.026 + 0.020
	POS (0.504%)	265	335	0.027 + 0.020
Steady-state	POS (0.058%)	265	380	0.040 + 0.020
	POS (0.11%)	265	380	0.047 + 0.020
	POS (0.504%)	265	380	0.048 + 0.020
Steady-state	POS (0.058%)	320	380	0.135 + 0.020
	POS (0.11%)	320	380	0.134 + 0.020
	POS (0.504%)	320	380	0.144 + 0.020

4. *Model compound studies*

In elegant work, DeSchryver and co-workers have explained the observation of complex kinetics of fluorescence decay observed in vinyl aromatic polymer in terms of emission from racemic and meso stereo-isomers of 2,4-disubstituted pentane model compounds. We have recently begun a programme of work on simpler models. 1,-3 di-aromatic substituted propanes. We recognise that these are not ideal models for polymers since they do not have asymmetrically substituted carbon atoms, but, since they represent the simplest possible linked systems capable of excimer formation, we wished to study them in the same detail as the polymers. The compounds studied, αα dinaphthyl propane I, αβ -dinaphthyl propane II, and ββ dinaphthyl propane III were subjected to preliminary investigation in dilute solutions in tetrahydrofuran (THF) and methylene chloride (CH_2Cl_2). Steady-state spectra are shown in Figure 9[21].

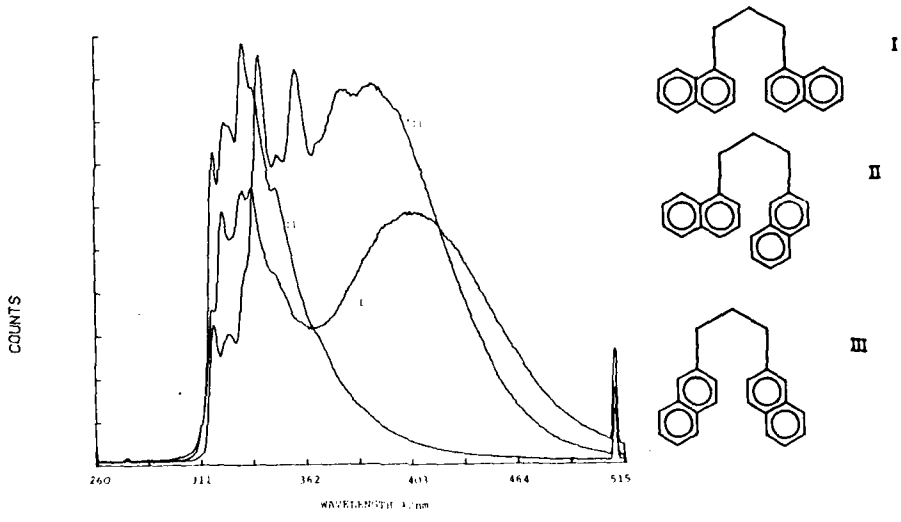

Figure 9 Steady-state fluorescence spectra for I, II and III in dichloromethane solution

Extensive measurements of fluorescence decays shows the following features:

(1) I in the THF obeys Birk's kinetics (Scheme 1) perfectly (see Table 8) for excitaton at 300nm.
(2) I in CH_2Cl_2 displays very complex kinetics for excitation at 257.25 or 300nm, with two-component fits generally incapable of reproducing experimental decay curves (Table 8).
(3) II in THF exhibits a single extremely long-lived (τ > 100ns) component. In CH_2Cl_2 at 300nm excitation this is

reduced to ~ 13.8ns. For 257.25nm excitation in CH_2Cl_2 kinetics become more complex.
(4) III in THF displays complex kinetics, with the 100ns decay time observed in II prominent.
(5) III in CH_2Cl_2 at both excitation wavelengths exhibited very complex kinetics (not shown in Table 8).

It is clear that the excimer formation and decay in these simple systems is very complex, and much further work will be required to gain a thorough understanding of the process involved. This work is currently in progress.

We have also reported briefly on the photophysics of poly-N (9-carbazolyl) carbonyl-L-lysine (PKL), a conformationally 'pure' polymer[28].

Table 8 Decay characteristics[a] of model compounds I, II and III in solution[21]

Compound	λ_{ex}[a] (nm)	λ_{em}[c] (nm)	Solvent	A_1	τ_1 (ns)	A_2	τ_2 (ns)	A_3	τ_3 (ns)	χ^{2d}	DW[e]
I	300	345	THF	0.97	15.8	0.10	39.4	-	-	1.26	1.86
I	300	450	THF	-2.49	16.0	2.58	38.0	-	-	1.41	2.1
I	300	320	CH_2Cl_2	1.38	6.20	0.17	13.20	-	-	1.22	1.69
I	300	450	CH_2Cl_2	-2.3	6.69	2.48	25.24	-	-	1.39	1.67
I	257.25	320	CH_2Cl_2	0.25	6.05	0.033	11.66	-	-	1.12	1.86
I	257.25	450	CH_2Cl_2	-0.25	7.03	0.30	29.01	-	-	1.34	1.91
I	257.25	320	CH_2Cl_2	0.25	6.54	0.013	14.41	0.07	1.08	1.04	2.02
II	300	345	THF	0.41	100.75	-	-	-	-	1.11	1.95
II	300	350	CH_2Cl_2	1.50	13.78	-	-	-	-	1.10	1.67
II	257.25	350	CH_2Cl_2	0.20	13.5	0.05	-	-	-	1.09	2.15
III	300	345	THF	0.91	5.6	0.02	100.9	0.03	37.63	1.2	1.96
III	300	450	THF	-0.78	5.1	0.62	100.3	0.3	36.2	1.76	2.05
III	257.25	310	CH_2Cl_2	0.38	3.33	0.009	33.25	-	-	1.17	2.12
III	257.25	450	CH_2Cl_2	-0.19	2.49	0.12	60.78	0.09	18.40	1.31	2.21

[a] Decay curves fitted to functions of the form $I(t) = \Sigma A_i \exp(-t/\tau_i)$.
[b] Excitation wavelength.
[c] Emission wavelength 300-350nm corresponds largely to monomer region, 450nm to excimer region.
[d] and [e] Fitting parameters, cf. Reference 1.

5. Time-dependent fluorescence anisotropy measurements

The methods used to measure time-dependent fluorescence anisotropy in poly(styrene) discuused above are outlined below. It should be stressed that these methods are not trivial, and great thought has been given to accurate measurements[29,30]. The methods are outlined fully in Appendix 2, and will not be repeated here. The time-dependence of the anisotropy r(t) is defined below, and can in principle be used to monitor molecular

$$r(t) = (I_{//}(t) - I_{\perp}(t))/I_{//}(t) + 2I_{\perp}(t) \qquad (21)$$

$$= r_o \sum_i a_i e^{-t/\tau_i} \qquad (22)$$

motion. At the outset of this work, a study of the literature revealed many unsatisfactory features. There appeared to be no general agreement upon how properly to carry out the experiment, and interpretation was difficult. Much of the work described here consists of a critical evaluation of methods and applications to two polymers systems in solution, poly(methyl methacrylate) PMMA covalently labelled with poly(1-vinyl naphthalene) and poly(acenaphthylene) respectively. Anisotropy is a more useful parameter than degree of polarisation in defining order and motion in molecular systems in that for fluorophore which decays exponentially with a single component.

The resulting anisotropy constructed from independent measurements of the fluorescence parallel $I_{//}(t)$ and perpendicular $I_{\perp}(t)$ to the plane of polarisation of excitation radiation is <u>independent</u> of the decay time of the fluorophore. For systems which decay with dual (or more) components this is not necessarily the case, although it would be if the <u>motional</u> properties of the two fluorophores giving rise to the two decay components were identical. Since there is no a priori way of ascertaining this, it seems prudent to employ fluorophores which are indeed single component. To assist in this a critical evaluation of the decay of standard substances which can be used to test single or dual exponentiality has been carried out[31].

Details of time-resolved anisotropy can also be obtained by deconvolution of individual $I_{//}(t)$ or $I_{\perp}(t)$ measurements, or difference measurements defined below

$$I_{//}(t) = e^{-t/\tau_F}(1 + 2r_o \sum_i a_i e^{-t/\tau_i}) \qquad (23)$$

$$I_{\perp}(t) = e^{-t/\tau_F}(1 - r_o \sum_i a_i e^{-t/\tau_i}) \qquad (24)$$

$$I_{//}(t) - I_{\perp}(t) = 3r_o e^{-t/\tau_F}(r_o \sum_i a_i e^{-t/\tau_i}) \qquad (25)$$

In these cases analysis of $I_{//}(t)$ and $I_{\perp}(t)$ are weighted, as usual, by Poisson statistics ($w_i = I_i^{-1}$). Fits of $I_{//} - I_{\perp}$ and

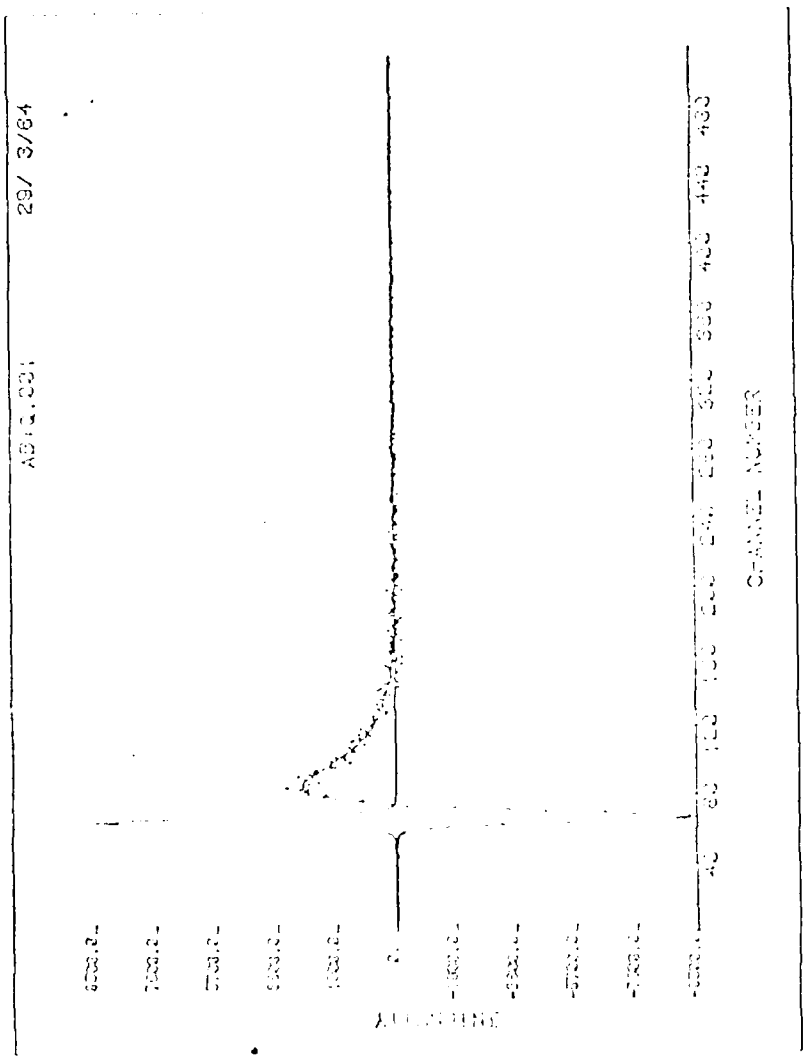

Figure 10 Plot of r(t) (see text) for perylene in glycerol. Channel number vs linear in time.

Table IV. Pre-exponential factors obtained for the decay of fluorescence anisotropy in perylene

$$r(t) = r_1 e^{-t/t_1} + r_2 e^{-t/t_2}$$

Study	λ_{ex}	r_1	r_2	t_2/t_1	$r_{(t=0)} = r_1 + r_2$
'limiting case'		0.10	+0.30	3.0	+0.40
($\zeta_{AE} = 0°$)					
Barkley et al	436 nm	0.10	+0.23	2.3	+0.33
Lakowicz et al	366 nm	0.13	+0.19	1.6	+0.32
Shinitsky et al	370 nm	temperature dependent coefficients			
'limiting case'		0.10	+0.30	3.0	+0.40
($\zeta_{AE} = 90°$)					
Barkley et al	370 nm	0.10	−0.23	−2.3	−0.13
this study	254 nm	0.077	−0.232	−3.0	−0.155

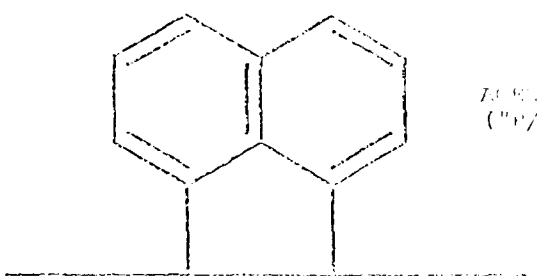

[illegible]
("perylene")

IV

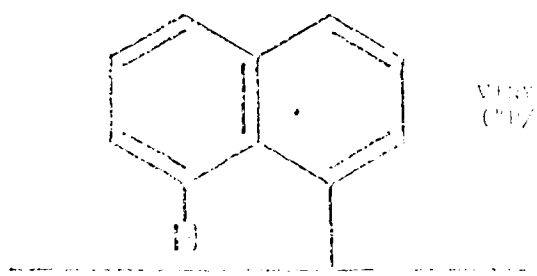

[illegible]
("perylene")

V

r(t) must propogate these Poisson weightings into the proper fitting functions. Thus for

$$I_{\parallel}(t) - I_{\perp}(t),\ w_i = (I_{\parallel} + I_{\perp})^{-1} \qquad (36)$$

and for r(t), $w_i = 3(I_{\parallel} + 2I_{\perp})/(2 + r + 5r^2 - 2r^3)$ (37)

These correct fittings are not universally employed in the literature, but are essential. Techniques are described in a chapter of a book published recently[11].

As an example of the use of these methods in extracting multiple components of anisotropy decay, we have carried out a complete study on the molecule perylene in the viscous medium, glycerol/water mixtures[29,30]. A typical experimental result is shown in Figure 10, from which it can be seen that the anisotropy decay is two-component, beginning with a large negative value, and becoming positive before decaying to zero. The initial negative value is due to the fact that in this sample the excitation is to the second excited singlet state, emission being from the lowest singlet, for which the electronic transition moment is approximately orthogonal. Diffusion coefficients and preexponential factors derived from this work, which is described more fully in Appendix 2, are shown in Tables 9 and 10.

Table 9. The Principal diffusion coefficients of Perylene in Glycerol/water solution at 25°C. λ^3_{ex} = 257 nm.

Solution composition (%/V)	Viscosity (centipoise)	D_1 (10^7 sec^{-1})	D_2 (10^7 sec^{-1})	D_1/D_2
[illegible]	0.[illegible]	7.0 ± 1.0	3.7 ± 0.[illegible]	2.0 ± 1.4
[illegible]	111.1	4.9 ± 0.5	2.7 ± 2	0.[illegible] ± 1.1
[illegible]	200.[illegible]	2.7 ± 0.1	18 ± 1	0.2 ± 0.[illegible]
				ave =
				0.[illegible] ± 0.[illegible]

(iii) Polyvinyl naphthalene and ethers thereof

The methods described in the above and in Appendix 2 have been used to study segmental relaxation in poly(vinyl acetate) and poly(methyl methacrylate) labelled with copolymerized acenaphthalene and vinyl naphthalene, structures IV and V below)[25,32,33]. Results are summarized in Tables III-V.

The polymers used in this study were of sufficiently high molecular weight, that their rotational tumbling motions, under the conditions considered, can be assumed to occur on the 10^{-6} second time scale. Thus the magnitude of the rotational

correlation times given in Tables 11 to 15 indicate that segmental motions are responsible for depolarising the fluorescence. Consequently these time constants (τ_{rpt}) are not, infact true rotational correlation times since

$$\frac{1}{\tau_{Rot}} = \frac{1}{\tau_{seg}} + \frac{1}{\tau_{mac}} \qquad (28)$$

where τ_{seg} is the segmental rotational correlation time and τ_{mac} the rotational correlation time for the motion of the entire polymer, however, as the polymers used were of high molecular weights, it is possible to ignore the contribution from the τ_{mac} term, that is

$$\tau_{Rot} \simeq \tau_{seg} \qquad (29)$$

Table 11 Summary of the anisotropy and fluorescence decay parameters for PMMA/ACE in dichloromethane at the temperatures considered

T /K	τ_F /ns	r_o	τ_{Rot} /ns
295 + 2	15.5 + 0.1	0.13 + 0.01	1.3 + 0.1
275 + 2	15.7 + 0.1	0.13 + 0.01	2.2 + 0.2
260 + 2	15.4 + 0.2	0.13 + 0.01	3.2 + 0.5
245 + 2	15.5 + 0.2	0.13 + 0.01	4.5 + 0.7
230 + 2	15.6 + 0.1	0.11 + 0.02	5.6 + 0.7

Table 12 Summary of the anisotropy and fluorescence decay parameters for PMMA/1-VN in dichloromethane at the temperatures considered

T /K	τ_F /ns	r_o	τ_{Rot} /ns
295 + 2	15.9 + 0.2	0.15 + 0.01	1.3 + 0.2
275 + 2	15.6 + 0.2	0.16 + 0.01	2.2 + 0.5
260 + 2	15.5 + 0.1	0.14 + 0.01	2.7 + 0.3
245 + 2	15.4 + 0.1	0.15 + 0.01	3.6 + 0.5
230 + 2	15.4 + 0.1	0.16 + 0.01	4.9 + 0.7

Table 13 Sumamry of the anisotropy and fluorescence decay parameters for PMA/ACE in dichloromethane at the temperatures considered

T /K	τ_F /ns	r_o	τ_{Rot} /ns
295 + 2	17.4 + 0.2	0.10 + 0.01	0.8 + 0.3
260 + 2	17.4 + 0.3	0.10 + 0.01	1.3 + 0.2
245 + 2	17.4 + 0.3	0.11 + 0.01	1.8 + 0.3
230 + 2	17.5 + 0.3	0.12 + 0.02	2.5 + 0.3

Table 14 Summary of the anisotropy and fluorescence decay parameters for PMA/1-VN in dichloromethane at the temperatures considered

T /K	τ_F /ns	r_o	τ_{Rot} /ns
295 + 2	15.1 + 0.1	0.13 + 0.01	0.5 + 0.1
275 + 2	14.9 + 0.1	0.13 + 0.01	0.8 + 0.1
260 + 2	14.8 + 0.1	0.14 + 0.01	1.0 + 0.2
245 + 2	14.9 + 0.1	0.14 + 0.01	1.3 + 0.2
230 + 2	14.9 + 0.1	0.15 + 0.01	1.7 + 0.3

The 1-vinyl naphthalene chromophore, unlike the acenaphthalene chromophore, is capable of motion independent of the polymer backbone. It is rather surprising that the anisotropy decay for the 1-vinyl naphthalene labelled polymers takes the same form as the anisotropy decay of the acenaphthalene labelled polymers. It is even more surprising that rotational correlation time a 1-vinyl naphthalene labelled polymer, at a given temperature is within experimental error equal to the rotational correlation time of the corresponding acenaphthylene labelled polymer. There are three possible, not necessarily exclusive, explanations:

a) The independent motions of the chromophore are too fast to detect. The effect of such motions is to lead to evaluations for the initial anisotropies which are too low. However as the initial anisotropies obtained for he polymers used in this study are in excellent agreement with values

Table 15 Summary of the activation energies for the segmental rotations and conformational changes labelled poly(methyl methacrylate) and poly(methyl acrylate) in dichloromethane

Polymer	Activation energy for segmental motion (E_{seg}) KJ mol^{-1}	Activation energy for conformational changes (E_{con} KJ mol^{-1}
ACE/PMMA	13 ± 4	5 ± 4
1-VN/PMMA	12 ± 2	4 ± 2
'PMMA'	12 ± 3	4 ± 3
ACE/PMA	9 ± 4	1 ± 4
1-VN/PMA	10 ± 2	2 ± 2
'PMA'	11 ± 3	3 ± 3

quoted for similar polymers in rigid glasses at 77K this is not thought to be the correct explanation.

b) The rotational correlation times for the segmental motions and the independent motions or the 1-vinyl naphthalene chromophores are sufficiently similar, over the temperature range considered, to be irresolvable.

c) The 1-vinyl naphthalene chromophores are prevented from performing any rotational motions independent of the polymer backbones due to steric hindrances. It is felt that the steric hindrances required to completely eliminate all independent motions are not present in the polymers considered.

d) The fluorescence polarisation properties of the 1-vinyl naphthalene chromophore are explained in terms of two emitting transition dipoles. These transition dipoles are aligned parallel and perpendicular to the bond about which the chromophore undergoes independent motion of the polymer backbone.

Rotation about this bond can not lead to these two transition dipoles interchanging their directions relative to the polymer backbone, for example, the chromophore cannot rotate into a position where the long axis polarised transition moment is perpendicular to the polymer backbone. Consequently for the 1-vinyl naphthalene labelled polymers, as with the acenaphthylene labelled polymers, it is only segmental motions which lead to depolarisation. This explanation does not take into account any 'rocking' motions of the 1-vinyl naphthalene molecule which would lead to fluorescence depolarisation. It is thus thought that the latter is the correct explanation with, perhaps, steric effects preventing the rocking motions.

Table 16 Comparison of values for the conformational activation energy for segmental motion and the rotational correlation time at 298K for poly(methyl methacrylate) quoted by various sources

Reference/ authors	Technique	τ_{Rot} (at 295K) 10^{-9} sec	Solvent	E_n KJ mol^{-1}	E_{seg} KJ mol^{-1}	E_{con} KJ mol^{-1}
Bullock et al [34]	esr. Polymer labelled at random ester groups along the chain	0.36	Toluene	9	20 + 1	11 + 1
A.M. North [35]	Dielectric relaxation	1.4	Toluene	9	27	18
A.M. North and I. Soutar [36]	Time resolved fluorescence anisotropy measurements Polymer labelled with 9-vinylanthracene chromophore	1.3	Toluene	9	-	-
G.J. Kettle and I. Soutar [37]	Steady state anisotropy measurements Polymer labelled with ACE and 1-VN chromophores	1.3 + 0.2	Toluene	9	-	-
This study [32,33]	Time resolved fluorescence anisotropy measurements Polymer labelled with ACE and 1-VN chromophores	1.3 + 0.1*	Dichloro-methane	8.2	12 + 3	4 + 3

* Measurement made at 295K

Table 17 Comparison of values for the conformational activation energy and the rotational correlation time at 298K for(methyl acrylate) quoted by various sources

Reference/ authors	Technique	τ_{Rot} (at 295K) 10^{-9} sec	Solvent	E_n KJ mol^{-1}	E_{se} KJ mol^{-1}	E_{con} KJ mol^{-1}
Bullock et al [34]	as in Table 16	-	Toluene	9	19 + 3	10 + 3
A.M. North [35]	as in Table 16	0.03	Toluene	9	23	14
A.M. North and I. Soutar [36]	as in Table 16	0.6	Toluene	9	-	-
This study	as in Table 16	0.6	Dich-chloro-methane	8.2	11 + 3	3 + 3

For each polymer sample the activation energy for segmental motion was evaluated from a linear regression of ln τ_{Rot} on 1/T. Results are summarised in Tables 16 and 17, and compared with literature values.

The activation energy for segmental rotation (E_{seg}) is dependent upon:

a) The activation energy for the conformational changes required for segmental motion (E_{con}).
b) The activation energy for viscous flow of the solvent (E_η).

The relative contributions of the above to the segmental (total) activatoin energy has been treated theoretically, the basis of which was Kramer's theory for the diffusion of a particle over a potential barrier, by Helfand. The rate constant (R) for segmental motion, or the rate at which substituent groups on a polymer backbone diffuse over a potential barrier, was found to be given by:

$$k = [\gamma/12\pi^2 a\eta][1/2 + (1/4 + m\gamma/(6\pi a\eta)^2)^{1/2}]^{-1} \exp(-E_{con}/RT) \quad (30)$$

where γ is the force constant for the potential barrier, m the mass of the particle, a the hydrodynamic radius of the particle and η is the viscosity of the solvent. In the limit of high viscous damping, that is when

$$1/4 >> \frac{m\gamma}{(6\pi a\eta)^2} \quad (31)$$

Equation (30) simplifies to

$$k = \gamma/(12\pi^2 a\eta) \exp(-E_{seg}/RT) \quad (32)$$

If an Arrhenius dependence of η upon temperature is assumed then equation (32) takes the form

$$k = c \exp[-(E_{con} + E_\eta)/RT] \quad (33)$$

where C is a constant. Thus the total activation energy for rotational motion is simply (in the limit of high viscous damping) the sum of the activation energies for segmental motion and viscous flow:

$$E_{seg} = E_{con} + E_\eta \quad (34)$$

It should be noted that there are two cases where the above treatment can <u>not</u> be used to remove the effect of the solvent:

a) If the solvating power of the solvent changes significantly with temperature. Non-linear Arrhenius plots of the segmental rotational correlation times of high

molecular weight poly(styrene) in cyclohexane, for example, is attributed to the increasing solvent power of cyclohexane with increasing temperature. If the solvent power of a solvent does change with temperature then as the temperature is reduced polymer-solvent interactions decrease resulting in the polymer chain adopting a more tightly-coiled conformation. This leads to an increase in the intra-chain steric interactions which oppose segmental motion and hence the segmental rotational correlation times are greater than expected.

b) If activation energies for conformational changes of a polymer in different solvents are compared they may not necessarily be the same. In different solvents polymers adopt different conformations depending on the relative magnitudes of the polymer-polymer and polymer-solvent interactions. In thermodynamically 'poor' solvents a polymer will adopt a tightly coiled configuration (due to the dominance of the polymer-polymer interactions), whereas in 'good' solvents they fully extended. Consequently intra-molecular steric interactions are greater in 'poor' solvents and so higher activation energies for conformational changes, as compared to those in 'good' solvents, are observed.

A linear regression of $\ln(1/\zeta)$ on $(1/T)$, gave a value of 8.2 KJ mol^{-1} for the activation energy for viscous flow of dichloromethane. This value enabled, by application of equation (34), the activation energies for conformational changes required for segmental motion to be evaluated (see Table 17) from the activation energies for segmental motion. It is clear from Table 17 that for both poly(methyl methacrylate) and poly(methyl acrylate) segmental motion is, to a high degree, solvent controlled; the activation energy for viscous flow represents approximately 70% of the segmental (total) activation energies. Consequently the activation energies for the conformational changes (approximately 30% of the total activation energy) are of the same magnitude as the associated errors. As no error was assumed to be associated with the value for the activation energy for viscous flow the errors, for a given sample, on the segmental and conformational activation energies are identical.

Table 16 compares the values obtained in this study for the rotational correlation times at 298K and the activation energy for conformational changes required for segmental motion of poly(methyl methacrylate) and poly(methylacrylate) respectively with values quoted by other groups[34-36]. (In all cases the polymers used were of sufficiently high molecular weights so that the 'observed' segmental motions were independent of molecular weight). Dilute solutions of the polymers were used in order to minimise inter-chain interactions. It should be realised that:

a) The segmental rotational correlation times of a given polymer in the two solvents may not be directly compared. However rotational correlation times of a polymer in toluene obtained by the different techniques (e.s.r., dielectric

relaxation and fluorescence depolarisation) it is possible to discern whether the different techniques are 'sensing' the same segmental motions.
b) Dichloromethane and toluene are thermodynamically 'good' solvents for poly(methyl methacrylate) and poly(methylacrylate). Consequently, in these solvents poly(methyl methacrylate) and poly(methylacrylate) adopt fully extended conformations. The conformational changes required for segmental motions and hence the activation energy for conformational changes should be approximately the same.

It is felt that the two techniques are sensing different motions and that the agreement on the value for the rotational correlation time at 298K (in toluene) is coincidental. To a certain extent the results from the experiments on poly(methylacrylate) substantiate this explanation. It is rather surprising that these two techniques give such differing results as, in this particular instance, they are extremely similar. In the dielectric relaxation experiments the motion of electronic dipoles residing on the ester carbonyl groups are monitored; these dipoles have components parallel and perpendicular to the polymer backbone. This situation can be seen to be directly analogous to the fluorescence anisotropy experiments carried out in this study.

Poly(methyl methacrylate)

The values for the rotational correlation times at 298K for this polymer in toluene from fluorescence anisotropy (both steady state and time-resolved) and dielectric relaxation measurements are in excellent agreement. It can thus be concluded that:

a) The two techniques, in this particular example, are 'sensing' the same motion in the fluorescence anisotropy experiments.
b) The segmental flexibility of poly(methyl methacrylate) was not influenced by the presence of anthracene, acenaphthylene or 1-vinyl naphthalene probes. The dielectric relaxation experiments did not require the polymer to be labelled). The rotational correlation time obtained by e.s.r. spectroscopy is an order of magnitude less than the dielectric relaxation/
fluorescence relaxation value. This disagreement is attributed to a rapid rotation of the spin label (a piperidinyl ring) about either the bond between the ester carbon and the oxygen atom (to which the label is attached) or between the oxygen atom and the spin label in addition to the segmental motion. The activation energy for the conformational changes evaluated by this technique (in this particular example) must be considered to be in error.

It is unexpected after the agreement on the value for the rotational correlation times at 298K in toluene that the

dielectric relaxation and fluorescence anisotropy techniques give such different values for the activation energy for the conformational changes required for segmental motion. There are three possible explanations:

a) The two techniques are monitoring different segmental motions.
b) The presence of the fluorescent probes modify the segmental motion. (It should be remembered that the acenaphylene probe is capable of motion independent of the polymer backbone whereas although the 1-vinyl naphthalene probe is capable of independent motions these motions do not lead to depolarisation of the fluorescence). The effect of the probes would tend to increase the activation energy required for the conformational changes due to the extra energy required to overcome the effect of solvent drag on the fluorophores. Even if the polymer adopted a different conformation in the vicinity of the probes to accomodate their presence it is not conceivable that this would lead to such a large decrease in the value for the activation energy.
c) The fluorimeter and analysis procedures used could not accurately resolve the rotational correlation times. This interesting but clearly controversial and unresolved feature of the work is currently being studied further.

6. Poly(diacetylenes)

Although not specified in the original proposal, these one-dimensional polymers are of such current interest, the work below was undertaken in collaboration with Professor D. Bloor, Queen Mary College, London.

The aim of this part of the project was to establish the nature, dynamics and decay of excitons in poly(diacetylenes). Little work (both experimentally and theroretically) had appeared concerning the behaviour of excitons in conjugated polymers. This knowledge is an important factor in a proper understanding of the interaction of free carriers and excitons, which have been shown in other materials to form bound states.

The project this necessitated experimentation to elucidate the conformation of PDA chains using light scattering, nmr spectroscopy, Raman spectroscopy; and then separate measurements of fluorescence decay measurements. The PDA backbone VI has in the ground state a conjugated π-bond structure, the absorption of which is excitonic in character.

$$\{RC - C \equiv C - CR'\}_n \qquad VI$$

9PA R = R' = $- (CH_2)_9 - OCO - CH_2$; 2 MTHF = 2 methyl tetrahydrofuran

4BCMU R = R' = $- (CH_2)_4 - OCO\ NH\ OCOC_4H_9$

Macroscopic single crystals of PDA fluoresce only weakly, but deformed systems have been shown to fluoresce. Thus PDA solutions and films have fluroescence yields in the range 0.001 - 0.003, and absorption spectra in the range 1.6 to 2.5 eV, depending upon the degree of disorder. Absorption and fluorescence spectra, from this work are discussed below in terms of the chromism observed. The two systems studied were 9PA, and 4BCMU with R groups defined as above.

Experimental observations

Low temperature PDA glasses

Rapidly freezing yellow 9PA/2MTHF or 4BCMU/2MTHF [38,39,40] solutions (Y-phase) results in a clear glass with a pink colour at 77K (R_Y-phase) - (refer to Scheme 4 below). Cycling the glass to R.T and requenching produces different low-temperature spectra depending on the dwell-time at R.T. If the dwell-time is short the solution remains pink (R-phase) and on quenching yields ths spectra in the R_R-phase. If the dwell-time is long or if the solution is warmed to the Y-phase, then on quenching to 77K, we obtain once again the R_Y-phase spectra. Spectra are shown in Figure 11.

Scheme 4 Temperature dependence for 9PA and 4BCMU in 2MTHF

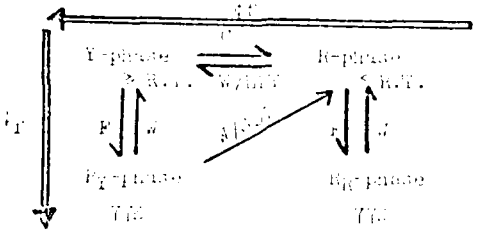

C: cool F: freeze W: warm SDT: short dwell-time LDT: long dwell time R.T: toom temperature increasing quantum yield ($_f$).

9PA glasses

The 77K spectra are consistent with an acetylenic polymer backbone structure. At least distinct species can be identified by studying these spectra with emission and absorption band origins at approximately

a) 519 and 514nm
b) 595 and 535nm
c) 610 and 560nm

respectively. The total fluorescence spectra of 9PA are more intense at 77K than at R.T.; the increase being approximately 100 fold. On quenching the R-phase the population of the third species (c) is drastically enhanced whilst the population of (b) is drastically reduced. It appears that species (c) are apparently created at the expense of the other two species. To explain the spectra of these conformations a small local deformation in the form of twisting about the C=C in the excited state is proposed. Locked-in conformations give rise to small Stokes shifted (long-lived) species (a). Those conformations involving large Stokes shifts (short-lived) species arises as a consequence of twisting of the C=C in the excited state. Time-resolved measurments will be discussed later.

4BCMU glasses

Whereas the 9PA R_R spectra are structured with well developed vibronic sidebands with shifts from the zero-photon (Z-P) peak of about 1500 and 2100 cm^{-1} characteristic of the C=C and C+C stretching modes of the acetylenic polymer backbone structure, the 4BCMU spectra are less structured. This makes it difficult to indentify zero-phonon bands. An analysis of the R.T. spectra indicates the presence of at least two species with emission and absorption bands occuring at 515 and 510nm, and 550 and 530nm respectively. The former species exhibit narrow

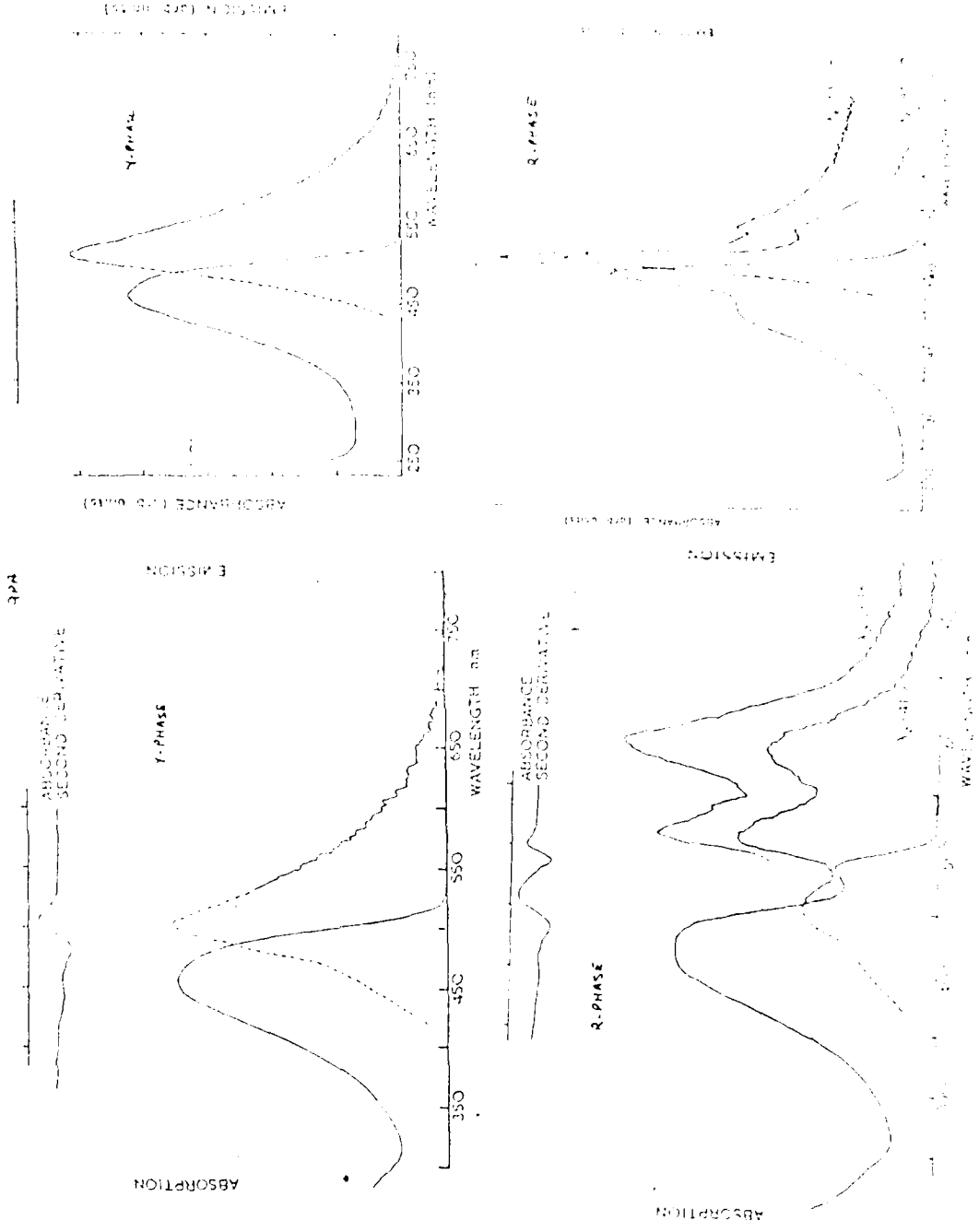

Figure 11 Absorption and emission spectra of PDA's vibronic emission when the excitation is in the region of the Y-P peak (510-520nm). At 77K this effect is very weak for 9PA; but similar effects have been seen for 9PA glasses at 4K. This superposition suggests that there is no fast energy transfer between the polymer species responsible for these emissions.

Comparison

The essential differences between 9PA and 4BCMU are:

i) The number of methylene groups - 9PA has 9 adjacent to the backbone whilst 4BCMU has 4.
ii) 4BCMU is able to establish hydrogen bonds between the sidegroups parallel to the main chain.

Figure 4 of Appendix III shows the emission spectra of the B_V and B_B phases for two different concentrations. One can immediately notice the presence of a sharp peak around 515nm for 4BCMU and 519nm for 9PA and presence of vibrational features for 9PA spectra in both the B_V and B_B phases in the low energy regions. By contrast the 4BCMU spectra are more blue-shifted; the emission arising from the second species being very weak indeed. This again suggests that the degree of order established in 4BCMU is higher than that in 9PA since we expect a decrease in fluorescence quantum yield with order; i.e. the precursor responsible for the 515/519nm emission has a higher quantum yield than that responsible for the redder emission(s). At this stage it is difficult to identify the nature of the 515/519nm emitting species which seems to show very little energy transfer to the longer segments and exhibiting narrow vibronic emission at 77K in 4BCMU and at 4K in 9PA. There are several possibilities for this precursor. These include chain ends, non-planar conformations, for example, cis-helix or a buckled trans-conformation locked-in by sidegroup interactions, and interchain contacts. Further experiments are in hand to try to distinguish between these possibilties.

The nature of the chromism in PDA's

Soluble PDA's with urethane containing sidegroups are known to display a visual batho-chromic shift when conditions are altered to favour the formation of hydrogen bonds between the sidegroups (parallel to the main chain). This effect was attributed to a conformational change of the backbone in terms of the extent of delocalisation of the -bond[40,41]. A concept of effective conjugated length was invoked by Chance and coworkers and others[42-45] to explain this effect. The blue-shifted species is thought to be a distribution of short conjugated segments. Chromism is achieved by either cooling or adding a poor or non-solvent to a solution in good solvent or increasing the concentration of the polymer. In the case of water-soluble PDA's, pH changes favour the formation of COOH terminal groups and the establishment of hydrogen bonds[46]. The formation of hydrogen bonds was identified by others as the essential driving force behind such a transition from a random coil to an extended, rigid-rod conformation which was proposed to account for the change in the absorption spectrum. However our investigations on the soluble PDA discussed above, 9PA (containing long parafinic sequences in their sidegroups) show that this material also exhibits chromism. Unlike the urethane containing sidegroups the sidegroups of 9PA do not interact strongly through hydrogen bond

[illegible] ... more general phenomenon ... still require the formation of ... bond between ... [illegible] ... Eckhardt et al., however, ... [illegible] ... remains to be established.

Backbone-driven processes

An evaluation of literature data on PDA's having [illegible] groups ([illegible]'s) adjacent to the polymer backbone with various morphologies suggests that there are specific configurations of the polymer backbone in different environmental conditions. For PDA solutions, for instance, the absorption maxima tend to occur in the range of 460 ± 10nm (Y phase). Depending on the number of methylenes adjacent to the backbone the absorption maxima for solution cast films, Langmuir-Blodgett films and red/blue 'solutions' tend to be in the range of [illegible] ± 10nm (R phase) and 6[illegible] ± 10nm (B phase). The former range corresponds primarily to more than [illegible]'s and the latter to [illegible]'s adjacent to the main chain. As polymerised crystals tend to show an absorption maximum in the B region; but depending on the strain imposed on the backbone they can also adopt any value in the range 520-760nm at room temperature. On this basis, chromism may well be explained as being a backbone-driven process (Y ⇄ R ⇄ B). At this stage we will not comment on the structure of the backbone in the various phases (see below). PDA's with [illegible]'s adjacent to the backbone seem to be exceptions, undergoing very little colour change upon extraction of the unreacted monomer. With solutions they exhibit a yellow-to-blue colour transition when undergoing this chromic effect. Exceptions, however, do occur whereby [illegible]'s-PDA's do not remain blue upon extraction of the unreacted monomer. In these cases, one may find that there is steric hindrance imposed by the groups adjacent to the [illegible]'s (for example, aryl or substituted aryl groups) thereby perturbing the backbone and causing the backbone to prefer a R phase conformation. The reverse effect may be true for blue [illegible]'s-PDA's, i.e. steric hindrance is actually removed, leaving the backbone unperturbed. The majority of PDA's, however, prefer the B-phase conformation.

Conclusions concerning Exciton phonon interacting and chromism in PDA's

On the basis of the data presented above one can postualte a correlation relting order/disorder, fluorescence yield, absorption profiles and extent of exciton-phonon coupling for the

different backbone configurations.

Y-phase	460 ± 10nm	Y^{H}-exciton
R-phase	535 ± 10nm	R^{H}-exciton
B-phase	610 ± 15nm	B^{H}-exciton

The different phases will be labelled with different type of excitons associated with them. The H superscript refers to room temperature excitons. The B^{H}-excitons are expected to be very anisotropic or coherent since PDA crystals are highly anisotropic. The other excitons are expected to be less coherent so that exciton-migration may occur by hopping as well. Of course, the extent to which these Y^{H}-excitons are localised is not known; probably over 6-7 repeat units. Figure 12 shows the above mentioned correlation.

X-ray studies reveal that the macroscopic single PDA crystals have the sidegroups attached to the backbone in an all-trans conformation. If one compares the R-phase absorption spectra of 4BCMU and 9PA obtained after addition of a poor solvent (Hexane) to a solution of good solvent ($CHCl_3$), one will notice that the relative intensities of the vibrational sidebands (v. .'s) compared to the zero-phonon bands (Z.P.B.'s) are different. We can say that the 4BCMU is more ordered than the 9PA since we know, from resonance Raman studies, that the more ordered polymer backbone have weakly associated V.S.'s. Recent studies on PFC* PDA clearly show that red polymer solutions have different absorption profiles (viz. the ratio of the heights of the Z.P.B.'s to the V.S.'s) as a result of the extent of homogeneity imposed onto the backbone. Nevertheless, all these spectra show an absorption peak or shoulder at 540nm. However, one would expect a decrease of the fluorescence yield with an increase in the exciton-phonon interaction and fluorescence yield or the extent of the localisation of the exciton wavefunction. Despite this competing process, the fluorescence quantum yield measured for the Y & R phases are low, ca. 0.1-0.3% and less than 10^{-4} for the B-phase. The non-radiative relaxation process in PDA chains is therefore extremely efficient. The nature of this non-radiative decay channel is still knot known. One possibility is the occurence of rapid intersystem crossing from the singlet exciton to the lowest triplet exciton. Results for other linear conjugated macromolecules suggest that this rapid intersystem crossing can only occur by singlet-singlet fission with the resulting triplets likely to decay rapidly by phonon emission since the backbone phonons range up to 0.25 eV in energy.

*In PFC

$R' = CH_3 - (CH_2)_n$

R = 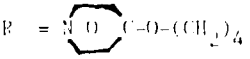 $-(CH_2)_4$

Figure 12 Correlation relating degree of order, ϕ_F, absorption and emission profiles and exciton-phonon interactions in PDA's.

Lifetime measurements in PDA's

We have used laser excitation to study fluorescence decay of the PDA 1OH in pure crystalline form[52,53]. Results are shown in Figures 13,14,15 and for room temperature and 77K respectively. From a modified version of a theoretical treatment of one-dimensional diffusion[54,55], the expected form of the decay is $\exp^{-}t^{\alpha}$, where $\alpha = 0.45$. Results here are best fitted by $\alpha = 0.425$, satisfactorily close to the theoretical value.

In glasses, the decay parameters have been shown to be much more complex, and this aspect of the requires further effort and support.

(iv) 4,4'-diphenylene di phenyl phenyl vinylene[56]

In collaboration with Dr J. Feast, University of Durham, and Dr Richard Friend, University of Cambridge, we have contributed briefly to the investigation of fluorescence in another conducint polymer poly(4,4'-diphenylene di phenyl vinylene) (VII) PDPV.

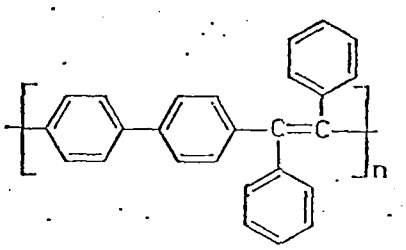

PDPV is a soluble conjugated polymer that shows a degree of conjugation similar to that in poly(paraphenylene). The optical properties of thin films exposed to AsF_5 show the appearance of features below the π-π^* gap at 3eV that can be interpreted in a model of dopant-induced polaron and bipolaron defects. When excited above the π-π^* gap, PDPV shows a strong luminescence peaked at 2.4eV. The Stokes' shift of leV can be accounted for by radiative decay from photogenerated polaron-exciton defect.

However, this explanation of the observed effects may not be unique, and further work is being carried out to elucidate the cause of the very large Stokes shift in fluorescence. The quantum yield of fluorescence has been shown to be of the order of 0.01, with a decay time of around 100ps. This work will continue.

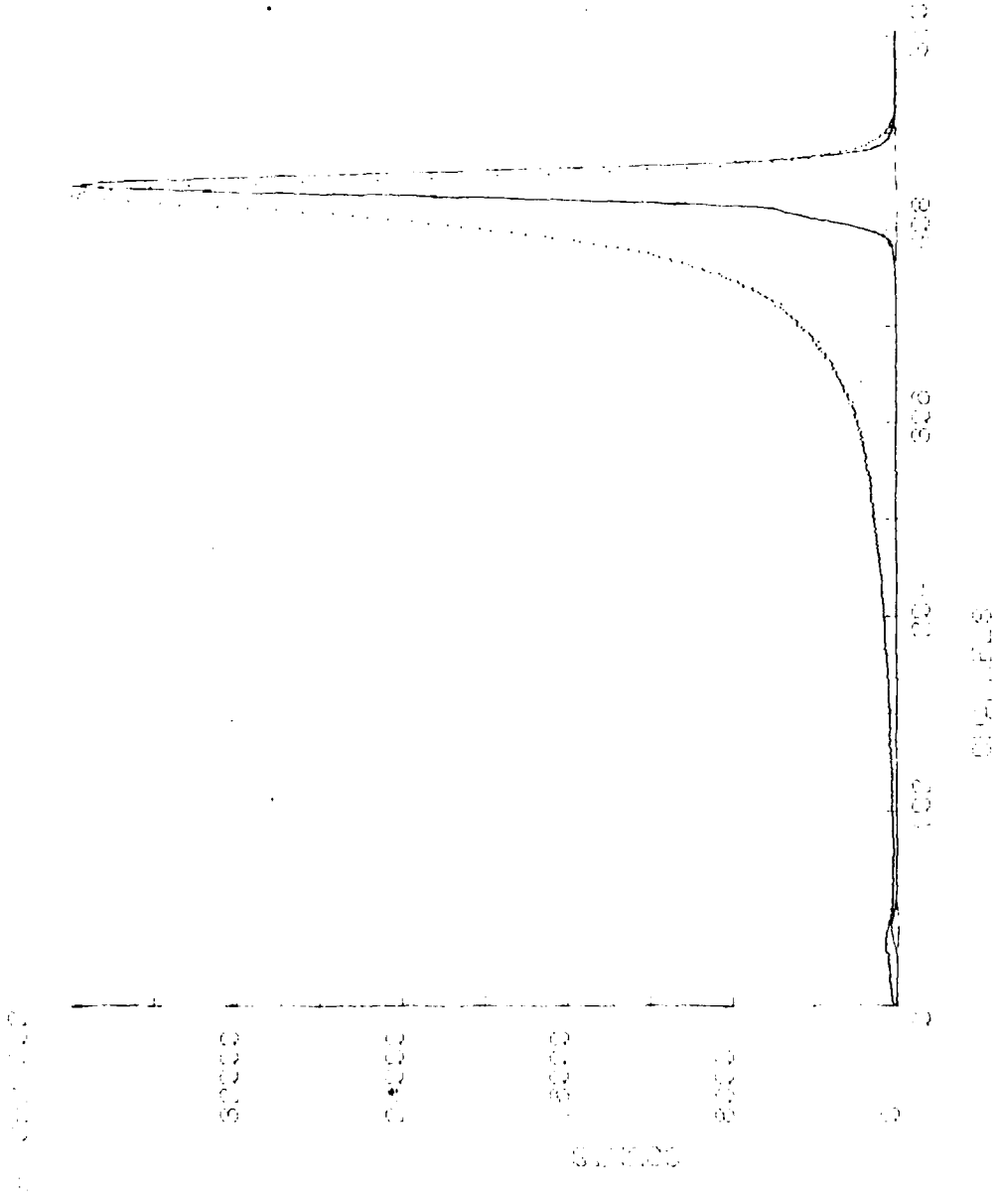

Figure 13 Decay of fluorescence from IOH, room temperature, raw data.

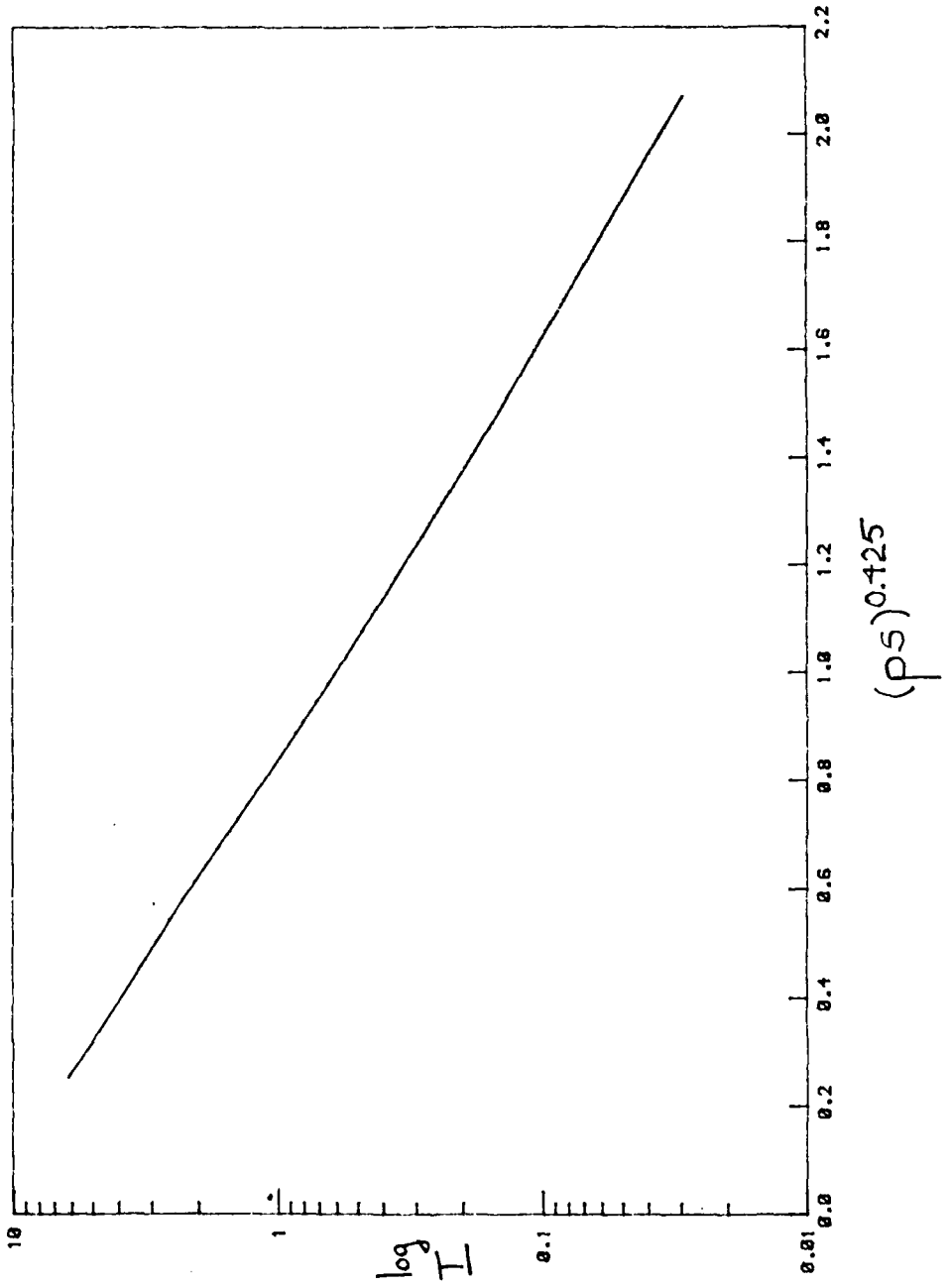

Figure 14 Data from Figure 13 plotted as log intensity vs. $t_{0.425}$

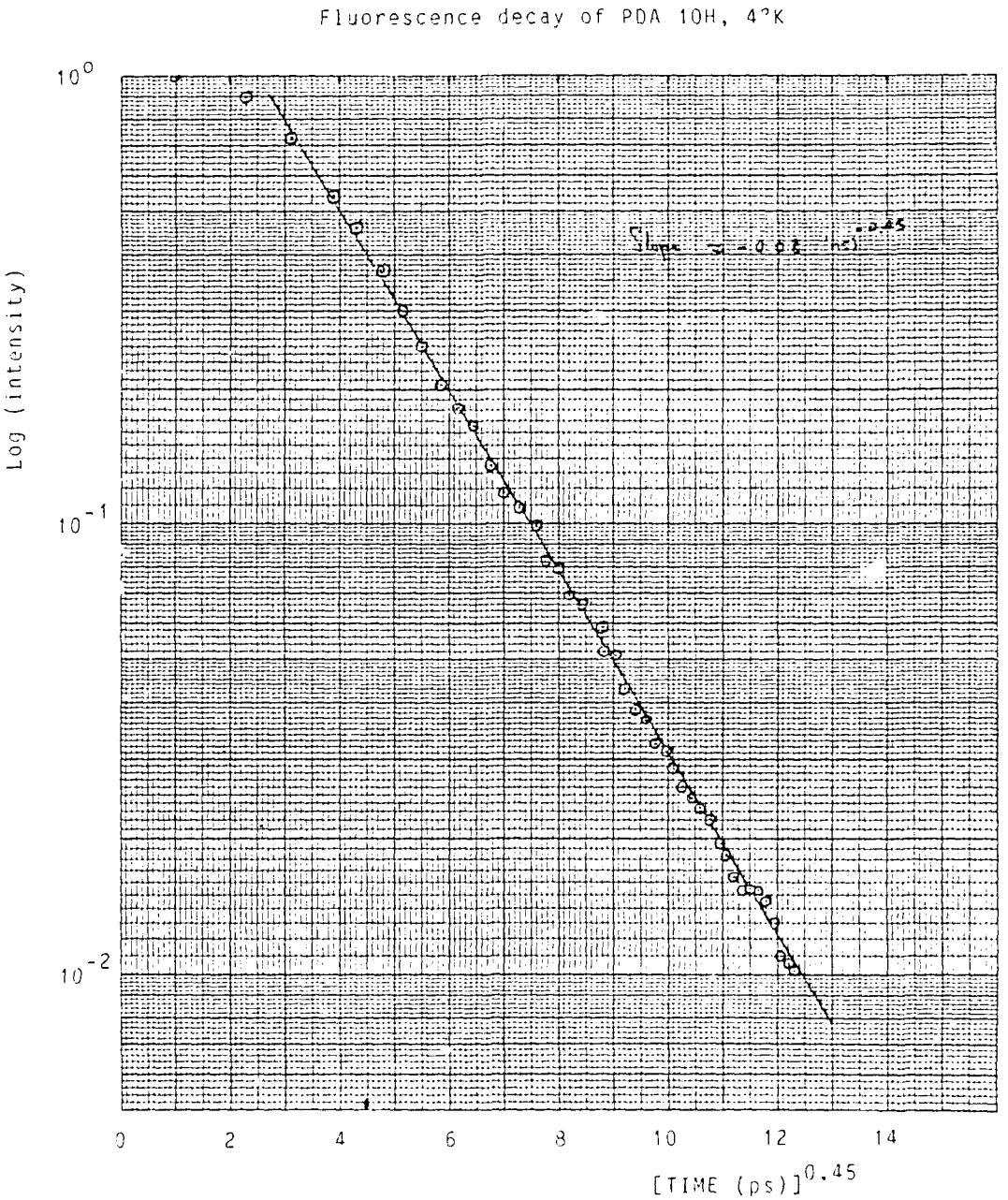

Figure 15 Fluorescence decay of PDA 10H, 4_{o}K, plotted as log intensity vs. $t_{0.45}$.

Acknowledgements

It is a pleasure to acknowledge the fruitful collaborative efforts of Dr Ian Soutar and his co-workers from the Department of Chemistry, Heriot-Watt University, and of Professor David Bloor and colleagues, Department of Physics, Queen Mary College, University of London on some aspects of the work described in this report. I would like also particularly to acknowledge the fine research efforts of Dr A.J. Roberts, Dr G. Rumbles, Dr Jean-Luc Gardette, Dr Andrew Langley, Mr Soonil Rughooputh, Professor R. Christensen, Mr R.C. Drake and Dr S.R. Meech, all of whom contributed to the work described here. Finally, the assistance of the Science and Engineering Research Council, who contributed part-financial aid for this work, is gratefully acknowledged.

6. Literature cited

[1] 'Time-correlated single-photon counting', D.V. O'Connor and D. Phillips, Academic Press, London 1984.

[2] G. Rumbles, Ph.D. Thesis, University of London 1984.

[3] J.B. Birks, 'Photophysics of Aromatic Molecules', Academic Press, London 1970.

[4] A.J. Roberts, D.V. O'Connor and D. Phillips, Annals. N.Y. Acad. Sci., 1981, 366, 109.

[5] D. Phillips, A.J. Roberts and I. Soutar, J. Polym. Sci. (Polym.Phys.), 1980, 18, 2401.

[6] D. Phillips, A.J. Roberts and I. Soutar, Polymer, 1981, 22, 293.

[7] D. Phillips, A.J. Roberts and I. Soutar, Eur. Polym. J., 1981, 17, 101.

[8] D. Phillips, A.J. Roberts and I. Soutar, Polymer, 1981, 22, 427.

[9] D. Phillips, A.J. Roberts and I. Soutar, J. Polym. Sci. (Polymer Physics), 1982, 20, 411.

[10] G.H. Fredrickson and C.W. Frank, Macromolecules, 1983, 16, 572.

[11] 'Analysis of fluorescence decay data from synthetic polymers: Heterogeneity, motion and migration', D. Phillips and I. Soutar in "Photophysical and photochemical tools in polymer science", Ed., M.A. Winnick, D. Reidel Publishers, (in press). (Copy appended, Appendix A).

[12] D. Phillips, A.J. Roberts, G. Rumbles and I. Soutar, J. Polym. Sci. (Polymer Physics), 1982, 20, 1759.

[13] 'Fluorescence of styrene-acrylonitrile copolymers', I. Soutar, J. Arciero, J-L. Gardette and D. Phillips, Brit. Polym. J., (To be submitted shortly).

[14] D. Phillips, A.J. Roberts, G. Rumbles and I. Soutar, Macromolecules, 1983, 16, 1597.

[15] T. Ishi, T. Handa and S. Matsunaga, Macromolecules, 1978, 11, 40.

[16] W.E. Lundsell, F.C. Robertson and I. Soutar, Eur. Polym.J., 1981, 14, 1603.

[17] J.M. Torkelson, S. Lipsky and M. Tirrell, Macromolecules, 1981, 14, 1603.

[18] J.R. MacCallum, Eur. Polym. J., 1981, 17, 797.

[19] J.R. MacCallum in 'Photophysics in synthetic polymers', Eds. D. Phillips and A.J. Roberts, Science Reviews Ltd., London 1982.

[20] D. Phillips, A.J. Roberts and I. Soutar, Macromolecules, 1983, 16, 1593.

[21] G. Rumbles and D. Phillips, Polymer Photochemistry, 1984, 5, 153.

[22] J.R. MacCallum and L. Rudkin, Nature, 1977, 266, 338.

[23] J.R. MacCallum, Polymer, 1982, 23, 175.

[24] J-L. Gardette and D. Phillips, Polymer Communications, 1984, 25, 366.

[25] R.C Drake, R.L. Christensen and D. Phillips, Polymer Photochemistry, 1984, 5, 141.

[26] M.C. Gupta, A. Gupta, J. Horwitz and D. Kliger Macromolecules, 1982, 15, 1372.

[27] F. de Schryer. Paper delivered at International Conference on Photochemistry, Berlin, June 1983.

[28] A.J. Roberts, L.L. Chapoy, D. Phillips and D. Biddle, Chem. Phys. Letters, 1984, 103, 271.

[29] 'The time-resolved fluorescence anisotropy of perylene', R.L. Christensen, R.C. Drake and D. Phillips, J. Phys. Chem, (to be submitted shortly) (Incorporated here as Appendix II).

[30] 'Time-correlated single photon counting using laser excitation', D. Phillips, R.C. Drake, D.V. O'Connor and R.L. Christensen, Analytical Instrumentation, (in press).

[31] D.V. O'Connor, A.J. Roberts, R.A. Lampert, S.R. Meech, L. Chewter and D. Phillips, Analytical Chemistry, 1983, 55, 68.

[32] 'Fluorescence polarisation studies in naphthalene labelled methyl acrylates', R.L. Christensen, R.C. Drake, D. Phillips and I. Soutar, Macromolecules, (to be submitted shortly).

[33] R.C. Drake, Ph.D. Thesis, University of London, 1985.

[34] A.T. Bullock, G.G. Cameron and V. Krajewski, J. Phys. Chem, 1976, 80, 1792.

[35] A.M. North, Chem. Soc. Review, 1972, 49, 1.

[36] A.M. North and I. Soutar, J. Chem. Soc. Faraday Trans., 1972, 68, 1101.

[37] G.J. Kettle and I. Soutar, Europ. Polym. J., 1978, 14, 895.

[38] S.D.D.V. Rughooputh, D. Phillips, D. Bloor and D.J. Ando, Chem. Phys. Letters, 1984, 106, 247.

[39] S.D.D.V. Rughooputh, D. Phillips, D. Bloor and D.J. Ando, Polymer Communications, 1984, 25, 242.

[40] S.D.D.V. Rughooputh, D. Phillips, D. Bloor and D.J. Ando, Chem. Phys. Letters, 1985, 114, 365.

[41] G.N. Patel, J.D. Witt and Y.P. Khanna, J. Polym. Sci., Polym. Phys. Edn., 1980, 18, 1383.

[42] R.H. Baughmann and R.R. Chance, Ann. N.Y. Acad. Sci., 1978, 313, 705.

[43] R.R. Chance, G.N. Patel and J.D. Witt, J. Chem. Phys., 1979, 71, 206.

[44] H.L. Shand, R.R. Chance, M. le Postollec and M. Schott, Phys. Rev. B., 1982, 25, 4431.

[45] G.N. Patel, R.R. Chance and J.D. Witt, J. Chem. Phys.,1979, 70, 4387.

[46] H.R. Bhattacharjee, A.F. Preziosi and G.N. Patel, J. Chem. Phys., 1980, 73, 1478.

[47] M. Sinclair, K.C. Lim and A.J. Heeger, Phys. Rev. Letters, 1983, 51, 1984.

[48] A.J. Berlinsky, F. Wudl, K.C. Lim, C.R. Fincher and A.J. Heeger, J. Polym. Sci. Polym. Phys. Edn., 1984, 22, 847.

[49] K.C. Lim and A.J. Heeger, 'Spectroscopic and light scattering studies of the conformational (rod-to-coil) transition of PDA in solution', (in press).

[50] G. Wenz, M.A. Muller, M. Schmidt and G. Wegner, Macromolecules, 1984, 17, 837.

[51] M.A. Muller, M. Schmidt and G. Wegner, Macromol. Chem. Rapid Commun., 1984, 5, 83.

[52] 'Luminescence of a fully polymerised poly(diacetylene)', D. Bloor, S.D.D.V. Rughooputh, D. Phillips, W. Hayes and K.S. Wong, "Proceedings of Winter School on electronic properties of polymers and related compounds", Eds., H. Kuzmany and S. Roth, Springer Verlag, (in press).

[53] S.D.D.V. Rughooputh, Ph.D. Thesis, University of London, 1985.

[54] B. Movaghar, G. Sayer, D. Wurtz and D.L. Huber, Solid State Comm., 1981, 39, 1179.

[55] B. Movaghar, B. Pohlmann and D. Wurtz, Phys. Rev. A., 1984, 29, 1368.

[56] W.J. Feast, R.H. Friend, M.E. Horton, I.S. Millichamp, D. Phillips and G. Rumbles, Synthetic metals, 1985, 10, 181.

7. Books and papers on the subject of polymer luminescence published during the tenure of Contract No. DAJA-37-82-C-B265 by Professor D. Phillips and co-workers.

Papers 1,2,11,12,13,14,20,21,24,25,28,29,30,31,32,37,38,39,52 and 56 listed under item 6, literature cited.

Plus

(a) 'Polymer photophysics', Ed. D. Phillips, Chapman and Hall, (in press, to be published August 1985).

(b) 'Time-correlated single photon counting: lasers and conventional sources', D. Phillips in "Excited state probes in Biochemistry and Biology", Eds., A.G. Szabo and L. Masotti, Plenum Press, (in press).

(c) 'Non-exponential kinetics', D. Phillips in "Excited state probes in Biochemistry and Biology", Eds., A.G. Szabo and L. Masotti, Plenum Press, (in press).

(d) 'Excited states in polymers', D. Phillips in "Excited state probes in Biochemistry and Biology", Eds., A.G. Szabo and L. Masotti, Plenum Press, (in press).

(e) 'Singlet energy migration, trapping and excimer formation in polymers', I. Soutar and D. Phillips in "Photophysical and Photochemical tools in polymer science", Ed., M.A. Winnick, D. Reidel Publishers, (in press).

APPENDIX I

ANALYSIS OF FLUORESCENCE DECAY DATA FROM SYNTHETIC POLYMERS: HETEROGENEITY, MOTION AND MIGRATION

David Phillips
The Royal Institution
21 Albemarle Street
London W1X 4BS

Ian Soutar
Department of Chemistry
Heriot-Watt University
Riccarton
Edinburgh

This article is concerned with the analysis of results obtained from experiments in which the time-dependence of fluorescence from synthetic polymers is analysed. Of the methods available to study such fluorescence, that utilizing time-correlated single photon counting detection is probably the most widely used. The method will not be described in detail here, but readers may refer to a recent comprehensive volume on the subject [1]. It is worthwhile here however including some discussion on the analysis of data obtained with the method.

Convolution

If the flash of light that excites the sample were infinitely narrow, and if the response of the detection system were infinitely fast, the observed decay curve would represent the true decay, or δ-pulse response, of the sample $G(t)$.

The form of the observed decay, $I(t)$, when the excitation function, $E(t)$, is not a δ function can be deduced from the theory of impulse functions and leads to the convolution concept. Convolution, or folding together, arises because molecules excited by photons at early times are decaying while others are being excited by photon in the tail of the excitation pulse. A simple deduction of the convolution equation can be obtained from consideration of Figure 1. The pump pulse is assumed to be a sum of δ pulses of amplitude $E(t')$ at any time t'. Here the number of sample molecules excited at time t' is proportional to $E(t')$ the number at any later time $x - t'$ is proportional to $E(t')G(x - t')$. The total number of excited state molecules at time x, written $[A^*](x)$ is then a sum over all times t' preceding time x, or, for an infinite sum,

$$[A^*](x) \propto \int_0^x E(t')G(x - t')dt'. \qquad (1)$$

This treatment neglects distortions introduced by the detection system, considered below.

Suppose that H(t) is the δ-pulse response of the detection system, and P(t) the measured time profile of the pump pulse, i.e., the instrument response function. P(t) is a convolution of E(t) and H(t).

$$P(t) = E(t) \otimes H(t). \qquad (2)$$

Writing the Laplace transform of a function X(t) as x(s) with

$$x(s) = \mathcal{L}\{X(t)\} = \int_0^\infty e^{-st} X(t)dt,$$

it follows that

$$p(s) = e(s).h(s). \qquad (3)$$

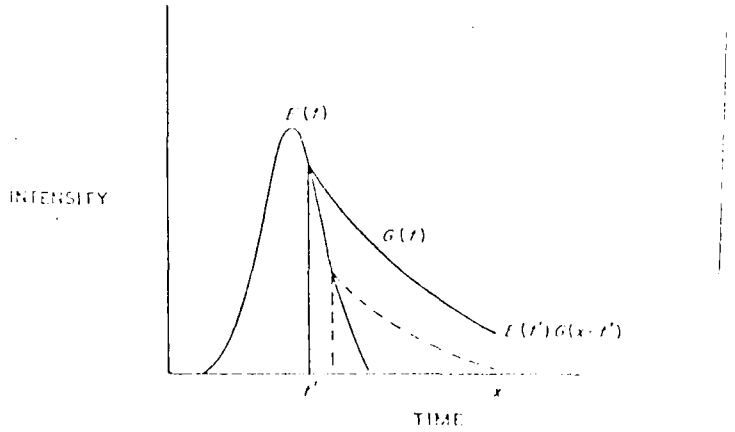

Figure 1. Schematic representation of the effect of convolution. E(t) idealized pump pulse profile; G(t) decay law (assumed simple exponential) of sample.

Similarly

$$a(s) = e(s).g(s) \qquad (4)$$

[illegible]

$$h(t) = a(t) \otimes b(t) \quad (5)$$

Therefore

$$h(t) = \exp(t) \otimes g(t) \otimes \delta(t) + p(t) \otimes g(t) \quad (6)$$

and

$$P(t) = P(t=0) + \int_0^t h(t')\,dt' = \int_0^t h(t')\,dt', \quad (7)$$

where $h(t)$ represents the response function to pulse of the sample distorted by convolution with both the pulse shape and the detector response, *i.e.*, the response of a delta. Using the convolution theorem, (6) can be solved for $a(t)$ by fitting $h(t)$ and $b(t)$, assuming under the assumption of instrumental distortion, as above. There are [illegible] objections to this, but the [illegible] procedure to [illegible] is that [illegible].

Least Squares Fitting

With this technique the decay [illegible] with the [illegible] counts are [illegible] weighted; however an [illegible] of the [illegible] curve [illegible] to the analytic [illegible] feature [illegible] still [illegible] distortion [illegible] present in the data. If the [illegible] is a single exponential, $f(t)$ is given by

$$f(t) = a_1 \exp(-t/\tau_1) \quad (8)$$

and in order to linearize the fitting function [illegible] (8) is expanded to first order in a Taylor's expansion as a function of the parameters a_1 and τ_1. A linear least squares search is then carried out to find values of the parameter increments Δa_1 and $\Delta \tau_1$ that minimize the reduced χ^2_ν given by

$$\chi^2_\nu = \frac{\sum_{i=n_1}^{n_2} w_i \left[f(t_i) - I(t_i) \right]^2}{n_2 - n_1 + 1 - p} \quad (9)$$

where w_i, the weighting factor, is the reciprocal of the number of counts [illegible] channel i, n_1 and n_2 are the first and last channels of the region of the decay to be analyzed, and p is the number of fitting parameters (two for a single exponential fit). The search for the minimum in χ^2_ν is performed according to Bargmann's technique.

When the criterion on χ^2_ν has been reached it is vitally important to have reliable criteria by which the fit can be judged. The actual

value should be close to 1; values of X^2_ν much less than 1 are symptomatic of poor statistics whereas values much in excess of 1 indicate a poor fit. If all distorted data are to be rejected we would accept results for which X^2_ν is less than 1.2, whereas if some level of distortion must be tolerated, fits with values of X^2_ν less than 1.4 may be acceptable if they are justified by some other criteria. Since acceptable values of X^2_ν are sometimes obtained for poor fits, it is usual to inspect a plot of the weighted residuals for nonrandom fluctuations. The weighted residual in channel i is given by

$$r_i = \sqrt{w_i}(Y(t_i) - I(t_i)) \tag{10}$$

It is generally less difficult to detect small deviations of the fitted from the observed curve in a plot of r_i vs. channel number rather than in the more traditional visual inspection of the two curves $Y(t_i)$ and $I(t_i)$. An even more sensitive plot is that of the autocorrelation function of the weighted residuals. The correlation of the residual in channel i with the residual in channel i + j is summed over a number of channels, n, and normalized, i.e.,

$$C_j = \frac{\frac{1}{n}\sum_{i=n_1}^{n_1+n-1} r_i \cdot r_{i+j}}{\frac{1}{n_3}\sum_{i=n_1}^{n_2} r_i^2} \tag{11}$$

In this expression $n_3 = n_2 - n_1 + 1$, the total number of channels in the portion of the decay used in the fit. An upper limit, usually $n_2/10$, is put on j so that the number of terms, $m = n_3 - j$, summed in the numerator is sufficient to give proper averaging. According to Equation (11) $C_{j=0} = 1$. In a successful fit C_j for $j = 0$ is randomly scattered about zero although, because of the finite value of m, some high frequency low amplitude fluctuations are generally observed. These are clearly distinguishable from the type of correlation indicative of an incorrect fitting function or of distorted data.

Judgements based on inspection of the aforementioned plots are subject to the inevitable bias associated with subjective tests. It is possible to calculate the Durbin Watson parameter D, which is, in certain cases, more sensitive than X^2_ν to small nonrandom oscillations in the residuals. It is calculated according to the equation

$$D = \frac{\sum_{i=n_1+1}^{n_2} (r_i - r_{i-1})^2}{\sum_{i=n_1}^{n_2} r_i^2} \tag{12}$$

Acceptable values for DW have been tabulated for up to 100 data points and five fittings parameters. Extrapolation of tables to more data points is quite straightforward. On the basis of our experience we conclude that single exponential fits yielding values of DW greater than 1.65 are generally successful. The corresponding values for double and triple exponential fits are 1.75 and 1.8, respectively. In addition we calculate a skewness factor, SK, given by

$$SK = \sqrt{\frac{n_3}{\left[\sum_{i=n_1}^{n_2} (r_i - r)^2\right]^3}} \sum_{i=n_1}^{n_2} (r_i - r)^3 \qquad (13)$$

and a kurtosis factor, K, given by

$$K = \frac{n_3 \sum_{i=n_1}^{n_2} (r_i - r)^4}{\left[\sum_{i=n_1}^{n_2} (r_i - r)^2\right]^2} \qquad (14)$$

In these equations r is the mean of the weighted residuals. For normally distributed residuals SK has a mean of zero and a standard deviation of $(6/n_3)^{1/2}$. Although we calculate these parameters routinely they are difficult to interpret and therefore we find them less useful than the Durbin-Watson parameter.

A very useful test, particularly when there is doubt about the suitability of a chosen fitting function is variation of the fitting range. Variation in the recovered parameters when channels representing earlier times are included in the fit is indicative of an incorrect fitting function. Usually, but not always, instrumental distortions affecting the early times data points lead to non-normally distributed residuals but the same values for the recovered parameters irrespective of the fitting range.

These tests are applied rigorously to all of the data obtained in our laboratories and, we believe, do permit some discrimination between alternative trial forms of G(t). (see below).

Expected form of G(t)

Single-exponential decay

It is perhaps worth stating at the outset the conditions under which single exponential decay should be anticipated. Considering a single emitting component in the condensed phase, electronic excitation will be followed by rapid equilibrium of vibrational energy to produce the Boltzmann distribution of levels from which emission occurs. Since the equilibrium which maintains this distribution is usually

rapidly established compared with the timescale of electronic relaxation processes, the depopulation of the excited state can be represented by a single rate parameter, a pseudo-first order rate constant multiplied by concentration of excited species.

$$d[\frac{M^*}{dt}] = k'[^1M^*] \tag{15}$$

We are, of course, familiar with the division of the pseudo-first order decay constant k' into individual contributions, based upon a simple scheme such as that below,

$$M + h\nu \rightarrow {}^1M^* \qquad I_a \tag{16}$$

$${}^1M^* \rightarrow M + h\nu_F \qquad k_R \tag{17}$$

$${}^1M^* \rightarrow {}^3M^* \qquad k_{ISC} \tag{18}$$

$${}^1M^* + Q \rightarrow \text{Quenching} \qquad k_Q[Q] \tag{19}$$

such that $k' = k_R + k_{ISC} + k_Q[Q]$, with the usual relationships below holding.

$$\tau_F^{-1} = k_R + k_{ISC} + k_Q[Q] \tag{20}$$

$$\phi_F = \frac{k_R}{(k_R + k_{ISC} + k_Q[Q])} \tag{21}$$

It is important to remember that rate-constants relate to bulk properties of molecular systems. Thus for example, a normal thermal bimolecular rate-constant for the hypothetical reaction (22) represents the rate observed in the bulk, and is thus averaged over all initial energy distributions in A, B, angles and velocities

$$A + B \quad C + D \tag{22}$$

of approach, product internal energy distributions, trajectories and kinetic energies. *If experiments are performed in conditions such that these parameters are specified, then the probability of reaction observed will not relate to that observed in the bulk phase, and may have different functional form.*

The common causes of deviations from single exponential decay of fluorescence in molecular systems has been reviewed elsewhere [2], and thus a digest only is given here. Briefly, these are:-

Heterogeneity

For more than one simultaneously excited, non interacting species, the decay of total fluorescence will be described in

principle by (22). The situation with two non-interacting species is

$$I(t) = \sum_i A_i e^{-t/\tau_i} \qquad (23)$$

fairly commonly met, but as the number of species increases, interactions such as energy transfer are bound to become more probable, complicating the kinetics (or rather simplifying them in some concentration ranges).

In the extreme of a large number of non-interacting sites, such as molecules adsorbed on a solid surface, in defects in molecular crystals or in some polymeric species, the decay may be better described by a distribution of decay times, suitably weighted about some mean value.

A recent treatment by Albery et al [3] gives a rate-parameter k as a distribution represented by

$$k = \bar{k} \exp(\gamma x) \qquad (24)$$

Thus the decay of concentration C of a species from initial concentration C_o is given by

$$\frac{C}{C_o} = \frac{\int_{-\infty}^{+\infty} \exp(-x^2) \exp[-t \exp(\gamma x)]dx}{\int_{-\infty}^{+\infty} \exp(-x^2)dx} \qquad (25)$$

where

$$\tau = kt, \text{ and } \int_{-\infty}^{+\infty} \exp(-x^2)dx = \pi^{\frac{1}{2}}$$

The width of the distribution can be obtained simply by using this analysis by measuring $t_{\frac{1}{2}}$, and $t_{\frac{7}{8}}$, the times taken for decay by $\frac{1}{2}$ and $\frac{7}{8}$ initial concentration respectively, and Equation (26).

$$\gamma = 0.92 \left[t_{\frac{7}{8}}/t_{\frac{1}{2}} - 3\right]^{\frac{1}{2}} \qquad (26)$$

In simple cases of two or three or perhaps four components, the derived A_i and resolved integrated areas under decay curves, $A_i\tau_i$, are respectively measures of the initial concentration of each species modified in one case by the radiative rate-constant, the second by the

$$A = k_R [{}^1M^*]_o \qquad (27)$$

$$A = \phi_f [{}^1M^*_o] \qquad (28)$$

quantum yield of fluorescence. Without knowledge of respective values of k_R, or ϕ_f for each species, little can be said about initial concentrations.

It is possible in favourable cases to deconvolve successfully three components from a single experimental curve, although reliance on one such experimental curve would be foolhardy. This is

illustrated in Figure 2 which displays analysis by this method of simulated data obtained by convolving three components of respective A and τ (shown in Table 1 as initial values), with a real instrument response function using a cavity-dumped dye laser (see below) adding random noise to simulate the experiment, and then analysing. Recovered values of A and τ are very satisfactory for a three component fit (2b) but a two-component, (four parameter) fit is seen to be unacceptable. (Figure 2a) [4].

It is very important to stress here what these simulated fittings mean. A triple-component, (six parameter) fit will certainly under some circumstances simulate other, more complex forms of decay, and thus great care must be taken in interpretation of data using such a model. However, we have shown above that the technique can recover the correct functional form, of the decay parameters i.e., while a triple component fit is *not automatically the correct functional form*, it certainly is not automatically inappropriate. Evaluation of the data must rely on a range of experiments which test the model, and all

Table 1 Analysis of simulated three component decay curve

	Initial	Recovered
A_1	0.25	0.25
τ_1/ns	2.50	2.54
A_2	0.07	0.07
τ_2/ns	10.00	9.72
A_3	0.025	0.026
τ_3/ns	40.00	39.44

results must be compatible with this model. In many cases of multiple species, more information can be gained by observing fluorescence in a narrow wavelength range, thus reducing or even eliminating contributions from one or more species. Sequential work is of different wavelength regions fixing decay time measured at wavelengths where kinetics are simpler renders extraction of multiple components easier, through great care must be taken in such a procedure. The technique of 'global' analysis of data is particularly useful in such circumstances [5].

Relaxation processes

Of the many possibilities, that of reversible complex formation is pertinent to polymers. The basic general scheme 1 leads to the

prediction that the decay of uncomplexed fluorophore, $^1A^*$, termed here monomer, and, complex, $^1AQ^*$, should follow the functional forms shown.

Scheme 1

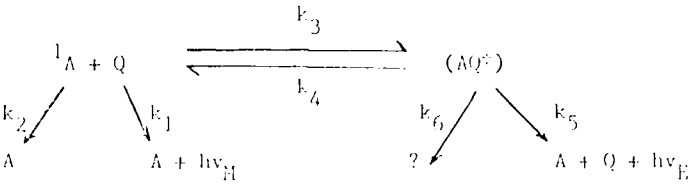

$$[^1A^*](t) = a_1 e^{-\lambda_1 t} + a_2 e^{-\lambda_2 t} \qquad (29)$$

$$[^1AQ^*](t) = a_3 e^{-\lambda_1 t} + a_4 e^{-\lambda_2 t} \text{ where } a_3 = -a_4 \qquad (30)$$

Table 2 Decay time data for CNN TFA (1 3 atm of Cyclohexane) at 168°C in the Gas Phase [6].

10^{-3} [TEA], M	monomer			exciplex			
	τ_1, ns	τ_2, ns	$a_1/(a_1+a_2)$	τ_1, ns	τ_2, ns	a_3	a_4
0		24.1					
0.222	8.17	11.96	0.64	8.64	12.05	-0.46	0.46
0.530	5.41	10.13	0.82	5.80	11.60	-2.69	2.68
0.837	4.07	10.50	0.90	4.16	11.11	-3.68	3.70
2.13	2.00	11.23	0.93	1.96	10.97	-2.33	2.33
3.36	1.31	10.35	0.98	1.31	10.38	-1.93	1.92

That such kinetics can be observed in some systems is typified by the results shown in Table 2, for an exciplex-forming system α-cyanonaphthalene-triethylamine in the vapour phase, where it can be seen that the relationship $a_3 = -a_4$ is obeyed precisely [6]. Indeed, the precision of these measurements is such that deviations from expected values of a_3 and a_4 can be used as a monitor of ground state complex formation [6].

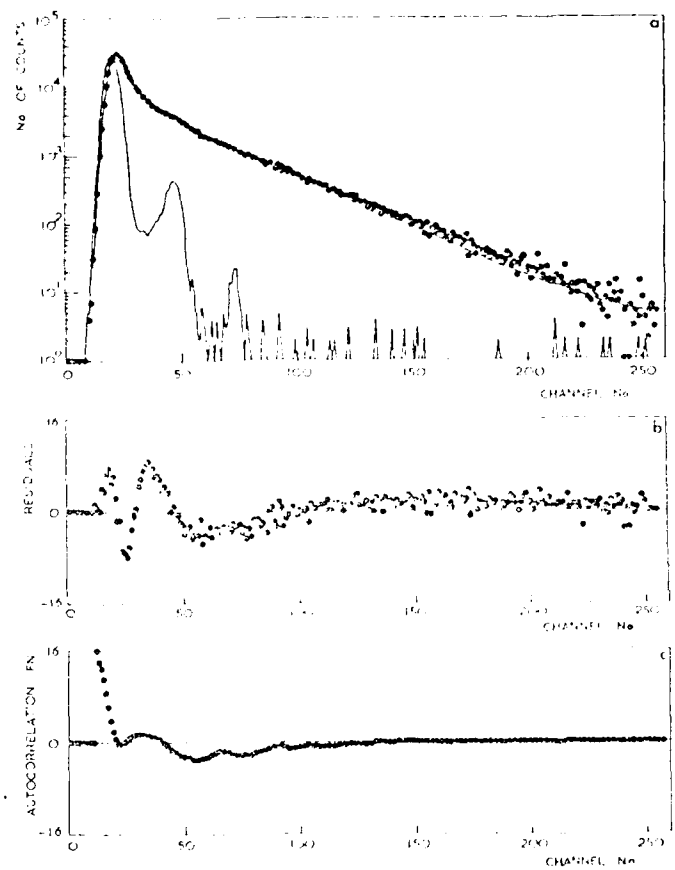

Figure 2a. Plots of (a) two-component fit to simulated three-component fluorescence decay (see text); (b) weighted residuals; (c) auto-correlation function.

Motion

The simplest correction to single-exponetial decay laws occurs as a result of transient effects in translational diffusional processes. An extensive review of the causes and consequences of these transient effects has been given elsewhere, and would be out of place here. In the diffusional quenching of molecule A* by B assuming the simple scheme below

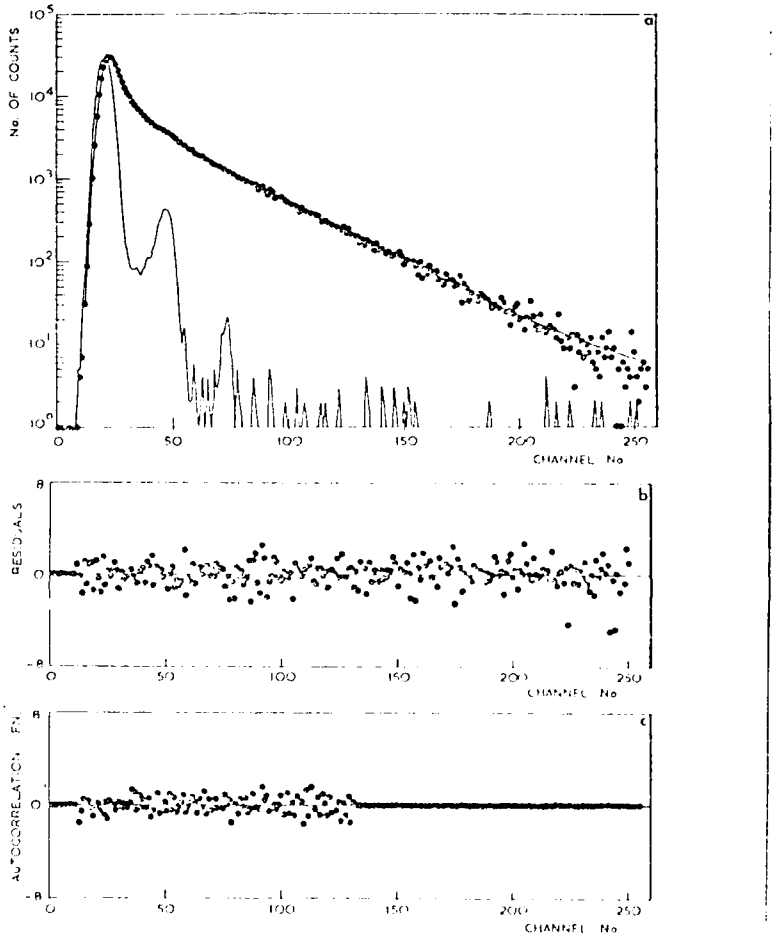

Figure 2b. Plots of (a) three-component fit to the same simulated three-component fluorescence decay as Figure 2a; (b) auto-correlation function.

$$A + h\nu \rightarrow {}^{1}A^{*} \tag{31}$$

$${}^{1}A^{*} \rightarrow A \tag{32}$$

$${}^{1}A^{*} \rightarrow A + h\nu \tag{33}$$

$$A^* + B \xrightarrow{k(t)} products \qquad (34)$$

the decay law of A*, monitored by fluorescence, has been shown to be

$$I(t) = \exp(-At - Bt^{\frac{1}{2}}) \qquad (35)$$

where

$$A = \frac{1}{\tau_o} + 4\pi\sigma D_{AB} N' [B] \qquad (36)$$

and

$$B = 4\pi D_{AB} \sigma^2 N' [B] \qquad (37)$$

where D_{AB} is the translational diffusion coefficient, and σ is the sum of the radii of the two species.

The exponential-t$^{\frac{1}{2}}$ term in (35) has been observed in quenching reactions in solution, but only on fast ($\lesssim$ 1 ns) timescales [7]. This is an important point, that some deviations from simple exponential decay laws will only be observable if the appropriate experimental timescale is employed. For the restricted rotational motion, Hagabi et al [8] have proposed the decay law should obey a similar functional form,

$$I(t) = A \exp[-(at + bt^{\frac{1}{2}}] + B \exp(-ct) \qquad (38)$$

although the theoretical basis for this is not clear. Decay laws for fluorescence anisotropy, which can be very complex, will not be discussed here.

Energy transfer and migration

This subject has been reviewed extensively, and this discussion will not be amplified here. In the simple case where randomly distributed immobile donors and acceptors are considered at a donor concentration such that donor-donor transfer is negligible, the time-dependence of donor fluorescence is

$$I(t) = \exp[-(t/\tau) - \gamma (t/\tau)^{3/s}] \qquad (39)$$

where

$$\gamma = (4/3)\pi [\Gamma(1 - 3/s)] N_A C_0^{3} \qquad (40)$$

with $S = 6$ for dipole-dipole transfers and N_A is the number of acceptor molecules / cm^3, C_0 is a constant proportional to the overlap of donor emission and acceptor absorption. In this case of dipole-dipole interaction formulated by Forster, the decay exhibits an exponential decay plus an additional exp(-t$^{\frac{1}{2}}$) dependence. For exchange energy transfer, the decay rate has a different dependence.

$$I(t) = \exp[-t/\tau - \alpha g(\beta t)] \tag{41}$$

where

$$g(z) = 6z \sum_{n=0}^{\infty} (-z)^n/[n!(n+1)^4] \tag{42}$$

and the constants α,β can be related to macroscopic constants as with γ. In both cases the decay is represented by an initial non-exponential component followed at long times by the decay of the unquenched donor.

In cases where energy migration is a dominant feature of luminescence, as in molecular crystals, various forms of decay are expected depending upon circumstances, but relying upon solutions, usually complex, to the basic rate equations where E(t) is the time-

$$\dot{E}(t) = -[k_E + k_L(t)]E(t) \tag{43}$$

$$\dot{T}(t) = -k_T T(t) + k_L(t)E(t) \tag{44}$$

dependent population of the initially excited (exciton) state, T(t) the population of the trap state, k_E the decay rate constant for band states, k_T the decay rate constant for trap states, and $k_L(t)$ the time-dependent trapping rate functions, the form of which depends upon the effective transport topology [10]. For a strictly one-dimensional transport, Yaver has given the form of $k_L(t)$ as

$$k_L(t) = At^{-\frac{1}{2}} \tag{45}$$

for quasi-one-dimensional, two-dimensional, and three-dimensional diffusional processes, other forms are appropriate [10,11-14]. Thus very extensive theoretical and picosecond experimental work on electronic excited state transport in finite volumes of randomly distributed molecules has been reported, which shows that there are significant deviations in the behaviour of finite volume systems compared with the infinite volume systems considered above. The treatment is mathematically complex and the results will not be given here explicitly [12-14]. Frederickson and Franck [15] have used this treatment to suggest possible forms for the decay of monomer and growth and decay of excimer fluorescence in vinyl aromatic polymers where electronic energy migration might be a dominant process. This treatment is presented elsewhere in the volume, and will be discussed briefly below.

Heterogeneity in polymers

Even a polymer sample of narrow molecular weight distribution is just that, a distribution. Since the fluorescence process can be extremely sensitive to the environment of the fluorophore, in principle, a range of environments is being observed even in a non-interacting fluorophore, that is a molecule which does not interact with neighbouring chromophores through excimer formation or energy

transfer or migration. This situation however, corresponds to that observed in a free chromophore in solution, and the decay should be modelled adequately by a rate constant. This is certainly not the case for interacting chromophores, where the local environment will be critical in determining the decay rate of any particular fluorophore. In a homopolymer, the principal cause of heterogeneity will be the tacticity of the polymer, isotactic, syndiotactic and atactic polymers being expected to behave very differently, as outlined elsewhere in this volume. In cases where nominally 'atactic' polymers consist of isotactic and syndiotactic sequences, the decay may in favourable simple cases be interpretable in terms of a summation of exponential decays of two kinetically distinct species. For a wide distribution of sites, a kinetic model recognising this heterogeneity may be more appropriate, although this yields information of limited usefulness.

In copolymers, heterogeneity of environment of a chromophore by virtue of composition becomes of overriding concern.

Motion in polymers

In a small molecule, rotational motion of a fluorophore in solution occurs on a picosecond timescale and the observed emission is thus averaged over all molecular orientations. In a synthetic polymer whole chain motion is in general very slow, but local motions may occur on the same timescale as fluorescence, and if these local motions, such as segmental motion, determine the rate of a process leading to emission, then the appropriate form of the rate expression for emission must be employed, as discussed earlier [8].

Electronic energy transfer, migration in polymers

Energy migration is thought to occur in many vinyl aromatic polymers, for example, and if this process is rate determining for any observed fluorescence then the form of the expression used to model the fluorescence growth or decay must be correct, as described above.

What prospect is there for analysing data, and recovering form appropriate for some of the processes identified above? In cases where the system is very carefully chosen to minimise the likelihood of observing a particular form of decay, these might be good. For example, in figure 3 we show the decay of fluorescence from a crystal of a poly(diacetylene) which is highly ordered [16], leading to one-dimensional exciton diffusion, and with a very short trap decay time such that the form of the expression appropriate for the decay, an exponential t^{-3} dependence, is clearly obeyed (figure 4) [11].

What of more complex systems, such as dilute solutions of flexible vinyl aromatic polymers?

In our early work, it became clear that simple Birks kinetic schemes representing excimer formation and decay were inadequate for modelling fluorescence in excimer forming polymers [17,22]. The empirical observation that multiple (dual and triple) exponential terms could model successfully the decay of monomer and excimer fluorescence in poly(vinyl naphthalene) led us to propose simple models which

largely recognised the heterogeneity of the sample, and discriminated between two classes of monomer site, one which could rapidly lead to excimer formation through energy migration and rotational coupling, and one which could not, discussed in the previous article. These findings have been criticised by two groups, who derive, from entirely different reasoning, a monomer decay function of the form in Equation (46). (C.F. Equation (46) is the simplified form given by Frederickson and Franck) [13].

$$I(t) = A \exp[-(at + bt^2)] + B \exp(-ct) \qquad (46)$$

It has been shown that functions of the form of Equation (46) can in general simulate (through adjustment of the parameters) some curves of the form observed in systems of isomer and excimer decay.
Alternatively, the functional type (47) has been shown to simulate that

$$I(t) = \exp[(a + bt + ct^2)] \qquad (47)$$

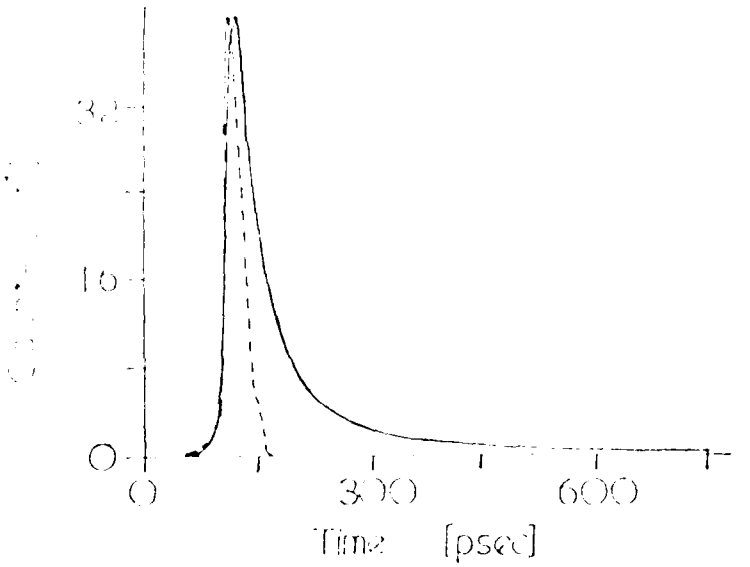

Figure . [illegible] (full curve). [illegible] dashed curve [13].

[illegible] fit, [illegible] [illegible] to data, acceptability [illegible].

[illegible] [illegible], the analysis [illegible] and the [illegible].

ecane. However, it is of relevance to note that in the copolymer series studied to date [1,9,22] the two shorter decay components obtained in triple exponential analysis increase as the basic homopolymer repeat unit are replaced by comonomers which will induce chain flexibility. It is difficult to rationalise these results with the trend expected in the presence of rotational diffusional as described by Equation (66).

In the specific case of styrene polymers, we can test the simplest alternative model, expression (67), against a multiple exponential model, where we have chosen, Figure 5, to fit a dual component fit is acceptable statistically for all polymer emission decays. Figure 7, 8 show that the stretched exponential (67) is certainly acceptable.

One drawback to Equation (67) is that reverse dissociation of the excimer is ignored, although there is spectroscopic evidence that for some systems this is not relevant, new studies in polarised light decay [ ] based on rotational expansion terms [ ] [illegible] with difficulty be distinguished [illegible].

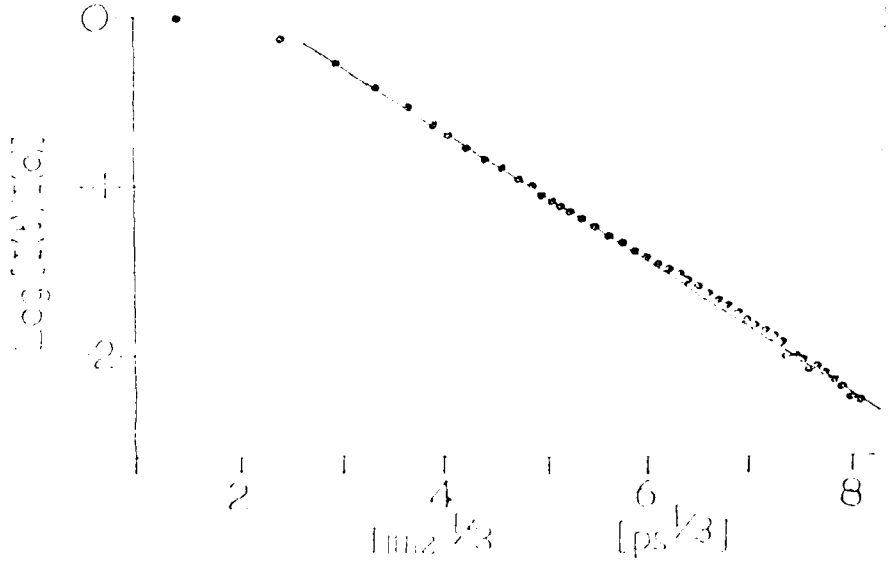

[illegible]

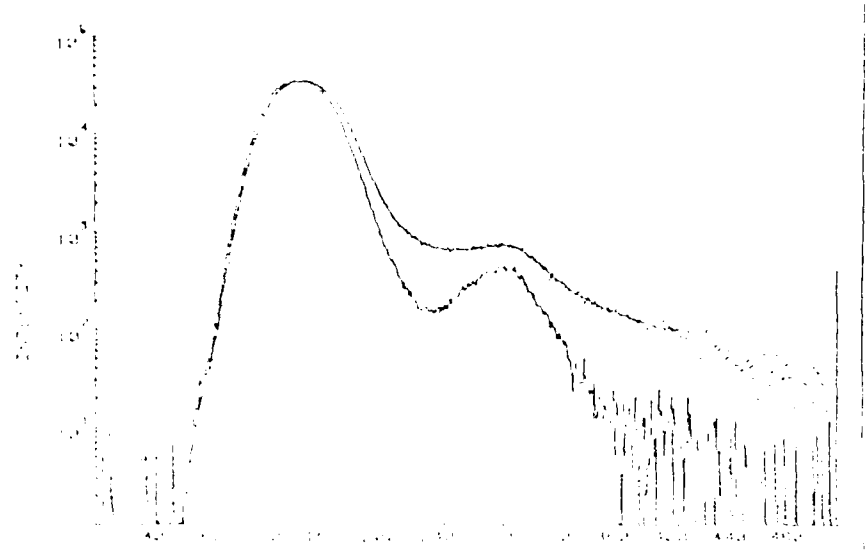

10⁴
10³
10²
10¹
10⁰

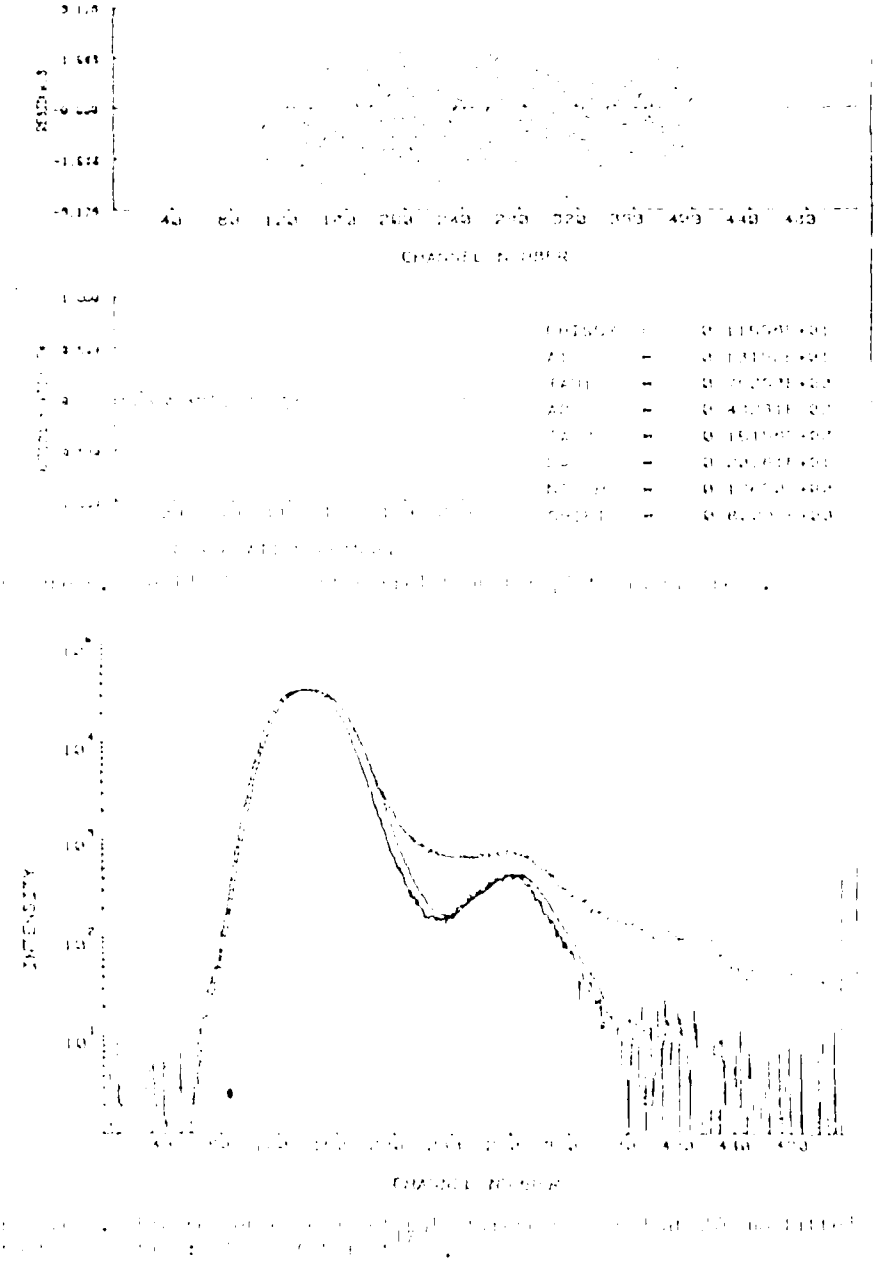

progress by devising experiments which will provide a means of identifying the processes which are rate-determining in any system. It is axiomatic in using such methods that the simplest model fully compatible with all results must be selected, since one can always replace this model by one which is more complex mathematically. This however, may defy interpretation in physical terms. A demonstration that a very complex model is as compatible as a more simple model with a particular set of data is not in itself cause for abandonment of the simplest model. The way forwards as always, is to devise experiments which further test the validity of the simpler model, and at the point where this can be shown demonstrably, experimentally to be inadequate, to abandon it in favour of the simplest refined model which is then fully compatible with the results. This is the approach we have taken and will continue to take.

It is clear that the origins of the photophysical behaviour of polymers will continue to be the subject of lively debate for some time. Activity in a field which has proved to be rapidly expanding and stimulating during the past decade seems likely to maintain momentum in the next few years.

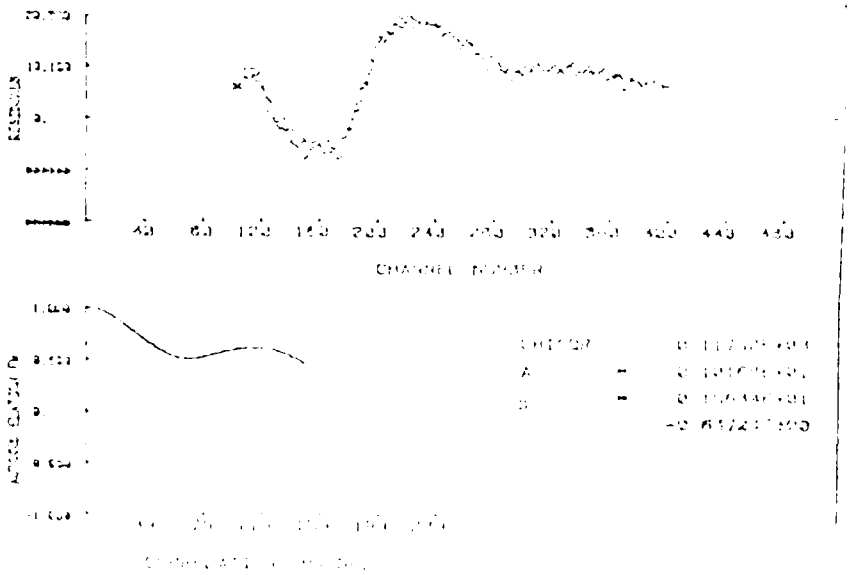

Figure 5. Residuals and correlation function for plots in Figure 4.

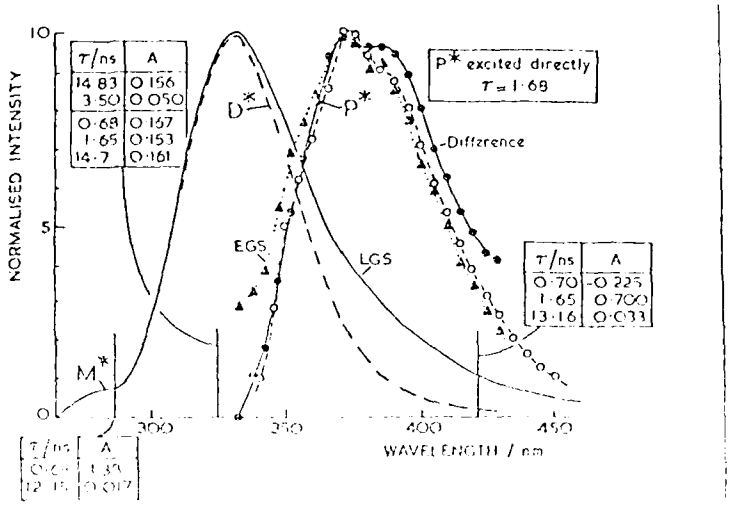

Figure 9. Fluorescence spectra and decay characteristics of P95 containing poly(styrene). M*, styrene monomer region, dual decay kinetics. D*, styrene excimer region, triple decay characteristics (double fit shown does not correlate with other wavelengths, thus meaningless). P* is P95 fluorescence, triple decay characteristics when styrene excited (see box), but single, $\tau = 1.68$ ns when excited directly. EGS is early gated time resolved spectrum which matches closely spectrum of P* excited directly, and difference between late-gated spectrum LGS and known spectrum of D*.

Acknowledgements

It is a pleasure to acknowledge the contributions to this work of A.J. Roberts, G. Rumbles, I-L. Gardette, S.D.D.V. Rughooputh and F. Prato. Financial support for our work in this area from the Science and Engineering Research Council and U.S. Army European Research Office are gratefully acknowledged.

References

1. 'Time-correlated single photon counting', D.V. O'Connor and D. Phillips, Academic Press, 1984.

2. 'Luminescence techniques', D. Phillips in "Excited state probes in biochemistry and biology", ed., A.G. Szabo and L. Masotti, Elsevier Press, New York.

3. V.L. Ermolaev, E.N. Larkert, K.K. Rohatgi and J.F. Parsont, J. Amer. Chem. Soc., 1969, 91, 1.

4. A.J. Roberts, D.V. O'Connor and D. Phillips, Ann. N.Y. Acad. Sci., 1981, 366, 109.

5. J.R. Knutson, J.M. Beechem and L. Brand, Chem. Phys. Letters, 1983, 102, 501.

6. D.V. O'Connor, L. Chester and D. Phillips, J. Phys. Chem., 1982, 86, 3400.

7. T.L. Nemzek and W.R. Ware, J. Chem. Phys., 1975, 62, 477.

8. H. Itagaki, F. Horie and I. Mita, Macromolecules, 1983, 16, 1395.

9. A. Kawski, Photochem. Photobiol., 1984, 38, 487.

10. 'Exciton coherence', M.D. Fayer in " pectroscopy and excitation dynamics of condensed olecular systems". ., V.M. Agranovich and R.M. Hochstrasser, North Holland, Amsterdam, 1983, p. 1.

11. [illegible] Hunt, [illegible] Thornton, J. Phys. [illegible] Biology, 1983, 16, [illegible].

12. [illegible], J. Chem. Phys., 1979, [illegible].

13. [illegible], J. Chem. Phys., 1983, [illegible].

14. [illegible], J. Chem. Phys., 1983, [illegible].

15. [illegible] Biophys. Res. Comm., 1984, 120, 452.

16. 'Time resolved fluorescence depolarization of polydiacetylene', O. Bloor, [illegible], D. Phillips, J. Phillips, J. Rees and J. Wood in "Electronic properties of polymers and related compounds", ., P. Kuzmany and [illegible], Springer Verlag, (in press).

17. A. [illegible] Roberts, D. [illegible] and D. Phillips, J. Polym. Sci., (Polym. Letters), 1983, 21, 125.

18. D. Phillips, A.J. Roberts and D. [illegible], J. Polym. Sci. Polymer Physics, 1983, 21, 1693.

19. D. Parelli, A.J. [illegible] and D. [illegible], Biochem., 1981, 20, 203.

20. D. Parelli, A.J. [illegible] and D. [illegible], Eur. Polym. J., 1981, 17, 1021.

21. D. Phillips, A.J. [illegible] and D. [illegible], Biochem., 1981, 20, 467.

22. D. Phillips, A.J. Roberts and I. Soutar, J. Polym. Sci., (Polymer Physics), 1982, 20, 611.

23. D. Phillips, A.J. Roberts and I. Soutar, Macromolecules, 1983, 16, 1593.

APPENDIX II

The Time Resolved Fluorescence Anisotropy of Perylene*

Ronald L. Christensen
Department of Chemistry
Bowdoin College
Brunswick, Maine 04011

Rodney C. Drake and David Phillips
Davy Faraday Research Laboratory
The Royal Institution
21 Albermarle Street
London W1X 4BS United Kingdom

* Paper to be published in J. Phys. Chem., preprint here without diagrams, which appear in body of report.

ABSTRACT

Time-resolved fluorescence anisotropies of perylene in glycerol/water solutions have been studied on nanosecond time scales. Anisotropy decays were obtained using mode locked, cavity dumped laser excitation and single-photon counting detection. The anisotropies are well characterized by a double exponential model and give rotational decay times which can be related to diffusion about the in-plane and out-of-plane molecular axes. The pre-exponential factors are determined by the relative orientations of the absorption and emission transition dipoles and are not sensitive to solvent viscosity, temperature, or other external parameters. The perylene /glycerol/water system appears to be a useful standard for comparing and evaluating different experimental techniques and analysis procedures for nanosecond and subnanosecond measurements of fluorescence anisotropies.

1. Introduction

Time-resolved fluorescence anisotropy measurements can provide detailed information on the reorientational dynamics of molecules in solution. Until recently, however, this information has been limited to single rotational correlation times which are only strictly appropriate for the diffusion of spherically symmetric systems. Improvements in instrumentation and data analysis techniques during the last decade have lead to increasingly accurate measurements of fluorescence lifetimes.[1,2,3] These capabilities also have lead to parallel improvements in determinations of fluorescence anisotropies.

The advances in time-resolved techniques have fostered a re-examination of theories of the rotational motions of molecules in liquids. Models considered include the anisotropic motion of unsymmetrical fluorophores,[4,5] the internal motions of probes relative to the overall movement with respect to their surroundings,[6] the restricted motion of molecules within membranes (e.g., "wobbling" within a cone),[7] and the segmental motion of synthetic macromolecules.[8,9] Analyses of these models points to experimental situations in which the anisotropy can show both multiexponential and nonexponential decay. Current experimental techniques are capable of distinguishing between these different models. It should be emphasized, however, that to accurately extract a single, "average" rotational correlation time demands the same precision of data and analysis as fluorescence decay experiments which exhibit dual exponential decays. Multiple or non exponential anisotropy experiments are thus near the limits of present capabilities and generally demand favorable combinations of fluorescence and rotational diffusion times.

Another key issue with regard to determinations of anisotropy decays are the wide variety of approaches to the calculation of rotational lifetimes. This is in contrast to the situation for the determination of unpolarized

fluorescence decays. In the later case, stable, cavity dumped dye laser excitation sources, time-correlated single photon counting, and standard procedures for deconvoluting fluorescence decays have lead to the acceptance of decay times as relatively easily measured parameters by which to characterize molecular fluorescence.[2,3] Indeed, these measurements have reached the stage where fluorescence decay standards are available to calibrate new experimental techniques.[1]

The anisotropy of a system, r(t), is derived from measurements of the fluorescence decays with polarizations parallel and perpendicular to the polarization of excitation:

$$r(t) = (I_{\parallel}(t) - I_{\perp}(t)) / (I_{\parallel}(t) + 2I_{\perp}(t)) = D(t)/S(t) \qquad (1)$$

The different approaches to analyzing the time dependence of the anisotropy generally arise from different methods by which deconvolutions of $I_{\parallel}(t)$ and $I_{\perp}(t)$ are translated into a deconvoluted r(t). For example, the rotational parameters can be extracted by individually deconvolving I (t), individually deconvolving I (t), deconvolving D(t), deconvolving both D(t) and S(t) and reconstructing r(t), simultaneously fitting $I_{\parallel}(t)$ and $I_{\perp}(t)$, simultaneously analyzing several decay curves ("global analysis")[10], etc. These and other methods recently have been discussed in some detail by Cross and Fleming.[11] At this point, there is no general agreement on which of these methods is most accurate, most efficient, least subject to typical systematic errors, etc., and it is fair to state that a critical comparison of various experimental and analysis techniques has not yet appeared.

An important complication in such a comparison is that several previous studies have not fully appreciated that the statistical procedures applied to unpolarized fluorescence decay cannot be directly transferred to the analysis

of D(t), r(t), etc. Whereas $I_{\parallel}(t)$ and $I_{\perp}(t)$ individually follow the Poisson statistics routinely employed in previous fluorescence decay measurements, deconvolution of D(t) and S(t) must employ properly propagated weights which are distinctively non-Poisson.[12]

This paper addresses the issue of the "best" experimental techniques and analysis procedures by reconsidering perylene (figure 1), a molecule whose fluorescence anisotropy has been shown to be characterized by dual exponential decay.[13-17] The purposes of this study are:

1. to investigate and critically compare rotational correlation times and pre-exponential factors obtained for perylene's anisotropy.
2. to develop a standard fluorophore/solvent system which would provide a useful focal point for evaluating the various procedures used to analyze and interpret polarized emission decays.

Perylene initially was identified as an anisotropic rotator in steady state polarization measurements. Weber et al.'s observation of wavelength dependent Perrin plots indicated the presence of at least two distinct rotational motions.[13] The subsequent development of time-resolved techniques lead to more detailed analyses of perylene's anisotropy by Brand, et al. and Zinsli et al.[16] These investigations indicated that the rate of rotation about the symmetry axis (z axis in figure 1) is about an order of magnitude larger than the rate of rotation perpendicular to the z axis. We have extended these earlier investigations by taking advantage of improvements in fluorescence decay measurements brought about by mode locked laser excitation, single photon counting, and the use of proper statistical weights in the deconvolution of experimental decays. Our measurements provide additional insights on perylene's photophysical behavior and establish useful

and convenient samples for comparison and evaluation of anisotropy measurements on nanosecond and subnanosecond time scales.

2. Theoretical Background

The fluorescence anisotropy of the general, unsymmetric rigid rotor was first given by Belford et al.[5] and subsequently discussed by several other workers.[6,7] These treatments lead to the following expressions:

$$I_{\parallel}(t) = e^{-t/\tau_f}\left(1+2\sum_{i=1}^{5} a_i e^{-t/\tau_i}\right) \tag{2}$$

$$I_{\perp}(t) = e^{-t/\tau_f}\left(1-\sum_{i=1}^{5} a_i e^{-t/\tau_i}\right) \tag{3}$$

$$D(t) = I_{\parallel}(t) - I_{\perp}(t) = 3e^{t/\tau_f}\sum_{i=1}^{5} a_i e^{-t/\tau_i} \tag{4}$$

$$S(t) = I_{\parallel}(t)+2I_{\perp}(t) = 3e^{-t/\tau_f} \tag{5}$$

$$r(t) = D(t)/S(t) = \sum_{i=1}^{5} a_i e^{t/\tau_i} \tag{6}$$

where the τ_i are functions of the rotational diffusion coefficients around the three principal molecular axes and the a_i's are functions of the direction cosines relating the absorption and emission transition dipoles to the principal rotation axes. For perylene, these expressions can be further simplified by assuming that the rotational diffusion constants about the two in-plane axes are identical. This approximation reduces the number of terms in the summations from five to three and the anisotropy then can be expressed as[6]

$$r(t) = 2/5e^{-6D_{\perp}t}\sum_{k=0}^{2} e^{-k^2(D_{\parallel}-D_{\perp})t}\, F_k(\theta_A, \theta_E, \phi_{AE})$$

where θ_A and θ_E are the polar angles between the absorption and emission dipoles and the unique symmetry axis (z in figure 1), ϕ_{AE} is the difference

in their azimuthal angles, and where $D_{//}$ and $D_{\perp}$ refer to the rates of rotation about the unique symmetry axis and any axis perpendicular to this axis

$$F_0 = 1/4\ (3\cos^2\theta_A - 1)\ (3\cos^2\theta_E - 1)$$

$$F_1 = 3/4\ \sin 2\theta_E \sin 2\theta_A \cos\phi_{AE}$$

$$F_2 = 3/4\ \sin^2\theta_E \sin^2\theta_A \cos 2\phi_{AE}$$

For perylene one additional simplification comes into play. Group theoretical considerations require that all $^1\pi\pi^*$ transitions are polarized within the molecular plane.[18] This means that both $\theta_A = \theta_E = \pi/2$ and

$$r(t) = 0.10e^{-6D_{\perp}t} + 0.30 \cos 2\phi_{AE} e^{-(2D_{\perp}+4D_{//})t} \qquad (7)$$

It should be recognized that the diffusion constants for rotation about the two in plane symmetry axes are not rigorously equivalent. As discussed by Small and Isenberg[19], however, these rotational constants would have to be greatly different for more than two exponentials to be observed. This is due to the close interconnection between the original five exponentials which shows that $\tau_1 \approx \tau_5$ and $\tau_2 \approx \tau_3$ in equations 2-6. We thus expect the fluorescence anisotropy of perylene to be well fitted by equation 7 with the pre-exponential factors relating to the angle between the in plane absorption and emission dipoles.

3. Experimental

3.1 Collection of Data

A diagram of the time-resolved fluorescence spectrometer employed in our studies is given in Figure 2. The excitation source was a 4w mode locked, cavity dumped Argon-ion laser (Spectra Physics Model 166). A radio

frequency synnthesizer (Racal Dana 8082) and amplifier (E.N.I. 403CA) were employed to provide the mode locking signal. Synchronization of the mode locked pulses with the cavity dumper was achieved by frequency doubling part of the mode locking signal (to give the same repetition rate as the mode locked pulses) and using this as the reference signal for the cavity dumper drive electronics.

The mode locked pulses (approximately 97MHz) were reduced to a lower repetition rate (single shot - 4MHz) to allow samples to fully relax between excitation events. Vertically polarized output pulses of the 514 nm line were rotated by $\pi/2$ using a Fresnal double rhomb (A.G. Electro Optics) and then focused (using a 10 cm focal length lens) into a temperature tuned ammonium dihydrogen phosphate crystal (Coherent Model 440 UV generator). This produced vertically polarized pulses at 257 nm with a full width at half maximum of 150 ps. Residual, undoubled light was removed by a Corning 7 54 filter. Samples were contained in 1 cm^2 quartz cuvettes. The 480 nm fluorescence was viewed at right angles to the excitation beam and was filtered (using a 420 nm cutoff filter) and polarization selected (using a Polaroid HNP'B sheet polarizer) before being focused on the slits of a Pilger Watts 0.33m-D330 monochromator. Spectral resolution of the emitted light was typically 2 nm.

The fluorescence was detected by using conventional single photon counting methods.[1,2,20] The signal from the photomultiplier (Philips XP2020Q) was sent through nanosecond variable delay lines (Ortec 463, Canberra 2058) and a constant fraction discriminator (Ortec 473A) to a time-to amplitude converter (Ortec 467). In order to use the full repetition rate of the laser, the time-to amplitude converter was operated in an inverted configuration with the voltage ramp being initiated by a signal from the

photomultiplier and terminated by a TTL logic pulse from the cavity dumper. Pulse pile up effects were avoided by arranging for the ratio of laser pulses to detected photons to be greater than 200:1. The data from the time to amplitude converter were processed by a multichannel analyzer (Norland Inotech 5300) and stored in one half of the memory (512 channels). The instrument response function was collected by scattering the 257 nm exciting light off a dilute, aqueous suspension of latex particles (Sigma, average particle diameter of 109 nm) with a transmission matching that of the perylene samples (~10%). The data were then transferred to a Perkin Elmer 7-32 Computer for subsequent analysis.

The fluorescence decay times were obtained from decays for which the analyzing polarizer was set at the "magic angle" (54.7° from the vertical)[21,22] and data accumulated until 20,000 counts were collected in the maximum channel. The instrumental response function was then recorded to a maximum of 20,000 counts using the procedures described above. In order to minimize errors due to long term drifts in the laser intensity and detection electronics, the polarized fluorescence decays were collected by alternating the polarization direction of the emission along with the memory addresses in the multichannel analyzer. These changes were carried out under microprocessor control which alternated the collection of $I_{\parallel}(t)$ and $I_{\perp}(t)$ every 60 seconds until approximately 40,000 counts were accumulated in the maximum channel of $I_{\perp}(t)$.

3.2 Corrections for Polarization Bias of Detection System

The relative number of photons collected in the $I_{\parallel}$ and $I_{\perp}$ channels will in general be biased by the polarization dependence of the detection system. This effect must be taken into account by rewriting equation 6:

$$r(t) = (I_{\parallel}(t) - G\, I_{\perp}(t))\,(I_{\parallel}(t) + 2G\, I_{\perp}(t)) = D(t)/S(t) \qquad (8)$$

where G is the "instrumental anisotropy" of the system. Several methods have been employed to determine G.[1,11] The approach used here is referred to as "tail matching," a method in which data are collected to insure that G=1.

If the rotational correlation times are shorter than the fluorescence lifetime, then at long times after excitation $I_{//}(t)$ and $I_{\perp}(t)$ should become identical ($r(t) \to 0$). For the perylene sample used in this study, tail matching was achieved by integrating and matching the total number of counts in $I_{//}$ and $I_{\perp}$ in channels corresponding to times between 22 and 24 ns after excitation. This procedure was checked by comparing the integrated counts for time intervals at earlier and later stages of the fluorescence decays. Matches over several regions of the decays showed that for sufficiently long times, $I_{//}(t)$ and $I_{\perp}(t)$ were indeed superimposible. The tail matching regions used were as "early" as possible in order to achieve a high signal to noise ratio in the integrated regions (S/N > 100/1). Tail matching will not be valid for many other systems, e.g., those with residual,long term anisotropies. It does work well with our samples and has the additional benefit of correcting for fluctuations in the exciting light intensities which are not already accounted for by alternating the detection polarization as described above.

3.3 Analysis of Data

All decay curves were assumed to follow the following equation:

$$I(t) = \int_{c}^{t+\delta} P(t')G(t+\delta-t')dt'$$

Where the observed decay intensity, $I(t)$ is a convolution of the true decay, $G(t)$, with the instrument response function $P(t)$. The time shift parameter δ represents the shift in zero time between the excitation function and the decay curve. Use of this parameter corrects for the different photomultiplier transit times of the exciting and emitting photons but can be strictly justified

only when this difference is small.[1,2] For our experiments the use of δ was justified by the improved quality of the single exponential fits to the magic angle decays.

Deconvolution of decay curves was achieved by least squares iterative techniques which have been described in great detail elsewhere.[1,2,23,24] This method convolves a trial decay function (single exponential, double exponential, etc.) with the instrument response function. The difference between the calculated and experimentally recorded decays is minimized by varying the parameters in the trial function. The quality of the fit is measured by the reduced chi squared, χ^2_ν where

$$\chi^2_\nu = \sum w_i[Y(t_i) - I(t_i)]^2/(n_2 - n_1 + 1 - p) \qquad (10)$$

where w_i is the weighting factor and $Y(t_i) - I(t_i)$ is the difference between the calculated and observed intensities in channel i, n_1 and n_2 are the first and last channels of the section of the decay to be analyzed, and p is the number of parameters in the least squares fit. Statistical criteria for judging goodness of fit have been discussed in considerable detail by Lampert, et al.[1]

Equation 9 applies to I(t), the fluorescence intensity observed under magic angle or rapid rotation conditions, $I_{//}(t)$, $I_{\perp}(t)$, and any linear combination of these latter two functions, i.e., D(t) and S(t). For I(t), $I_{//}(t)$, and $I_{\perp}(t)$ the weighting factors employed in equation 10 follow Poisson Statistics with

$$w_i = 1/\sigma_i^2 = 1/I(t_i) \qquad (11)$$

For D(t), S(t), and r(t) the Poisson errors in $I_{//}(t_i)$ and $I_{\perp}(t_i)$ must be propagated in order to obtain proper weights[12]:

$$\text{for } D(t),\ w_i = 1/(I_{//}(t_i) + I_{\perp}(t_i)) \qquad (12)$$

$$\text{for } S(t),\ w_i = 1/(I_{//}(t_i) + 4I_{\perp}(t_i)) \qquad (13)$$

$$\text{for } r(t),\ w_i = 3\,(I_{//}(t_i) + 2I_{\perp}(t_i))/(2 + 3r(t_i) - 3r^2(t_i) - 2r^3(t_i)) \qquad (14)$$

As discussed earlier, the anisotropy parameters can in principle be extracted from $I_{//}(t)$, $I_{\perp}(t)$, D(t), or r(t) (equations 2 6). (This assumes that the fluorescence lifetime can be determined from magic angle experiments[21,22] or from S(t)). For single exponential anisotropies, analyses of $I_{//}(t)$ and/or $I_{\perp}(t)$ do yield accurate correlation times. For anisotropies involving two exponentials, however, $I_{//}(t)$ and $I_{\perp}(t)$ require accurate fits to triple exponential functions. Even with excellent data, there are a relatively small number of samples for which the fluorescence and rotational lifetimes are well enough separated to give meaningful fits. These problems are illustrated with the following synthetic data:

Data curves for $I_{//}(t)$ and $I_{\perp}(t)$ were constructed by convolving an experimentally recorded instrument response function with decay functions representative of those actually obtained for our perylene samples:

$$G_{//}(t) = 1.0 \exp(-t/4.8) - 0.46 \exp(-t/0.63) + 0.16 \exp(-t/2.0)$$

and $$G_{\perp}(t) = 1.0 \exp(-t/4.8) + 0.23 \exp(-t/0.63) - 0.08 \exp(-t/2.0)$$

Poisson noise was added to (or subtracted from) the curves for $I_{//}(t)$ and $I_{\perp}(t)$. Triple exponential fits of $I_{//}(t)$ and $I_{\perp}(t)$ were unable to recover the correct parameters. However, double exponential analysis of the synthesized difference function, $I_{//}(t) - I_{\perp}(t)$, and a single exponential fit to S(t) accurately extracted the expected lifetimes and pre-exponential factors, as seen in the following comparison:

$$\text{expected } r(t) = 0.23 \exp(-t/0.72) + 0.80 \exp(-t/3.4)$$

$$D(t)/S(t) = 0.23 \exp(-t/0.71) + 0.82 \exp(-t/3.4)$$

We thus conclude that for data similar to that obtained for perylene, the reduction in the number of parameters seems to provide an important reason for analyzing D(t) rather than separately fitting $I_{//}(t)$ and $I_{\perp}(t)$.

3.4 Samples

In anticipation of developing samples which might serve as useful standards for anisotropy measurements, we have employed comercially available fluorophore/solvent combination which require no further purification and provide a wide range of viscosities and rotational correlation rates under ambient temperature conditions.

Perylene was Aldrich Gold Label (99+%). The glycerol was Aldrich Gold Label (99.5+%), Spectrephotometric grade and was shown by NMR techniques to contain less than 1% water. The water used for the glycerol/water solutions was MCB Omnisolve, HPLC grade. All of these were used as supplied by the manufacturers, without additional purification. The glycerol/water mixtures showed negligible fluorescence under the excitation conditions used for accumulating data on the perylene samples.

The perylene solutions were all $1x10^{-6}$M and had absorbances of less than 0.05 at 257 nm. No attempt was made to remove O_2 from the samples. The glycerol/water solutions used in these measurements were 80, 85, and 90% (volume glycerol/volume solution) and have <1% uncertainty in their compositons. This uncertainty is due to the water (<1%) in the "pure" glycerol. Solutions were kept tightly capped to avoid the pick up of additional water from the atmosphere. Steady state polarization measurements showed that these relatively viscous samples picked up negligible quantities of water even when cuvettes were left open to air for several days.[25]

All measurements reported in this paper were performed at 25±1°C. The relationships between solution composition and viscosity are given by Miner and Dalton.[26] The 80, 85, and 90% (v/v) solutions correspond to 82.9, 87.3, and 91.5% solutions in terms of weight percentages of glycerol. These solutions have viscosities of 63.5, 111.1, and 204.0 centipoise at 25°C.

4. Results and Discussion

4.1 Summary of Anisotropy Data

Polarized fluorescence decays ($I_{//}(t)$ and $I_{\perp}(t)$ were obtained for perylene in glycerol/water solutions which were 80, 85, and 90% (v/v) glycerol and which were maintained at 25±1°C. The anisotropy parameters were analyzed by separately fitting D(t) and S(t) and then constructing r(t) from their quotient. Difference curves were well described by double exponential decays whereas S(t) was well fit by a single exponential [illegible] expected for fluorescence from a single component.

A plot of D(t) for a typical sample (perylene in 85% glycerol [illegible] given in figure 3. These data show an inversion in sign [illegible] and $I_{\perp}(t)$), indicative of the different signs of the two [illegible] in equation 7. This characteristic feature of perylene's [illegible] anisotropy) function can be traced to the relative [illegible] absorption and emission transition dipoles. [illegible] approximately short axis (x) polarized with [illegible] long axis (y) polarized (see figure 1). [illegible] dipoles, the initial anisotropy [illegible] rotation about the [illegible] rotation perpendicular [illegible] ($I_{//}(t) + 2I_{\perp}(t)$) [illegible] of the [illegible]

AD-A185 409 MOLECULAR MOTION AND ENERGY MIGRATION IN POLYMERS(U) 2/2
ROYAL INSTITUTION OF GREAT BRITAIN LONDON (ENGLAND)
D PHILLIPS JUN 85 DAJA37-82-C-0265

UNCLASSIFIED F/G 7/6 NL

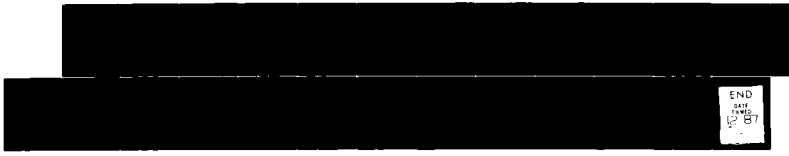

END
DATE FILMED
10 87

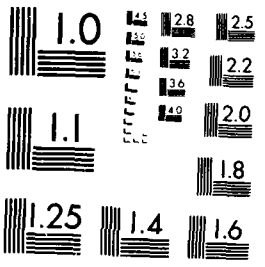

This would be followed by relatively slower ($t=(6D_{\perp})^{-1} \alpha D_{\perp}^{-1}$) decay to $r(t)=0$. Such a model accounts qualitatively for the difference (and anisotropy) curves presented in this paper. The precise form of these decay curves depends on the actual orientation of transition dipoles and the rates of rotational diffusion. These parameters can be determined from the double exponential fits as discussed in following sections of this paper.

The unpolarized fluorescence decays from both S(t) and magic angle measurements of all samples were well described by single exponential kinetics. A comparison of these two methods for the 85% solution is given in figure 4. The fluorescence lifetimes given in Table 1 are the average values of all measurements on a given sample. Our ability to obtain good fits for these curves indicates that the wavelength dependent response of our photomultiplier is well accounted for by the "time-shift" parameter introduced in equation 9. The fluorescence lifetimes are essentially independent of solution composition and viscosity. The average lifetime (4.77±0.05 ns) is in excellent agreement with the value obtained by Brand et al.[15] for perylene in pure glycerol (4.7±0.1 ns) and has been shown to be independent of temperature (over the range 10-40°C).

A summary of our anisotropy measurements is given in Table 1. These parameters are derived from those obtained for D(t) and S(t) as follows:

$$D(t) = d_1 e^{-t/\tau_1} + d_2 \cdot e^{-t/\tau_2} \; ; \; S(t) = s_o e^{-t/\tau_f}$$

$$r(t) = d_1/s_o \exp(-t(1/\tau_1 - 1/\tau_f) + d_2/s_o \exp(-t(1/\tau_2 - 1/\tau_f)$$

$$= r_1 \exp(-t/\tau_1^{rot}) + r_2 \exp(-t/\tau_2^{rot}) \qquad (15)$$

The pre-exponential lifetimes and rotational lifetimes given in equation 15 can be compared with those given by the two exponential model (equation 7) to determine the rotational diffusion rates $D_{\parallel}$ and $D_{\perp}$ as well as the relative orientation of the transition dipoles in perylene.

4.2 Preexponential factors/orientation of transition dipoles

The data in Table 1 show that r_1 and r_2 are essentially independent of solvent composition. This supports the model described by equation 7 which shows the pre-exponential factors to depend only on properties of the solute (directions of absorption and emission dipoles) and to be insensitive to solvent viscosity, temperature, composition, etc. The limiting anisotropy ($r(0) = r_1+r_2$) obtained in our experiments (average = -0.157±0.011) compares well with steady state measurements on frozen solutions with viscosities sufficiently high to prevent rotational diffusion. For example, r(0) = -0.149 for perylene in glycerol at -78°C and with an excitation wavelength of 256 nm.[25] The r(0)'s should be compared with a limiting anisotropy of -0.200 for absorption and emission polarizations which are exactly orthoganol (ϕ_{AE} = 90°). In the absence of other depolarizing effects, our value of r(0) (r_1+r_2) leads to ϕ_{AE} =78±2°. ϕ_{AE} also can be directly calculated by comparing our r_2(-0.233±0.006) with the r_2 given in equation 7. This gives ϕ_{AE} = 71±1°.

It appears, therefore, that perylene's absorption and emission dipoles are not orthogonal for excitation at 257 nm. It is important to note, however, that limiting values of r(0) (e.g., 0.400 for colinear dipoles, -0.200 for perpendicular dipoles) are rarely obtained, even when the excitation and emission involve the same electronic transition. It has been suggested[29,30] that rapid (subnanosecond) internal motions, e.g., low frequency torsional vibrations ("librations") provide additional depolarization mechanisms which

might not be directly observed on nanosecond time scales and which also might not be quenched in low temperature, "rigid" environments. This possibility finds some support in picosecond anisotropy measurements which have recovered r(0) = 0.40 in several systems.[30,31] If these effects are present in our experiments they might be corrected for by calculating ϕ_{AE} from the ratio of r_2 and r_1 rather than from their absolute values (note that $r_1 < 0.10$ and this cannot be rationalized by nonorthogonal dipoles--see equation 7). This gives $r_2/r_1 = 3 \cos 2\phi_{AE}$ and for our data leads to $\cos 2\phi_{AE} = -1.01$ or $\phi_{AE} \sim 90°$. If this result is correct, then the absolute values of our pre-exponential factors may be systematically low. However, ~~although our pre-exponential factors may be systematically low~~, it is important to stress that $\phi_{AE} = 90°$ is rather unlikely. Whereas, the strongly allowed $S_0 \leftrightarrow S_1$ transition is most likely due to a linear transition dipole, the relatively weak absorption at 257 nm probably involves vibronic coupling with other electronic states. This would lead to mixed polarization throughout the absorption band. These effects are clearly evident in plots of anisotropy as a function of wavelength.[13] For $\lambda > 360$ nm the anisotropy is relatively high and constant. In the region of the 257 nm absorption, however, the anisotropy is very sensitive to wavelength and it is unlikely that r=0.20 at 257 nm or any other wavelength. It thus seems reasonable to conclude that $70° < \phi_{AE} < 90°$ with a better specification of this angle awaiting shorter time scale anisotropy measurements.

4.3 Rotational Correlation Times/Diffusion Coefficients

The rotational correlation times indicated in Table 1 can be related to the rates of rotation about the symmetry axis ($D_{\parallel}$) and about any perpendicular axis ($D_{\perp}$). Use of a "cylindrical" model (i.e., symmetry axis is C_{∞} rather

than C_2) is justified both by the good fits to equation 7 and the large differences between $D_{\parallel}$ and $D_{\perp}$. Following Small and Isenberg[19], we might consider the case of rotation about two perpendicular in plane axes (e.g.,x and y) where the rotation rates differ by a factor of two. Even in this case (certainly an exaggeration for perylene), the rotational decays (see equation 6) would be governed by $D_{\parallel}$, and thus will give rise to no more than three discernable decay times (the cylindrical case). The further restrictions brought about by the in plane orientation of the transition dipoles further simplify the anisotropy decay to the two exponential model given in equation 7.

The rotational diffusion rates can be calculated from rotational correlation times given in Table I:

$$\tau_1^{rot} = (6D_{\perp})^{-1} \text{ and } \tau_2^{rot} = (2D_{\perp} + 4D_{\parallel})^{-1}$$

The results of these calculations are presented in Table 2. Figure 5 illustrates the viscosity dependence of the diffusion rates.

It is important to note that $D_{\parallel}/D_{\perp}$, like r_1 and r_2, is independent of solvent viscosity ($D_{\parallel}/D_{\perp} = 6.7 \pm 0.3$ for our samples). These parameters thus should prove particularly useful in comparing experimental techniques and analysis procedures for anisotropy measurements on a variety of perylene samples. The viscosity independence of $D_{\parallel}/D_{\perp}$ shows that the in-plane and out-of-plane rotations are equally affected by changes in solvent environment. This clearly would not be the case if $D_{\parallel}$ were well described by "slipping' boundary conditions as opposed to the "sticking" boundary conditions appropriate to $D_{\perp}$.[14,15,32] Both motions must require displacement of solvent molecules as is most clearly seen in a comparison of diffusion constants associated with free rotation ($D \sim 10^{11} sec^{-1}$) with those obtained here ($D \sim 10^7$-$10^8 sec^{-1}$).

4.4 Summary of Anisotropy Parameters for Perylene

A tabulation of $D_{//}/D_{\perp}$ values obtained using several measurement techniques and analysis procedures is given in Table 3. The parameters from earlier, steady state studies[13,14] tend to be less accurate than those from time-resolved measurements.[15-17,33] This reflects the inherent difficulties in extracting time dependent information from steady state data. $D_{//}/D_{\perp}$ values from several time-resolved studies (Zinsli, et al.,[16] Barkley, et al.,[15] and the present work) and from a recent phase modulation study (Lakowicz et al.[17]) are in general agreement. These studies also demonstrate that $D_{//}/D_{\perp}$ is essentially independent of both solvent viscosity and temperature. Combinations of solvents and temperatures which change $D_{//}$ and $D_{\perp}$ by more than two orders of magnitude have no perceptible effect on their ratio. Any discrepancies between $D_{//}/D_{\perp}$'s from different studies, therefore, must arise from differences in the methods by which these parameters are obtained.

The generally good agreement in the rotational correlation times and diffusion rates contrasts the equally striking disparity in values given for the pre-exponential factors. These factors are considerably more sensitive to the quality of data and analysis procedures and thus provide a natural focal point for comparing different methods used for studying fluorescence anisotropy. The pre-exponential factors should be completely specified by properties of isolated perylene molecules (i.e., the relative orientations of the absorption and emission transition dipoles) and should be ~~sensitive~~ insensitive to solvent, temperature, or the procedures by which these parameters are obtained.

Comparing pre-exponential factors from different experiments is somewhat complicated by the wavelength dependence of these numbers (see equation 7). Previous experiments, however, fall into two distinct groups: those in which perylene is excited into the lowest energy absorption band ($r(0) \sim 0.400$ and

$\phi_{AE} \sim 0$) and those in which excitation is into the spectral feature centered at 256-257 nm ($r(0) \gtrsim -0.200$ and $\phi_{AE} < 90°$). The first set of experiments all involve excitation in spectral regions (λ>350nm) where r(0) is wavelength independent[13] and should lead to common preexponential values. These measurements along with data for short wavelength excitation conditions are summarized in Table 4.

Zinsli's temperature dependent preexponentials arise from a model[16] which superimposes temperature dependent, librational motions (cf. the low frequency, torsional motions discussed in section 2.4) on the rotational diffusion model employed in this and other studies. The simpler, double exponential model accounts for the observed kinetics and temperature independence of the preexponentials over the 10-40°C range investigated. Librational motions of perylene may well be important, (e.g., in explaining r(0)'s < 0.400 for long wavelength excitation of perylene) but appear to require a model different from that proposed by Zinsli.

Gratton, Lackowicz and others[17,34-38] recently have applied multifrequency, phase modulation techniques to the measurement of multiexponential anisotropy decays. In the case of perylene[17], rotational correlation times and diffusion rates are comparable to those determined by time-resolved methods. Pre-exponential factors obtained by these two methods, however, are not in good agreement. The ratio, r_2/r_1, determined by modulation techniques[17] leads to $\phi_{AE} = 29°$ which is clearly inconsistent with the expected colinearity of absorption and emission dipoles for excitation into perylene's lowest energy absorption band. Although frequency-domain techniques show considerable promise for unraveling complex (multiexponential and nonexponential) anisotropy decays, more work is needed to reconcile these initial results with those obtained from time-domain measurements.

The anisotropy parameters (rotational diffusion rates and pre-exponential factors) of Barkley et al.[15] are in relatively good agreement with those of the present investigation. Any comparison, however, must consider some fundamental differences in the analysis procedures employed in the two studies. The apparent use of Poisson distributed weights, rather than the weights given by equations 12, 13, and 14 must lead to systematic errors in fits to D(t), S(t), and r(t). This can be illustrated by comparing fits to simulated S(t) and D(t) curves using correct and incorrect (Poisson) statistical weights (Table 5). The simulated parameters (which duplicate those we have obtained for perylene) can only be recovered by using the proper weights. The use of Poisson statistics makes little difference in fitting S(t). For fits to D(t), however, these weights lead to systematic errors in the relevant parameters. The pre-exponential factors are particularly sensitive, e.g., r_2/r_1 changes from -2.9 to -2.0 in changing from the correct weights (equation 13) to the Poisson weights used in the earlier work. Such differences may contribute to the apparent discrepancies between r_1,r_2, and r_2/r_1 values obtained in the two studies.

The "global analysis" procedures employed by Barkley et al.[10,15] also require comment. The anisotropy parameters were obtained by simultaneously fitting decay data obtained at two excitation wavelengths

$$r(t) = r_1 e^{-t/\phi_1} + r_2 e^{-t/\phi_2} \qquad \lambda_{ex} = 430 \text{ nm}$$

$$r(t) = r_1 e^{-t/\phi_1} - r_2 e^{-t/\phi_2} \qquad \lambda_{ex} = 256 \text{ nm}$$

The rotational correlation times, ϕ_1 and ϕ_2, should indeed be independent of the wavelength used for excitation. On the other hand, equation 7 shows

that $r_2(430) = -r_2(256)$ if and only if $\phi_{AE}(430) = \phi_{AE}(256) \pm \pi/2$. Excitation at either wavelength results in the same emission dipole ($S_1 \rightarrow S_0$). We thus can express the restrictions expressed in the above pair of equations as $\phi_A(430) = \phi_A(256) \pm \pi/2$ where ϕ_A is the relative orientation of the (in-plane) transition dipoles for the two absorptions.

This restriction would be satisfied if the 430 nm absorption ($S_0 \rightarrow S_1$) were long axis (y) polarized and if the 256 nm absorption ($S_0 \rightarrow S_n$) were short axis (x) polarized. The first of these conditions may well be attained. There is less justification for the 265 nm absorption being perfectly, short axis polarized. The steady state polarization (and anisotropy) of perylene depends on excitation wavelength for absorption in the 256 nm region.[13] The absorptions are sufficiently weak to implicate the mixed polarizations associated with vibronic coupling as discussed in section 4.2. That $\phi_A(430) \neq \phi_A(256) \pm \pi/2$ also is suggested by the pre-exponential factors obtained by Barkley et al. (r_2=-0.24 and r_2/r_1=-2.4 versus $r_2 = -0.30$ and $r_2/r_1 = -3.0$ for short axis absorption followed by long axis emission). "Global analysis" clearly provides a useful approach for cases in which there are known, verifiable relationships between different decay curves, e.g., in simultaneously fitting $I_{\parallel}(t)$ and $I_{\perp}(t)$.[11] In the present situation, however, the assumption that $r_2(430) = r_2(256)$ may place artificial restrictions on these parameters.

5. Conclusions

The fluorescence anisotropy of perylene in solutions of glycerol/water is well described by a bi-exponential model. For excitation at 257 nm,

$$r(t) = (0.077\pm0.006)\exp(-t(6D_{\perp})) - (0.233\pm0.006)\exp(-t(2D_{\perp}+4D_{\parallel})) \quad (16)$$

A double exponential model should be rigorously correct for rotations in

molecules with cylindrical symmetry (i.e., possessing a C_∞ axis) and with electronic transitions polarized in the plane perpendicular to the C_∞ axis.[5,6] The first of these conditions is effectively met[19] by the comparable rotational diffusion rates about any of the in-plane axes (e.g., $D_x \approx D_y$--see figure 1). The second requirement is satisfied by the $^1\pi\pi^*$ transitions monitored in this experiment.

The above equation appears to describe perylene for a broad range of solvent viscosities and temperatures.[15] Although $D_{//}$ and $D_\perp$ depend on solvent, $D_{//}/D_\perp$ is constant ($\sim$7/1), indicating that the in-plane and out-of-plane rotations are equally affected by changes in environment. Both rotations must displace solvent molecules, thus blurring the distinction between "sticking" and slipping" often applied to the two motions.[14,15,32] In contrast to the rotational diffusion rates, the pre-exponential factors are insensitive to solvent, being completely specified by the relative orientation of electronic transition moments.[5,6] Our results indicate that the absorption and emission dipoles are displaced by at least 70°. Orthogonal dipoles cannot be excluded, but there is little evidence from this or other studies to support such a conclusion.

The experiments establish a physical basis for the bi-exponential model. The primary purpose of this study, however, is to establish perylene/glycerol/water as a potential standard for time-resolved anisotropy measurements which cannot be simply described by single exponential kinetics. Our samples provide several advantages:

1. The components are readily available and can be used without futher purification.

2. The photophysical properties of perylene are well understood and lead to straightforward interpretation of the parameters describing the bi-exponential anisotropy decay.
3. The apparent constancy of r_1, r_2, and $D_{\parallel}/D_{\perp}$ over a range of solvent compositions and temperatures means that the results expressed by equation 16 should be applicable to both longer and shorter (subnanosecond) time scales.
4. *The pre-exponential factors, unlike the more easily measured* rotational correlation times, are particularly sensitive to experimental techniques and analysis procedures.

The anisotropy parameters (r_1, r_2, and $D_{\parallel}$, and $D_{\perp}$) were obtained by separately deconvolving properly weighted sum and difference curves and then reconstructing the anisotropy according to the two exponential model. This procedure reduces the number of parameters in the least squares analysis, a critical simplification for systems exhibiting multi or non-exponential kinetics. Other analysis techniques, e.g., the simultaneous analysis of parallel and perpendicular decays[11] and "global" analysis,[10] may well have advantages, but these may not be realized for complicated anisotropy decays such as those of perylene.

Our analysis focuses on the relevant differences between the parallel and perpendicular decays. Individual decays tend to be dominated by changes due to the fluorescence lifetime. Goodness of fit calculations thus may be less sensitive to parameters governing the anisotropy and may depend on the fitting range employed, especially when the anisotropy decays more quickly *than the fluorescence. It also should be stressed that simultaneous fitting* and "global analysis" will be advantageous only if the relationships between the various decay curves are well-established. Simultaneous analysis of

parallel and perpendicular decays obtained under identical ~~eation~~ excitation conditions clearly is justified. On the other hand, the simultaneous fitting of anisotropies obtained at different excitation wavelengths may well put artificial restraints on the parameters extracted from such fits.

Improvements in time-resolved fluorescence techniques have pushed anisotropy measurements beyond the determination of single, average correlation times. Movements of macromolecules in solution have been shown to involve non-exponential and multi-exponential anisotropy decays. Considerable theoretical effort has provided models for the restricted motion of membrane probes,[7] the internal motion of biopolymers,[8,9] and the rotational motion of unsymmetrical fluorophores.[6] The samples described in this paper may lead to a critical comparison of the methods and models by which these complicated motions can be measured and understood.

Acknowledgements

This research was supported by the Engineering Research Council, The Royal Society, the United States Army European Research Office, and a DuPont Fund Grant to Bowdoin College.

References

1. Lampert, R.A.; Chewter, L.A.; Phillips, D.; O'Connor, D.V.; Roberts, A.J.; Meech, S.R. Anal. Chem. 1983, 55, 68.

2. O'Connor, D.V.; Phillips, D. "Time-Correlated Single Photon Counting," Academic Press: London, 1984.

3. "Time-Resolved Fluorescence Spectroscopy in Biochemistry and Biology," Cundall, R.B., Dale R.E., Eds.; Plenum Press: New York, 1980.

4. Tao, T. Biopolym. 1969, 8, 609.

5. Belford, G.G.; Belford, R.L.; Weber, G. Proc. Natl. Acad. Sci. USA 1972, 69, 1392.

6. Szabo, A. J. Chem. Phys. 1984, 81, 150.

7. Kinoshita, K.; Kawato, S.; Ikegami, A. Biophys J. 1977, 20, 289.

8. Valeur, B.; Monnerie, L. J. Polym. Sci. Polym. Phys. 1976, 14, 11.

9. Dubios-Violette, E.; Geny, F.; Monnerie, L.; Parodi, O. J. Chem. Phys. 1969, 66, 1865.

10. Knutson, J. R.; Beechem, J.M.; Brand, L. Chem. Phys. Lett. 1983, 102, 501.

11. Cross, A.J.; Fleming, G.R. Biophys J. 1984, 46, 45.

12. Wahl, Ph. Biophys. Chem. 1979, 10, 91.

13. Shinitsky, M.; Dianoux, A.-C.; Gitler, C.; Weber, G. Biochem. 1971, 10, 2106.

14. Mantulin, W.W.; Weber, G. J. Chem. Phys. 1977, 66, 4092.

15. Barkley, M.D.; Kowalczyk, A.A.; Brand, L., J. Chem. Phys, 1981, 75, 3581.

16. Zinsli, P.E. Chem. Phys. 1977, 20, 299.

17. Lakowicz, J.R.; Cherek, H.; Maliwal, B.P.; Gratton, E. Biochem. 1985, 24, 376.

18. Cotton, F.A., "Chemical Applications of Group Theory," 2nd ed.; Wiley-Interscience: New York, 1971.

19. Small, E.W.; Isenberg, I. Biopolymers 1977, 16, 1907.

20. Ware, W.R. In "Creation and Detection of the Excited State"; Lamola, A.A., Ed.; Marcel Dekker: New York, 1971; Vol. 1A, p. 213.

21. Spencer, R.D.; Weber, G., J. Chem. Phys. 1970, 52, 1654.

22. Mielenz, K.D.; Cehelnik, E.D.; McKenzie, R.L., J. Chem. Phys. 1976, 64, 370.

23. O'Connor, D.V.; Ware, W.R.; Andre, J.C., J. Phys. Chem. 1979, 83, 1333.

24. McKinnon, A.E.; Szabo, A.G.; Miller, D.R., J. Phys. Chem. 1977, 81, 1564.

25. Albin, J. Senior Honors Thesis, Bowdoin College, 1984.

26. Miner, C.S.; Dalton, N.N. "Glycerol"; Reinhold Publishing Corporation: New York, 1953; pp. 278-282.

27. Albrecht, A.C. J. Mol. Spect. 1961, 6, 84.

28. Albrecht, A.C. Prog. React. Kinet. 1970, 5, 301.

29. Yguerabide, J. Meth. Enzymology 1972, 26, 498.

30. Fleming, G.R.; Morris, J.M.; Robinson, G.W. Chem. Phys. 1976, 17, 91.

31. Porter, G.; Sadkowski, P.J.; Tredwell, C.J. Chem. Phys. Lett. 1977, 49, 416.

32. Fleming, G.R.; Knight, A.E.W.; Morris, J.M.; Robbins, R.J.; Robinson, G.W. Chem. Phys. Lett. 1977, 51, 399.

33. Lakowicz, J.R.; Knutson, J.R. Biochemistry 1980, 19, 905.

34. Gratton, E.; Limkeman, E. Biophys. J. 1983, 44, 315.

35. Gratton, E.; Jameson, D.M.; Hall, R.D. Annu. Rev. Biophys. Bioeng. 1984, 13, 106.

36. Lakowicz, J.R.; Prendergast, F.G.; Hogen, D. Biochem. 1979, 18, 508.

37. Gratton, E.; Limkeman, M.; Lakowicz, J.R.; Maliwal, B.P.; Cherek, H.; Laczko, G. Biophys. J. 1984, 46, 479.

38. Gratton, E.; Jameson, D.M. Anal. Chem. 1985, 57, 1694.

Table 1. Anisotropy decay parameters and fluorescence lifetimes of perylene in glycerol/water mixtures at 25°C (λ_{ex}=257nm)

Solution Composition (V/V)	viscosity (centipoise)	τ_f (10^{-9}s)	r_1	τ_1^{rot} (10^{-9}s)	r_2	τ_2^{rot} (10^{-9}s)	r(o)
80%	63.5	4.81± 0.02	0.08± 0.02	2.5± 0.5	-0.23± 0.02	0.56± 0.07	-0.15± 0.03
85%	111.1	4.79± 0.04	0.07± 0.01	3.4± 0.5	-0.24± 0.01	0.72± 0.02	-0.17± 0.02
90%	204.0	4.71± 0.02	0.082± 0.003	6.2± 0.2	-0.23± 0.01	1.32± 0.07	-0.15± 0.01
	Averages:	4.77± 0.05	0.077± 0.006		-0.233± 0.006		-0.157± 0.011

Table 2 The Principle Diffusion Coefficients of Perylene in Glycerol/ Water Solution at 25°C. (λ_{ex} = 257nm)

Solution Composition (V/V)	Viscosity (centipoise)	$D_{\perp}$ (10^7 sec^{-1})	D_{11} (10^7 sec^{-1})	$D_{11}/D_{\perp}$
80%	63.5	7.0± 1.0	42 ± 6	7.0± 1.4
85%	111.1	4.9± 0.8	32 ± 2	6.5± 1.1
90%	204.0	2.7± 0.1	18 ± 1	6.7± 0.4
				ave = 6.7± 0.3

Table 3. $D_{11}/D_{\perp}$ values for perylene

References/authors	Technique	Solvent	$D_{11}/D_{\perp}$
Mantulin and Weber[14] 1977	Single Frequency Phase Modulation	propylene glycol	28
Shinitzky, et al.[13] 1971	Steady state polarization measurements at different excitation wavelengths.	propylene glycol and propylene glycol/glycerol mixtures	10
Lakowicz and Knutson[33] 1980	"Lifetime-resolved" emisssion anisotropy using quenchers	propylene glycol	1-10
Zinsli[16] 1977	Time resolved emission anisotropy; analysis of the difference curve	parafin	10± 2
Barkley[15] et al 1981	Flashlamp pumped, time resolved fluorescence anisotropy; global analysis of the difference curves	'pure'glycerol	10± 1
Lakowicz et[17] al 1985	Multifrequency Phase Modulation	propylene glycol (9°C)	8.8
This Study	Mode locked, cavity dumped laser excitation; Time resolved fluorescence anisotropy; analysis of difference curves	glycerol/water mixtures	6.7± 0.3

Table 4. Pre-exponential factors obtained for the decay of fluorescence anisotropy in perylene

$$r(t)=r_1e^{-t/t_1} + r_2e^{-t/t_2}$$

Study	λ_{ex}	r_1	r_2	r_2/r_1	$r_{(o)}=r_1+r_2$
"limiting case" ($\phi_{AE}=0^0$)		0.10	0.30	3.0	0.40
Barkley, et al.[15]	430nm	0.10	0.24	2.4	0.34
Lakowicz, et al.[17]	442nm	0.12	0.19	1.6	0.31
~~Shinitsky et al.~~ Zinsli, et al.[16]	395nm	temperature dependent coefficients			
"limiting case" ($\phi_{AE}=90^0$)		0.10	-0.30	-3.0	-0.20
Barkley, et al.[15]	256nm	0.10	-0.24	-2.4	-0.14
this study	257nm	0.077	-0.233	-3.0	-0.16

Table 5

Data Set	Synthetic Parameters *					Fits to S(t) and D(t) Parameters recovered using correct weighting factors				
	τ_{f1} ns	r_1	τ_1^{rot} ns	r_2	τ_2^{rot} ns	τ_{f1} ns	r_1	τ_1^{rot} ns	r_2	τ_2^{rot} ns
1	4.77	0.08	6.20	-0.23	1.32	4.79±0.02	0.077± 0.007	6.26± 0.08	-0.22± 0.01	1.28 ± 0.04
2	4.77	0.08	3.40	-0.23	0.72	4.77± 0.02	0.082± 0.004	3.40± 0.04	-0.23± 0.01	0.71± 0.02
3	4.77	0.08	2.50	-0.23	0.56	4.78± 0.01	0.079± 0.003	2.52± 0.06	-0.23± 0.01	0.56± 0.02

* Synthetic S(t) and D(t) curves were constructed from convoluted parallel ($i_{\parallel}(t)$) and perpendicularly polarized ($i_{\perp}(t)$) decays. Poisson noise was added (or subtracted) to $I_{\parallel}(t)$ and $I_{\perp}(t)$ before synthesis of sum and difference functions.

Fits to S(t) and D(t) Parameters recovered using incorrect (Poisson) weighing factors				
τ_{f1} ns	r_1	τ_1^{rot} ns	r_2	τ_2^{rot} ns
4.79± 0.02	0.15± 0.01	4.00± 0.02	-0.03± 0.01	1.54± 0.01
4.79± 0.01	0.32± 0.01	1.72± 0.06	-0.47± 0.01	1.04± 0.01
4.78± 0.01	0.13± 0.01	1.82± 0.01	-0.27± 0.01	0.64± 0.03

APPENDIX III

SPECTROSCOPIC STUDIES OF POLYDIACETYLENE SOLUTIONS AND GLASSES. GLASSES OF A HYDROGEN-BONDING POLYMER

S.D.D.V. RUGHOOPUTH, D. PHILLIPS
Davy Faraday Laboratory, The Royal Institution of Great Britain, 21 Albemarle Street, London W1X 4BS, UK

D. BLOOR and D.J. ANDO
Department of Physics, Queen Mary College, Mile End Road, London E1 4NS, UK

Received 23 November 1984

In this communication we report some electronic spectral studies on a soluble polydiacetylene: poly[4,6-decadiyne-1,10-bis(butoxycarbonylmethylene urethane)], 4BCMU. The results obtained are comparable to our previous studies on another soluble polydiacetylene: poly[10,12-docosadiyne-1,22-bis(phenylacetate)], 9PA. The essential difference between these two systems is that 4BCMU contains sidegroups capable of forming hydrogen bonds parallel to the polymer chain whereas the 9PA sidegroups cannot.

1. Introduction and experimental methods

A number of reviews are now available which reflect the widespread interest in the field of solid-state polymerization of disubstituted diacetylenes [1–4]. Polydiacetylenes (thereafter referred to as PDAs) have the general structure

$$[RC{-}C{\equiv}C{-}CR]_n. \qquad (1)$$

Owing to the insolubility of most PDAs in common organic solvents, attempts to study their solution properties remained unsuccessful until Patel et al. discovered that appropriate choice of the sidegroups R and R′ provides soluble polymers [5,6]. The intense optical absorption maximum of the conjugated polymer backbone typically shifts some 5500 cm^{-1} to higher energy on dissolution of such PDA crystals. This has been attributed to disruption of the initially fully extended conjugated backbone to give a distribution of short conjugated segments [5–7].

The intense optical absorption of PDAs is well recognised as being excitonic in character. Very little work (either experimental or theoretical) has appeared related to exciton dynamics in such conjugated systems. This is principally due to the absence of fluorescence emission from PDA single crystals. Disordered and defected PDAs are known to be weakly fluorescent [8–14]. As part of our studies of fluorescence in such systems, we report here studies of absorption and fluorescence excitation and emission of a soluble PDA containing urethane sidegroups, 4BCMU, where

$$R = R' = -(CH_2)_4\,OCO\,NH\,COO\,C_4H_9$$

in structure (1). These supplement the similar studies, reported previously [8], carried out on another soluble PDA polymer, 9PA, where

$$R = R' = -(CH_2)_9\,OCO\,CH_2-.$$

The principal difference between these two polymers is that hydrogen bonds can be formed between the sidegroups, parallel to the polymer chain in 4BCMU and other urethane-sidegroup containing polymers [5,6,15], whereas the sidegroups of 9PA do not interact in this manner. The former compounds undergo a bathochromic shift when either

(a) a non-solvent is added to a solution in good solvent, or

(b) the solution is cooled, or

(c) the concentration of the polymer is increased.

0 009-2614/85/$ 03.30 © Elsevier Science Publishers B.V.
(North-Holland Physics Publishing Division)

The formation of hydrogen bonds has been implicated as the driving force behind a transition from a random coil to a more ordered form which produces these spectral changes [5–7]. The studies of 9PA have established that chromism is a more general photome-

non that does not necessarily require the formation of hydrogen bonds between the side groups as the essential driving force [5,16,17].

4BCMU polymer was prepared as described elsewhere [18]. Thus the polymer solutions were prepared

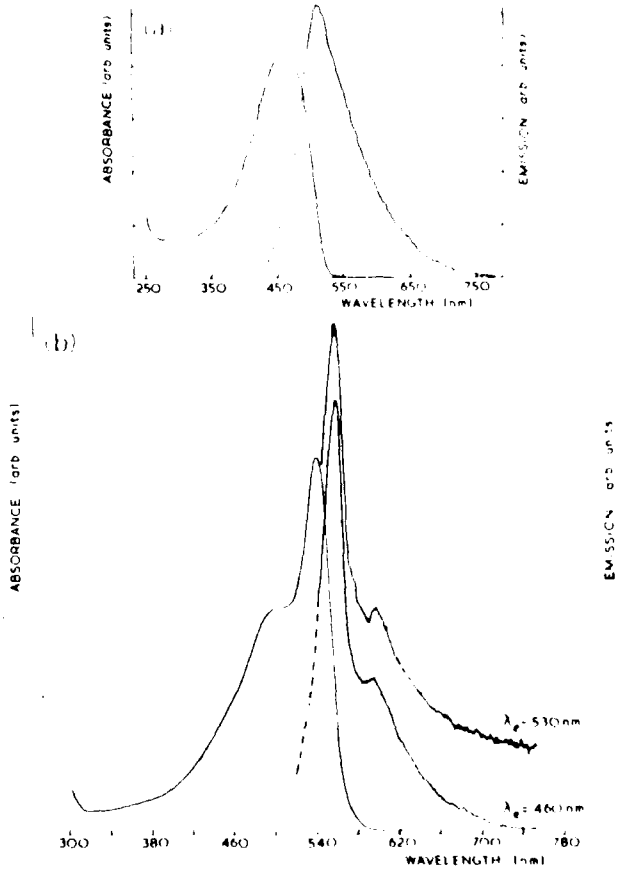

Fig. 1. (a) Absorption and fluorescence emission spectra of 4BCMU polymer in $CHCl_3$ at room temperature (25°C). Emission spectrum (uncorrected) corrected for Raman (dashed region) excited at λ_e = 410 nm (5 nm bandwidth) detected with 5 nm bandwidth, optical density (OD) at 410 nm is 0.086. Absorption spectrum scanned with a 2 nm slitwidth. (b) Absorption and fluorescence emission spectra of 4BCMU polymer in toluene at room temperature (R.T.) (dried). Emission spectrum (uncorrected) corrected for Raman (dashed region) excited at λ_e = 460 and 530 nm (5 nm bandwidth) detected with 5 nm bandwidth. OD at excitation wavelengths are less than 0.07. Absorption spectrum scanned with a 2 nm slitwidth.

using spectroscopic grade chloroform and 2-methyltetrahydrofuran (2-METHF) which had been refluxed carefully over $LiAlH_4$ and fractionally distilled prior to use. Absorption spectra were recorded using a Perkin–Elmer model 554 spectrophotometer, and fluorescence spectra were measured using either a Perkin–Elmer model MPF-4 or a home-built single photon counting microprocessor controlled spectrofluorimeter [19]. Low temperature glasses were formed by quenching solutions contained in a 2 mm diameter quartz tube in a Dewar flask containing liquid nitrogen.

2. Results and discussions

Solutions of 4BCML in 2-METHF and chloroform have a yellow colour, the absorption spectra are essentially identical with that of 9PA [8] – we denote this as the Y phase (see fig. 1a). Cooling the solution or adding a non-solvent (hexane) to a good solvent (2-METHF or chloroform) results in a red solution – we denote this as the R phase (see fig. 1b). Addition of good solvent or heating the cooled solutions converts them back to the Y phase. Our results are similar to those reported by other workers [5,6]. The quantum yield of fluorescence, ϕ_f, for the yellow solution of 4BCML in $CHCl_3$ was found to be approximately 2.0×10^{-3}, compared with the absolute yield of 4×10^{-3} of 1,8-anthronaphthalene sulphonate (ϕ_f for 9PA in $CHCl_3$ is approximately 2.45×10^{-3}) [8]. A yellow to red glass (depending on the initial polymer concentration) is obtained by rapidly freezing the Y-phase in 2-METHF to 77 K as displayed by fig. 2 (R_Y-phase). The fluorescence spectra are more intense at 77 K than at room temperature. The colour changes on freezing–melting cycles are similar to those observed for 9PA glass outlined in scheme 1 of ref. [8].

Quenching the R phase solution results in the spectra shown in fig. 3 (R_R phase). Fig. 4 compares the fluorescence emission spectra of 9PA and 4BCML for the corresponding R_Y- and R_R phases at 77 K. A feature apparent from the fluorescence emission of these

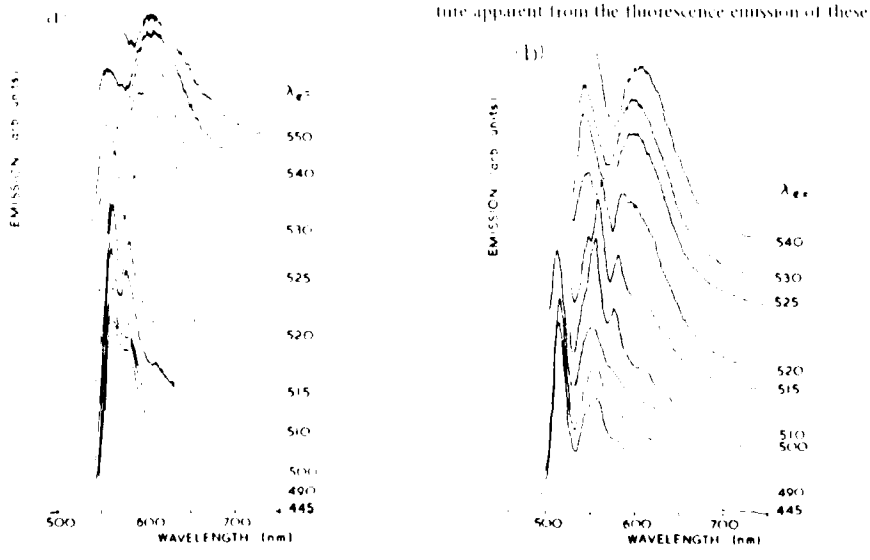

Fig. 2. Fluorescence emission spectra (uncorrected) of 4BCML-polymer in 2-METHF at 77 K of R_Y phase; corrected for scattered light (shielded from Dewar flask). Fluorescence excited at different wavelengths λ_{ex} (5 nm bandwidth) and detected with 5 nm bandwidth. The spectra are arbitrarily offset for clarity. Polymer concentrations (a) = 0.64 mg/ml, (b) = 0.064 mg/ml.

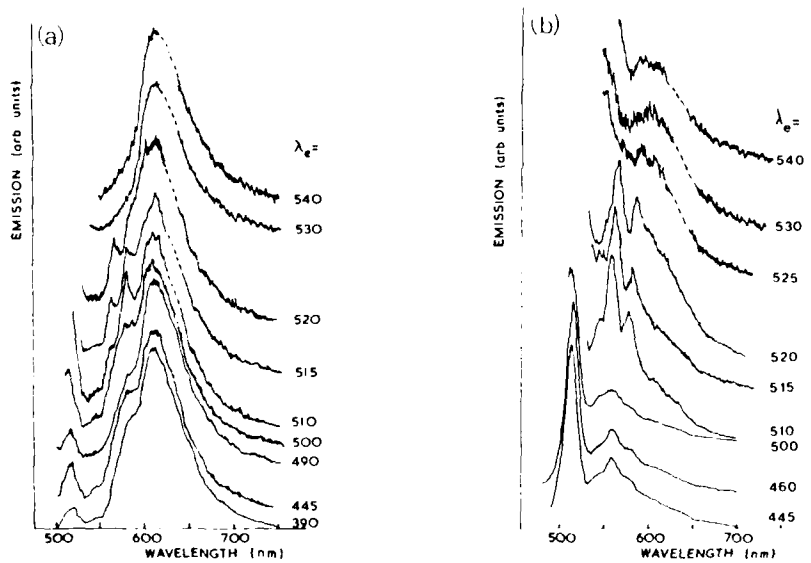

Fig. 3. Fluorescence emission spectra (uncorrected) of 4BC MU polymer in 2-MTHF at 77 K (R_R phase), corrected for scattered light (dashed) from Dewar flask. Fluorescence excited at different wavelengths λ_e (5 nm bandwidth), detected with 5 nm bandwidth. The spectra are arbitrarily offset for clarity. *Polymer concentrations* (a) ≈0.64 mg/ml; (b) ≈0.064 mg/ml.

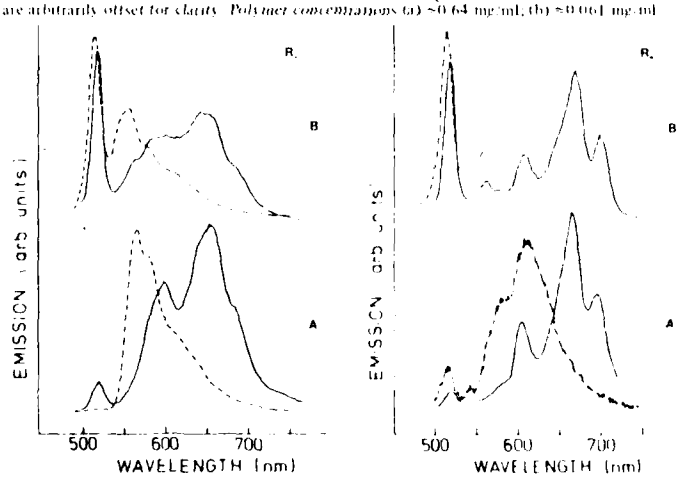

Fig. 4. Comparison of the fluorescence emission spectra (uncorrected) of 9PA polymer (solid) and 4BC MU polymer (dashed) in 2-MTHF at 77 K for the R_V- and R_R-phases. Fluorescence excited at 460 nm (5 nm bandwidth), detected with 5 nm bandwidth. Polymer concentrations (A) ≈0.6 mg/ml; (B) ≈0.06 mg/ml. The spectra are arbitrarily offset for clarity.

polymers is that the total fluorescence yield of the R_R-glass is less than that for the corresponding R_Y-glass by a factor of up to 3.5 depending on the initial concentration of the polymer. This is expected because of the lower entropy (greater order) of the R_R-phase. Whereas the spectral profiles of 9PA for the R_R phase show well developed vibronic sidebands with shifts from zero-phonon peaks of about 1500 and 2100 cm^{-1}, characteristic of the C=C and C–C stretching modes of the acetylene polymer backbone structure respectively, 4BCMU spectral profiles (fig. 3) are rather less structured. This makes it difficult to identify band origins. The R_Y-phase consists principally of two distinct molecular conformations with emission and absorption bands occurring roughly at 515 and 540 nm, and 550 and 530 nm, respectively. Quenching of the R_R phase, obtained after a short annealing time at room temperature, leads to a reduction of the 515 nm emission band together with the associated vibronic sidebands which appear as shoulders in fig. 3. The other conformation, dominant in the R_R phase (shoulder in R_Y), is apparently created to some extent at the expense of the initial conformation of R_Y-phase. The same trend is also observed for 9PA polymer [8]. For very dilute 4BCMU polymer solutions ($\leq 5 \times 10^{-4}$ mg ml^{-1}) the emission spectra representing R_Y and R_R phases are *virtually identical* except for a small intensity difference. Emission spectra were corrected for reabsorption. Though experimental problems limit the accuracy of this correction the emission intensity of the 515 nm peak of the R_Y-glasses was found to be virtually independent of the concentration of the Y phase solutions.

The changes in spectral profile with excitation wavelength can be explained as the superposition of the two spectra with emission origins at 515 and 550 nm. The former exhibits narrow vibronic emission when the excitation is in the region of the zero phonon peak (510–520 nm). Similar effects have been observed for 9PA glasses at 4 K [20]. This superposition suggests that there is no fast energy transfer between the polymer species responsible for these emissions. Since the ordering of high molecular weight semi flexible entangled polymers is *likely to be a slow process*, we believe that precursor species with similar conformations to those of the species frozen in the glasses, must exist in the polymer solutions [21]. The concentration dependence of emission and absorption we observe leads to the following conclusions. The precursor responsible for the 515 nm emission is present in nearly equal amounts in dilute R- and Y-phase solutions, *and the quantity of precursor or precursors*, responsible for the 550 nm emission increases with concentration for both R- and Y-phase solutions. These conclusions follow from the lower quantum efficiency for emission resulting from the species absorbing at 530 relative to that absorbing at 510 nm.

The R ⇌ Y transition for 3- and 4 BCMU has been interpreted as either a rod ⇌ coil transition of isolated chains [5–7,15,22,23] or as an aggregation phenomenon [24,25]. The absorption/fluorescence data of several PDAs clearly indicate that distinct, different backbone conformations occur in the Y- and R-phases. The absorption profiles for the Y phase of several PDAs suggest that the interactions between the sidegroups are minimal, if they occur at all. In the case of the urethane sidegroups containing PDAs, the dynamic nature of the Y-phase solutions will involve a competition between the formation and disruption of hydrogen bonds between the sidegroups, the latter being dominant. A clear-cut assignment of the microscopic structure in the R-phase is difficult because of conflicting experimental data. Both possibilities could occur for different PDAs. It is possible that sidegroup *interactions lock in local conformations in the R*-phase, preventing the formation of an extended rod-like conformation, and a chain folded microcrystalline morphology could result from the collapse of the Y-phase [26]. Such a conformation could occur independent of sidegroup hydrogen-bond formation. Thus, though the details of the polymer conformation will depend on the balance of inter- and intra-chain interactions, it seems likely that the Y- to R phase transition (and vice versa) is essentially backbone-driven, more or less independent of the sidegroup.

The interpretation of the fluorescence data given above indicates that aggregation of polymer chains occurs in both Y- and R phase solutions at all concentrations. There are several possibilities for the precursor of the 510 nm absorbing species. These include chain ends, non planar conformations, for example, *cis-helix* or a buckled trans locked in by sidegroup interactions. Further experiments are in hand to try to distinguish between these possibilities.

Acknowledgement

The authors are indebted to the Science and Engineering Research Council and the US Army European Research Office for financial support. Dr. D.A. McCarthy, Professor H. Baessler and our colleagues of the Royal Institution and Physics Department of Queen Mary College are thanked for helpful discussions.

References

[1] G. Wegner, in: Molecular metals, ed. W.E. Hatfield (Plenum Press, New York, 1979) p. 209.
[2] D. Bloor, in: Quantum theory of polymers, solid state aspects, eds. J. Ladik, J.M. Andre and M. Seel (Reidel, Dordrecht, 1984) p. 191.
[3] D. Bloor, in: Developments in crystalline polymers, Vol. 1, ed. D.C. Bassett (Appl. Sci., London, 1982) p. 151.
[4] R.H. Baughmann and R.R. Chance, Ann. NY Acad. Sci. 313 (1978) 705.
[5] G.N. Patel, R.R. Chance and J.D. Witt, J. Chem. Phys. 70 (1979) 4387; J. Polym. Sci. Polym. Phys. Ed. 16 (1978) 607.
[6] R.R. Chance, G.N. Patel and J.D. Witt, J. Chem. Phys. 71 (1979) 206.
[7] M.L. Shand, R.R. Chance, M. Le Postollec and M. Schott, Phys. Rev. B25 (1982) 4431.
[8] S.D.D.V. Rughooputh, D. Phillips, D. Bloor and D.J. Ando, Chem. Phys. Letters 106 (1984) 237.
[9] D. Bloor, D.N. Batchelder and J.H. Preston, Phys. Stat. Sol. 40a (1977) 279.
[10] H. Eichele and M. Schwoerer, Phys. Stat. Sol. 43a (1977) 465.
[11] B. Tieke and D. Bloor, Makromol. Chem. 180 (1979) 2275.
[12] H.R. Bhattacharjee, V.T. Priyadarsan and G.N. Patel, J. Chem. Phys. 73 (1980) 1438.
[13] J. Olmsted III and M. Strand, J. Phys. Chem. 87 (1983) 4290.
[14] C. Bubeck, B. Tieke and G. Wegner, Ber. Bunsenges. Physik. Chem. 86 (1982) 498.
[15] K.C. Lim, C.R. Fincher Jr. and A.J. Heeger, Phys. Rev. Letters 50 (1983) 1934.
[16] S.D.D.V. Rughooputh, D. Phillips, D. Bloor and D.J. Ando, Polym. Commun. 25 (1984) 242.
[17] C. Pluchetta, N.O. Rau, A. Hoult and R.C. Schulz, Makromol. Chem. Rapid Commun. 3 (1982) 249; C. Pluchetta, N.O. Rau and R.C. Schulz, Mol. Cryst. Liquid Cryst. 96 (1983) 141.
[18] G.N. Patel, Polym. Prepr. 19 (1978) 155.
[19] S.D.D.V. Rughooputh, D. Bloor, C. Stirkes and D. Phillips, to be published.
[20] H. Baessler, private communication.
[21] M. Gratley, A. Reiser, A.F. Roberts and D. Phillips, Macromolecules 14 (1981) 1752;
R.R. Chance, M.W. Washabeugh and D.E. Hoje, Proc. NATO ARW Polydiacetylenes, to be published.
[22] M. Sinclair, K.C. Lim and A.J. Heeger, Phys. Rev. Letters 51 (1983) 1768;
K.C. Lim, M. Sinclair, S.A. Casalnuovo, C.R. Fincher, F. Wudl and A.J. Heeger, Mol. Cryst. Liquid Cryst. 105 (1984) 329.
[23] A.J. Berlinsky, F. Wudl, K.C. Lim, C.R. Fincher and A.J. Heeger, J. Polym. Sci. Polym. Phys. Ed. 22 (1984) 847.
[24] G. Wenz and G. Wegner, Makromol. Chem. Rapid Commun. 3 (1982) 231.
[25] G. Wenz, M.A. Müller, M. Schmidt and G. Wegner, Macromolecules 17 (1984) 837.
[26] D.A. McCarthy, private communication.

END

DATE
FILMED

12 87

DTIC